Astrofisica Nucleare e Subnucleare

GeV Astrophysics V

Fermi LAT

The Large Area Telescope

- The LAT is a particle physics detector we've shot into space
  - We analyze individual events (one photon at a time) with high energy physics techniques to get photon sample
  - Lots of hard work to get (RA,DEC,E) behind the curtain
- Huge variations in response to different types of events
  - Bandpass = 4-5 decades in energy (< 20MeV to > 300 GeV)
  - Field of View = 2.4 sr (some response up to 70° off-axis)
- Several High Energy Astrophysics topics explored by the LAT

4FGL catalog

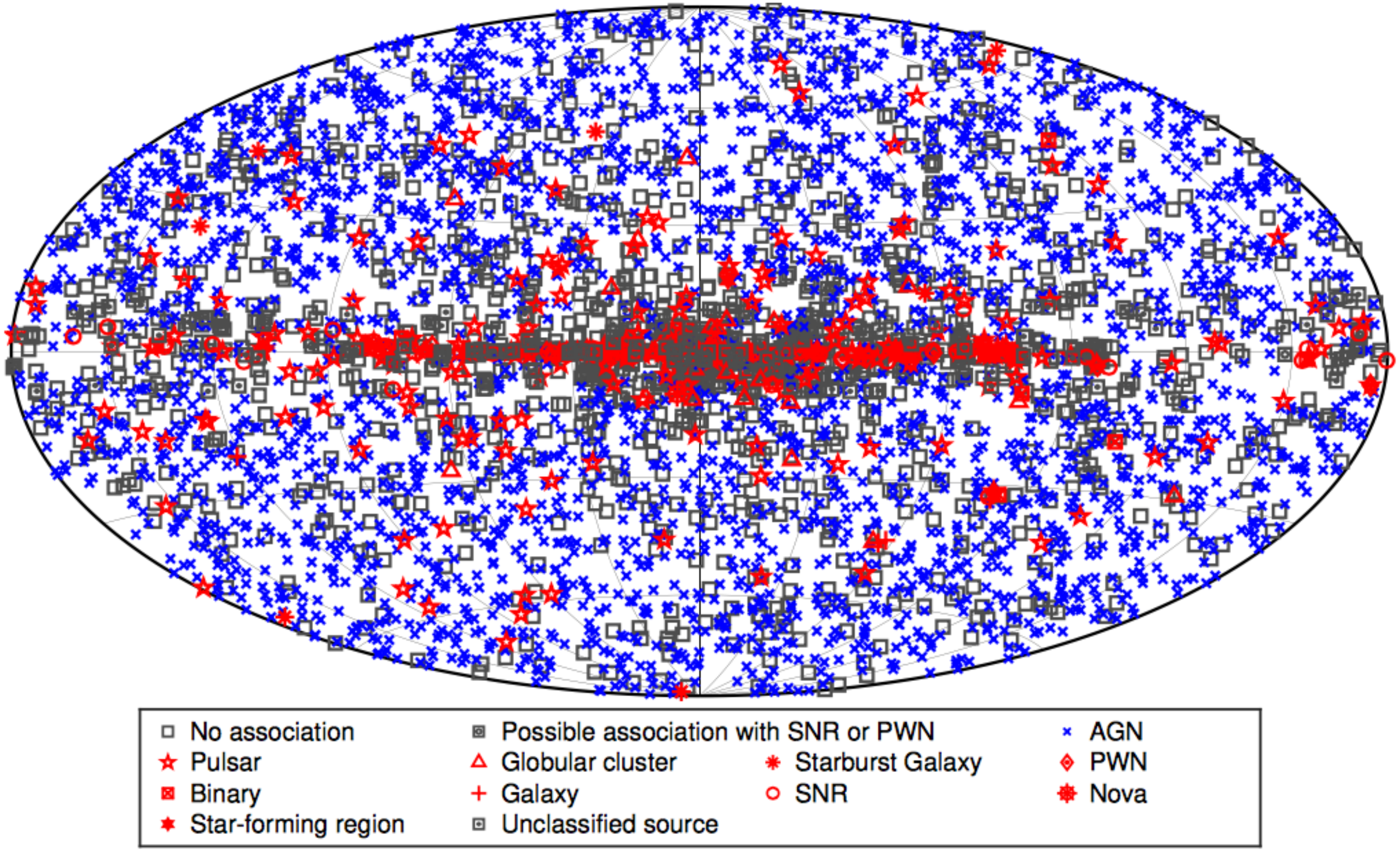

Abdollahi et al 2020

Source Analysis

- Source detections algorithms
- Spectral analysis
- Association studies
- Variability studies
- Source extension

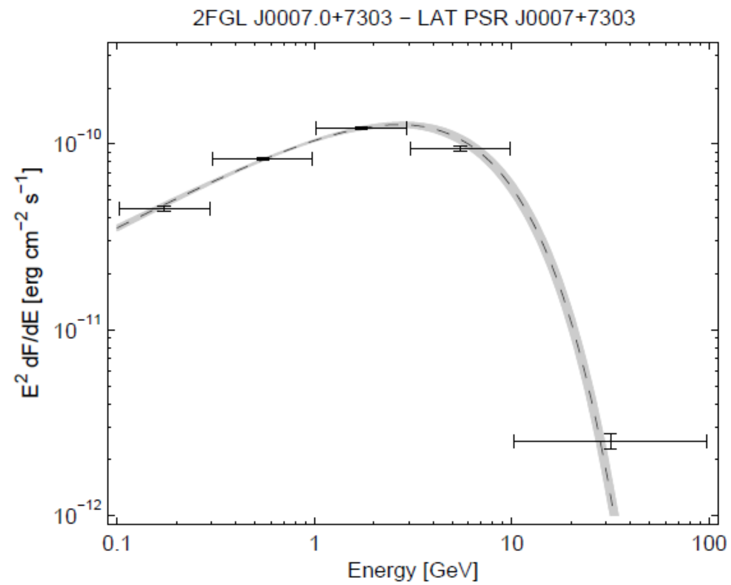

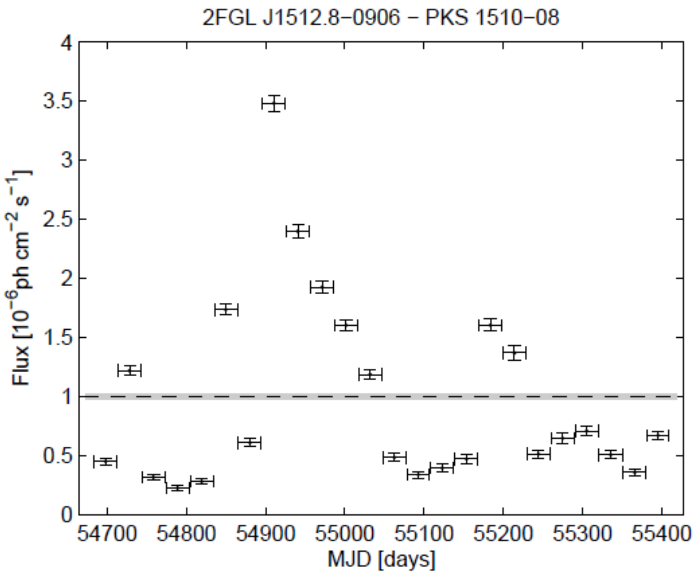

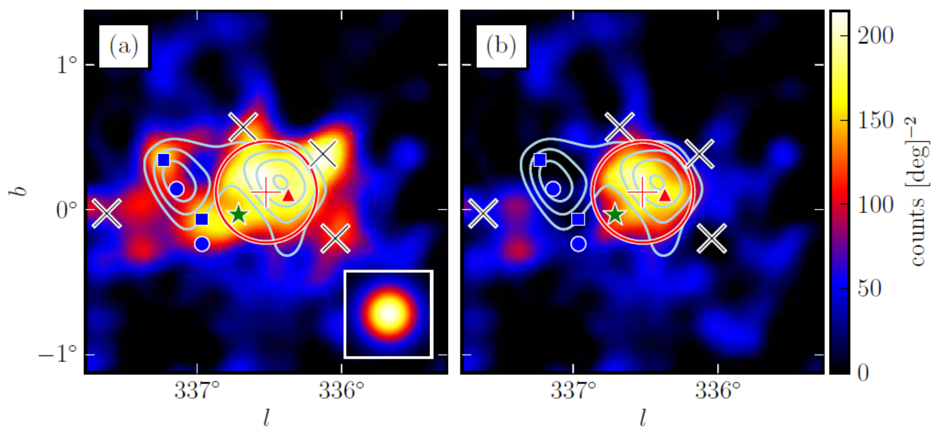

Abdo et al. 2011, Nolan et al. 2012

Lande et al. 2012

Fermi LAT
Data Analysis Tutorial

Tutorial

- Overview of the Fermi Large Area Telescope
  - **LAT data**

- **Fermi Science Tools**
  - **General Introduction**

- **Maximum Likelihood Overview**
  - **Source modeling**

- One study case:
  - **3c454.3: likelihood tutorial**

- **gtburst HE Analysis of GRBs**

New Pass8 data

Fermi
Science Support Center

Home | Observations | Data | Proposals | Library | HEASARC | Help | Site Map

Data

- Data Policy
- Data Access
- **Data Analysis**
  - + System Overview
  - + Software Download
  - + Documentation
  - + Cicerone
  - + Analysis Threads
  - + User Contributions
- Caveats
- Newsletters
- FAQ

Using LAT's New Pass 8 Data

The FSSC is now serving Pass 8 LAT data for analysis. The new version of LAT data provides a number of improvements over the reprocessed Pass 7 data, and is considered the best dataset for all types of LAT analysis. As of the release date (June 24, 2015) reprocessed Pass 7 data is no longer being served. However, existing Pass 7 reprocessed data has been archived and is available from the FSSC's FTP server.

Pass 8 provides a full reprocessing of the entire mission dataset, including improved event reconstruction, a wider energy range, better energy measurements, and significantly increased effective area. In addition, the events have been evaluated for their measurement quality in both position and energy. This allows the user to select a subset of the events if appropriate to improve analysis results. To support the use of these data selections, there have been some structural changes to the *Fermi* Science Tools.

Here we discuss the changes to the data and tools, and how they affect your analysis.

Pass 8 Bottom Line

Pass 8 contains a lot of changes, and the rest of this page may seem overwhelming. If you just want to get started doing a standard LAT analysis, here's the bottom line:

- Recommended event class for source analysis is "P8 Source" class (*evclass*=128).
- Add *evtype* parameter to your gtselect call (*convtype* parameter is deprecated). Recommended event type for source analysis is "FRONT+BACK" (*evtype*=3).
- Recommended zenith angle cut to eliminate Earth limb events ("zmax") is 90 degrees for events at 100 MeV and above.
- Recommended source list for analysis is the 3FGL Catalog. A python script is available at the User-Contributed Tools page that creates XML model files using the 3FGL catalog FITS file.

http://fermi.gsfc.nasa.gov/ssc/data/analysis/documentation/Pass8_usage.html

Overview of Fermi Science Tools

Maximum Likelihood Overview

Perform the fit: the likelihood

In high energy gamma rays it is never possible to really isolate a source because of limited statistics and strong and structured background.
Therefore statistical techniques have to be applied.
The most used method is the likelihood analysis based on the Poisson statistics.
The method requires to assume a model for the signal detected by the telescope.

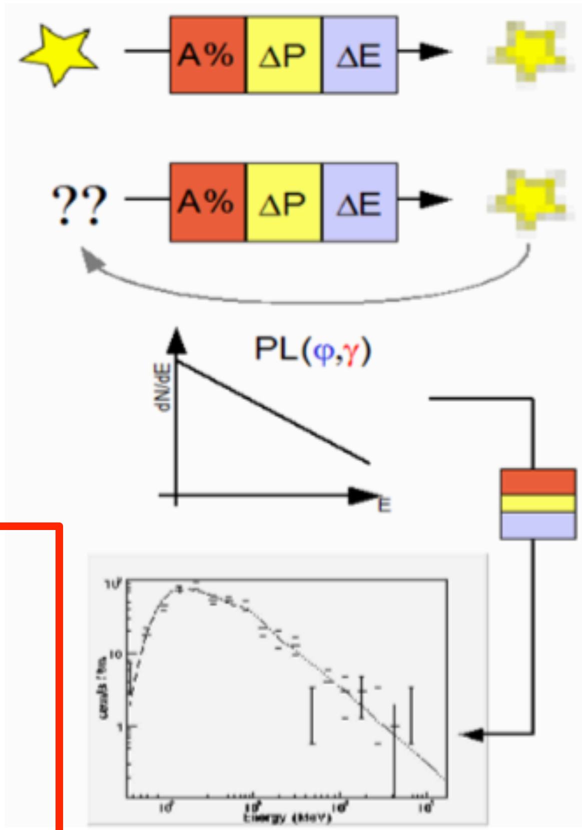

- Assume a **model**
- Model **convolved** with Instrument responce Function (IRF)
- Maximizing likelihood find the best set of parameters that reproduce the observed spectrum

- Maximum Likelihood Details

- Look Also at this very useful and complete presentation by Steve Fegan at Fermi Summer School 2014:
- https://confluence.slac.stanford.edu/download/attachments/169871661/ML_intro_SF_2014.ppt?version=1&modificationDate=1401204482000&api=v2

Likelihood Analysis

- Small number of counts in each bin, thus is characterized by the Poisson distribution.
- $\mathcal{L}$ is the product of the probabilities of observing n_k counts in each bin given the number of counts predicted by the model m_k

$$\mathcal{L} = \prod_k \frac{m_k^{n_k} e^{-m_k}}{n_k!}$$

- $\mathcal{L}$ can be rewritten as

$$\mathcal{L} = \prod_k e^{-m_k} \prod_k \frac{m_k^{n_k}}{n_k!} = e^{-N_{pred}} \prod_k \frac{m_k^{n_k}}{n_k!}$$

Likelihood Analysis

- If we let the bin sizes get infinitesimally small, then n_k = (0 or 1) and we are left with a product running over the number of photons:

$$\mathcal{L} = e^{-N_{pred}} \prod_i m_i$$

(This is the *unbinned* likelihood method).

- It's easier to handle the logarithm of $\mathcal{L}$ so we usually maximize:

$$\log\mathcal{L} = \sum_i \log(m_i) - N_{pred}$$

Instrument Response Function

It is often assumed that the IRF may be decomposed into three functions or matrices:

$$R(E', \hat{p}', E, \hat{p}, \vec{L}(t)) = D(E'; E, \hat{p}, \vec{L}(t))P(\hat{p}'; E, \hat{p}, \vec{L}(t))A(E, \hat{p}, \vec{L}(t)) \tag{2}$$

where

- $A(E, \hat{p}, \vec{L}(t))$ is the effective area, that is the projected area of the detector multiplied by its efficiency, that means the probability that a photon will react in the detector and produce a recognizable shower of particles.
- $D(E'; E, \hat{p}, \vec{L}(t))$ is the energy dispersion which reflects the imperfection of the energy measurement.
- $P(\hat{p}'; E, \hat{p}, \vec{L}(t))$ is the point spread function which reflects the imperfection of the measured direction.

Likelihood Analysis

- The source model considered is

$$S(E,\hat{p},t) = \sum_i s_i(E,t)\delta(\hat{p}-\hat{p}_i) + S_G(E,\hat{p}) + S_{\rm eg}(E,\hat{p}) + \sum_l S_l(E,\hat{p},t),$$

↑ Point Sources ↖ Galactic & EG diffuse Sources ↗ ↑ Other Sources

- This model is folded with the Instrument Response Functions (IRFs) to obtain the predicted number of counts in the measured quantity space (E', p', t'):

$$M(E',\hat{p}',t) = \int_{\rm SR} dE\,d\hat{p}\,R(E',\hat{p}',t;E,\hat{p})S(E,\hat{p},t)$$

Likelihood Analysis

- The function to maximize is:

$$\log \mathcal{L} = \sum_j \log M(E'_j, \hat{p}'_j, t_j) - N_{\rm pred}$$

- where the sum is performed over photons in the ROI. The predicted number of counts is $N_{\rm pred} = \int_{\rm ROI} dE' d\hat{p}' \, dt M(E', \hat{p}', t)$
- To save CPU time, a model-independent quantity, the exposure map (and cube), is precomputed:

$$\varepsilon(E, \hat{p}) \equiv \int_{\rm ROI} dE' \, d\hat{p}' \, dt \, R(E', \hat{p}', t; E, \hat{p})$$

- Then:

$$N_{\rm pred} = \int_{\rm SR} dE d\hat{p} \, S(E, \hat{p}) \, \varepsilon(E, \hat{p})$$

Test Statistic

$$\mathrm{TS} = -2\ \log \frac{\mathscr{L}_0}{\mathscr{L}_1}$$

$\mathscr{L}_0$ → Null hypothesis max likelihood, *h* parameters

$\mathscr{L}_1$ → Alternative hypothesis max likelihood, *m* parameters

- Where $\mathscr{L}_{max,0}$ is the maximum likelihood value for a model without an additional source ("the null hypothesis") and $\mathscr{L}_{max,1}$ is the maximum likelihood value for a model with the additional source at a specified location.

Test Statistic

Null hypothesis max likelihood, *h* parameters

$$TS = -2 \; \log \frac{\mathscr{L}_0}{\mathscr{L}_1} \underset{N \to \infty}{\to} \chi^2_{m-h}$$

non fixed parameters

Alternative hypothesis max likelihood, *m* paramete

- In the limit of a large number of counts, Wilk's Theorem states that the TS for the null hypothesis is asymptotically distributed as χ_n^2 where n is the number of parameters characterizing the additional source.
- As a basic rule of thumb, the square root of the TS is approximately equal to the detection significance for a given source.

Describing the Source Model: the XML model

- Typical source entry for an assumed powerlaw spectrum
- <!-- Point Sources -->

{<source name="……" type="PointSource">…
</source>
Your sources here

- <source name="3c454.3" type="PointSource">
- <spectrum type="PowerLaw2">
- <!-- Source is in ROI center -->
- <parameter error="0.00" free="1" max="1000" min="1e-06" name="Integral" scale="1e-04" value="1.000"/>
- <parameter error="0.00" free="1" max="0" min="-5" name="Index" scale="1" value="-2.000"/>
- <parameter free="0" max="3e6" min="20" name="LowerLimit" scale="1" value="100."/>
- <parameter free="0" max="3e6" min="20" name="UpperLimit" scale="1" value="300000."/>
- </spectrum>
- <spatialModel type="SkyDirFunction">
- <parameter free="0" max="360.0" min="-360.0" name="RA" scale="1.0" value="343.494812"/>
- <parameter free="0" max="90" min="-90" name="DEC" scale="1.0" value="16.149500"/>
- </spatialModel>
- </source>

XML model

- Test different models... power law * HE exponential cut-off
- <source name="3c454.3" type="PointSource">
- <spectrum type="PLSuperExpCutoff">
- <parameter free="1" max="1000" min="1e-05" name="Prefactor" scale="1e-07" value="1"/>
- <parameter free="1" max="0" min="-5" name="Index1" scale="1" value="-1.7"/>
- <parameter free="0" max="1000" min="50" name="Scale" scale="1" value="200"/>
- <parameter free="1" max="30000" min="500" name="Cutoff" scale="1" value="3000"/>
- <parameter free="0" max="5" min="0" name="Index2" scale="1" value="1"/>
- </spectrum>

- Look here for source model definition and XML model definitions:
- http://fermi.gsfc.nasa.gov/ssc/data/analysis/scitools/xml_model_defs.html
- http://fermi.gsfc.nasa.gov/ssc/data/analysis/scitools/source_models.html

- Useful python script to load 4FGL sources that belongs to your ROI in your XML file model (make4FGLxml.py)
- http://fermi.gsfc.nasa.gov/ssc/data/analysis/user/
-

Describing the Source Model: the XML model

- Backgrounds
- <!-- Diffuse Sources -->
- <source name="galactic_background"   type="DiffuseSource">
- <spectrum type="PowerLaw">
- <parameter free="1" max="10" min="0" name="Prefactor" scale="1" value="1"/>
- <parameter free="0" max="1" min="-1" name="Index" scale="1.0" value="0"/>
- <parameter free="0" max="2e2" min="5e1" name="Scale" scale="1.0" value="1e2"/>
- </spectrum>
- <spatialModel file=”gll_iem_v07.fits" type="MapCubeFunction">
- <parameter free="0" max="1e3" min="1e-3" name="Normalization" scale="1.0" value="1.0"/>
- </spatialModel>
- </source>
- <source name="extragalactic_background" type="DiffuseSource">
- <spectrum file=”iso_P8R3_SOURCE_V3_v1.txt" type="FileFunction">
- <parameter free="1" max="10" min="1e-2" name="Normalization" scale="1" value="1"/>
- </spectrum>
- <spatialModel type="ConstantValue">
- <parameter free="0" max="10.0" min="0.0" name="Value" scale="1.0" value="1.0"/>
- </spatialModel>
- </source>

Perform the fit: the likelihood approach

- Absolute value of likelihood meaningless!
- Comparison between model w/ and w/o source to reject H_0 = no source
- Many variables may be calculated BEFORE selecting the models
- IRFs depend on inclination angle:
  Livetime Cube: seconds in $\Delta\Omega$ with a given z,
  the time that the LAT observed a given position on the sky at a given inclination angle
  Exposure Map: integration of the effective area over the FoV weighted by the livetime over a position-energy grid, $N_{model} = \int \Phi_{model}(\Omega, E(t)) \times A_{LAT}(\Omega, E)$

The Livetime cube

- The LAT instrument response functions are a function of the inclination angle, the angle between the direction to a source and the LAT normal.
- The number of counts that a source should produce should therefore depend on the amount of time that the source spent at a given inclination angle during an observation.
- This livetime quantity, the time that the LAT observed a given position on the sky at a given inclination angle, depends only on the history of the LAT's orientation during the observation and not on the source model.

https://fermi.gsfc.nasa.gov/ssc/data/analysis/documentation/Cicerone/Cicerone_Likelihood/Exposure.html

The Exposure Map

- The likelihood consists of two factors: the first is dependent on the detected counts; and the second is equal to the exponential of the negative of the predicted total number of counts for the source model.
- The exposure map is the total exposure (effective area multiplied by live time) for a given position on the sky producing counts in the Region of Interest. Since the effective area is a function of the photon energy, the exposure map is also a function of this energy. Thus the counts produced by a source at a given position on the sky is the integral of the source flux and the exposure map (a function of energy) at that position.
- The exposure map should be computed over a Source Region that is larger than the Region of Interest by ~50%. This is necessary to ensure that all source photons are included due to the size of the LAT instrument PSF at low energies.

https://fermi.gsfc.nasa.gov/ssc/data/analysis/documentation/Cicerone/Cicerone_Likelihood/Exposure.html

Likelihood 1st step: gtltcube

- [/home]$ gtltcube zmax=90
- Event data file[filtered_gti.fits]
- Spacecraft data file[sc.fits]
- Output file[ltCube.fits]
- Step size in cos(theta) (0.:1.) [0.025]
- Pixel size (degrees)[1]
- ....

The "livetime cube" must be re-calculated when a new time-interval or a new ZA is selected

Likelihood 2nd step: gtexpmap

- [/home/]$ gtexpmap
- Event data file[filtered_gti.fits]
- Spacecraft data file[sc.fits]
- Exposure hypercube file[ltCube.fits]
- output file name[expMap.fits]
- Response functions[CALDB]
- Radius of the source region (in degrees)[30]
- Number of longitude points (2:1000) [120]
- Number of latitude points (2:1000) [120]
- Number of energies (2:100) [20]
- Computing the ExposureMap using ltCube.fits
- ...

Add 15° to the ROI radius

gtexpmap

Quick check with DS9: fields must be homogenous

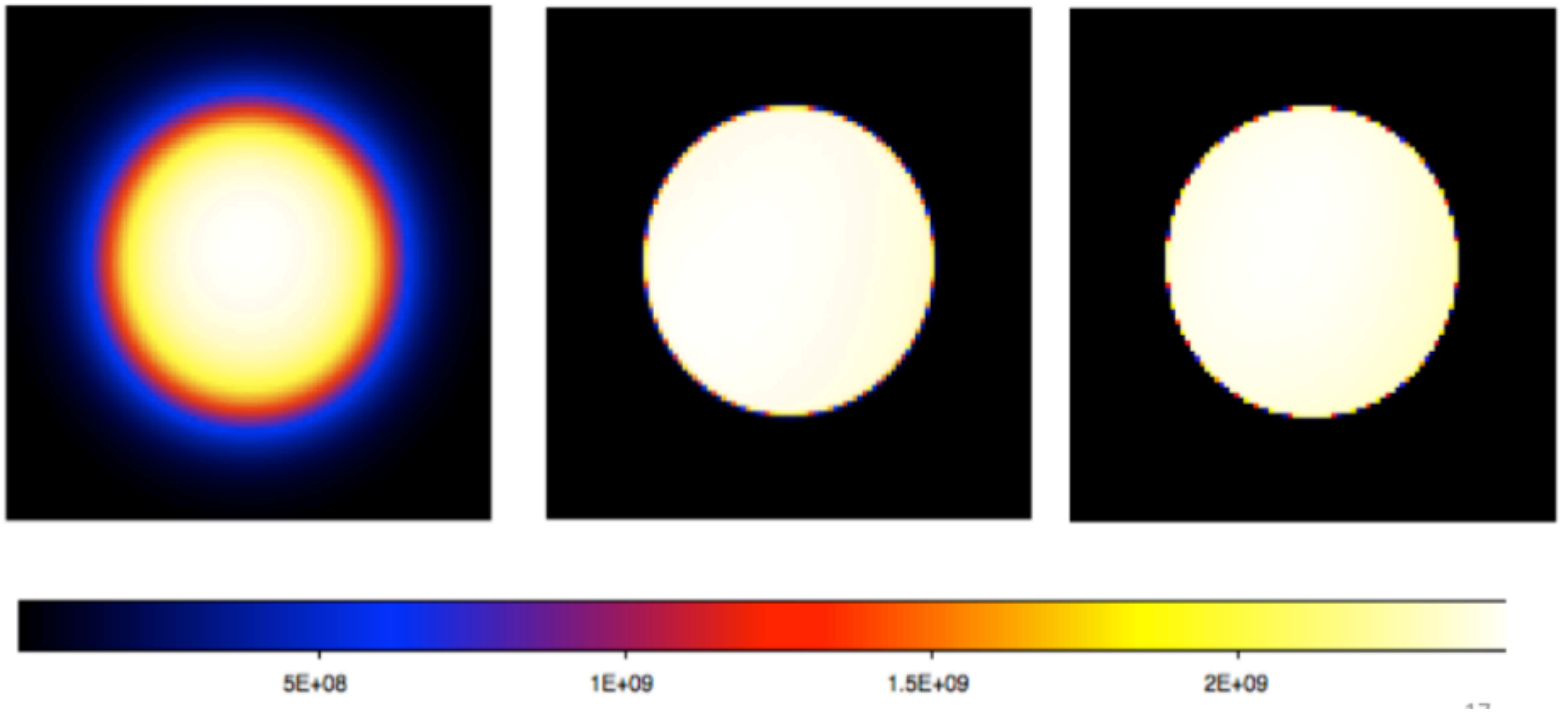

Likelihood 3rd step: the XML model

5. Create a source model XML file

The gtlike tool reads the source model from an XML file. The model file contains your best guess at the locations and spectral forms for the sources in your data. A source model can be created using the model editor tool, by using the user contributed tool **make3FGLxml.py** (available at the user-contributed tools page), or by editing the file directly within a text editor.

Here we cannot use the same source model that was used to analyze six months of data in the Unbinned Likelihood tutorial, as the 2-year data set contains many more significant sources and will not converge. Instead, we will use the 3FGL catalog to define our source model by running make3FGLxml.py. To run the script, you will need to download the current LAT catalog file and place it in your working directory:

```
prompt> make3FGLxml.py gll_psc_v16.fit 3C279_binned_gti.fits -o 3C279_input_model.xml
-G $FERMI_DIR/refdata/fermi/galdiffuse/gll_iem_v06.fits -g gll_iem_v06
-I $FERMI_DIR/refdata/fermi/galdiffuse/iso_P8R2_SOURCE_V6_v06.txt
-i iso_P8R2_SOURCE_V6_v06 -s 120 -p TRUE -v TRUE
This is make3FGLxml version 01r0.
The default diffuse model files and names are for pass 8
and assume you have v10r00p05 of the Fermi Science Tools or higher.
Creating file and adding sources from 3FGL
Added 312 point sources, note that any extended sources in ROI were modeled as point sources
because psForce option was set to True
prompt>
```

Note that we are using a high level of significance so that we only fit the brightest sources and we have forced the extended sources to be modeled as point sources. This only affects the lobes of Centarus A which are just outside the FOV.

It is also necessary to specify the entire path to location of the diffuse model on your system. The resulting XML model contains 312 sources. Clearly, the simple 4-source model we used for the 6-month Unbinned Likelihood analysis would have been too simplistic.

This XML file uses the spectral model from the 3FGL catalog analysis for each source. (The catalog file is available at the LAT 4-yr Catalog page.) However, that analysis used a subset of the available spectral models. A dedicated analysis of the region may indicate a different spectral model is preferred. For more details on the options available for your XML models, see:

- Descriptions of available Spectral and Spatial Models
- Examples of XML Model Definitions for Likelihood

Likelihood 3rd step

- python make4FGLxml.py gll_psc_v27.fit filtered_gti.fits -o 3c454.3.xml –G $FERMI_DIR/refdata/fermi/galdiffuse/gll_iem_v07.fits -g gll_iem_v07 –I $FERMI_DIR/refdata/fermi/galdiffuse/iso_P8R3_SOURCE_V2.txt -i iso_P8R3_SOURCE_V2 -s 120 -p TRUE

Describing the Source Model: the XML model

- Backgrounds
- <!-- Diffuse Sources -->
- <source name="galactic_background" type="DiffuseSource">
- <spectrum type="PowerLaw">
- <parameter free="1" max="10" min="0" name="Prefactor" scale="1" value="1"/>
- <parameter free="0" max="1" min="-1" name="Index" scale="1.0" value="0"/>
- <parameter free="0" max="2e2" min="5e1" name="Scale" scale="1.0" value="1e2"/>
- </spectrum>
- <spatialModel file=”gll_iem_v07.fits" type="MapCubeFunction">
- <parameter free="0" max="1e3" min="1e-3" name="Normalization" scale="1.0" value="1.0"/>
- </spatialModel>
- </source>
- <source name="extragalactic_background" type="DiffuseSource">
- <spectrum file=”iso_P8R3_SOURCE_V2.txt" type="FileFunction">
- <parameter free="1" max="10" min="1e-2" name="Normalization" scale="1" value="1"/>
- </spectrum>
- <spatialModel type="ConstantValue">
- <parameter free="0" max="10.0" min="0.0" name="Value" scale="1.0" value="1.0"/>
- </spatialModel>
- </source>

XML model

- Typical source entry for an assumed powerlaw spectrum
- <!-- Point Sources -->

<source name="......" type="PointSource">...
</source>
Your sources here

- <source name="3c454.3" type="PointSource">
- <spectrum type="PowerLaw2">
- <!-- Source is in ROI center -->
- <parameter error="0.00" free="1" max="1000" min="1e-06" name="Integral" scale="1e-04" value="1.000"/>
- <parameter error="0.00" free="1" max="0" min="-5" name="Index" scale="1" value="-2.000"/>
- <parameter free="0" max="3e6" min="20" name="LowerLimit" scale="1" value="100."/>
- <parameter free="0" max="3e6" min="20" name="UpperLimit" scale="1" value="300000."/>
- </spectrum>
- <spatialModel type="SkyDirFunction">
- <parameter free="0" max="360.0" min="-360.0" name="RA" scale="1.0" value="343.494812"/>
- <parameter free="0" max="90" min="-90" name="DEC" scale="1.0" value="16.149500"/>
- </spatialModel>
- </source>

XML model

- Test different models... power law * HE exponential cut-off
- <source name="3c454.3" type="PointSource">
- <spectrum type="PLSuperExpCutoff">
- <parameter free="1" max="1000" min="1e-05" name="Prefactor" scale="1e-07" value="1"/>
- <parameter free="1" max="0" min="-5" name="Index1" scale="1" value="-1.7"/>
- <parameter free="0" max="1000" min="50" name="Scale" scale="1" value="200"/>
- <parameter free="1" max="30000" min="500" name="Cutoff" scale="1" value="3000"/>
- <parameter free="0" max="5" min="0" name="Index2" scale="1" value="1"/>
- </spectrum>

- Look here for source model definition and XML model definitions:
- http://fermi.gsfc.nasa.gov/ssc/data/analysis/scitools/xml_model_defs.html
- http://fermi.gsfc.nasa.gov/ssc/data/analysis/scitools/source_models.html

- Useful python script to load 2FGL sources that belongs to your ROI in your XML file model (make3FGLxml.py)
- http://fermi.gsfc.nasa.gov/ssc/data/analysis/user/
-

Diffuse response

- [/home/]$gtdiffrsp
- Event data file[]filtered_gti.fits
- Spacecraft data file[] sc.fits
- Source model file[] 3c454.3.xml
- Response functions to use[] CALDB

Finally... gtlike performing the actual fit

- [/home/]$ gtlike plot=no
- Statistic to use (BINNED|UNBINNED) [UNBINNED]
- Spacecraft file[sc.fits]
- Event file[filtered_gti.fits]
- Unbinned exposure map[expMap.fits]
- Exposure hypercube file[ltCube.fits]
- Source model file[../xml_models/_3c454.3_model_ROI15.xml]
- Response functions to use[CALDB]
- Optimizer (DRMNFB|NEWMINUIT|MINUIT|DRMNGB|LBFGS) [DRMNFB]

Typically use DRMNGB/DRMNFB to find a rough estimate of the likelihood maxima and refine later on with **MINUIT (or NEWMINUIT)**

Likelihood output

- {'3c454.3': {'Integral': '0.146106 +/- 0.00271733',
- 'Index': '-2.29973 +/- 0.017189',
- 'LowerLimit': '100',
- 'UpperLimit': '300000',
- 'Npred': '4171.85',
- 'ROI distance': '0',
- 'TS value': '17548.4',
- 'Flux': '1.46192e-05 +/- 2.7178e-07',
- …
- extragalactic_background': {'Normalization': '1.20197 +/- 0.23541',
- 'Npred': '643.953',
- 'Flux': '0.000170707 +/- 3.34331e-05',
- },
- 'galactic_background': {'Prefactor': '0.739969 +/- 0.251827',
- 'Index': '0',
- 'Scale': '100',
- 'Npred': '357.929',
- 'Flux': '0.000215978 +/- 7.35023e-05',

gtlike creates two output files:
1) results.dat: fit results
2) counts_spectra.fits: the counts in a proper energy binning

Comparison of different models

- Powerlaw * HE exp cut-off
- {'3c454.3': {'Prefactor': '0.39194 +/- 0.00793161',
- 'Index1': '-2.12802 +/- 0.03056',
- 'Cutoff': '5495.55 +/- 934.857 (MeV)
- 'Npred': '4157.04',
- 'ROI distance': '0',
- 'TS value': '17604.2',
- 'Flux': '1.41693e-05 +/- 2.72878e-07
- (ph cm-2 s-1)

- ----> Comparing TS values for different models!
- For this source, in this time interval, the model with the HE exponential cutoff is favoured with respect to the Simple Powerlaw

You can repeat analyses by yourself also following instructive and complete Tutorials on the FSSC web-site:
- Standard Likelihood: http://fermi.gsfc.nasa.gov/ssc/data/analysis/scitools/likelihood_tutorial.html
- PyLike: http://fermi.gsfc.nasa.gov/ssc/data/analysis/scitools/python_tutorial.html

Analysis Tutorial - 3

Check the “Navigation” plot

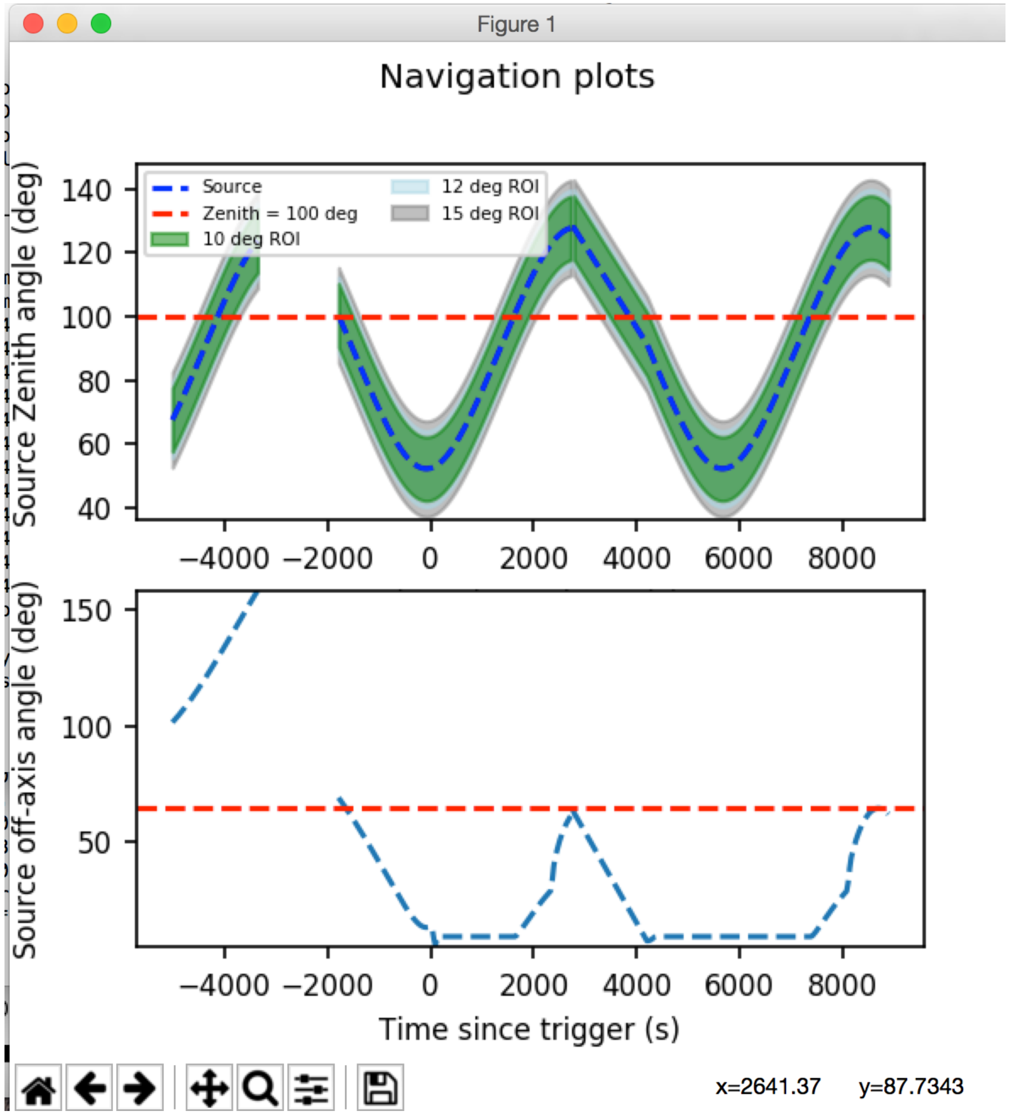

Likelihood with gtburst

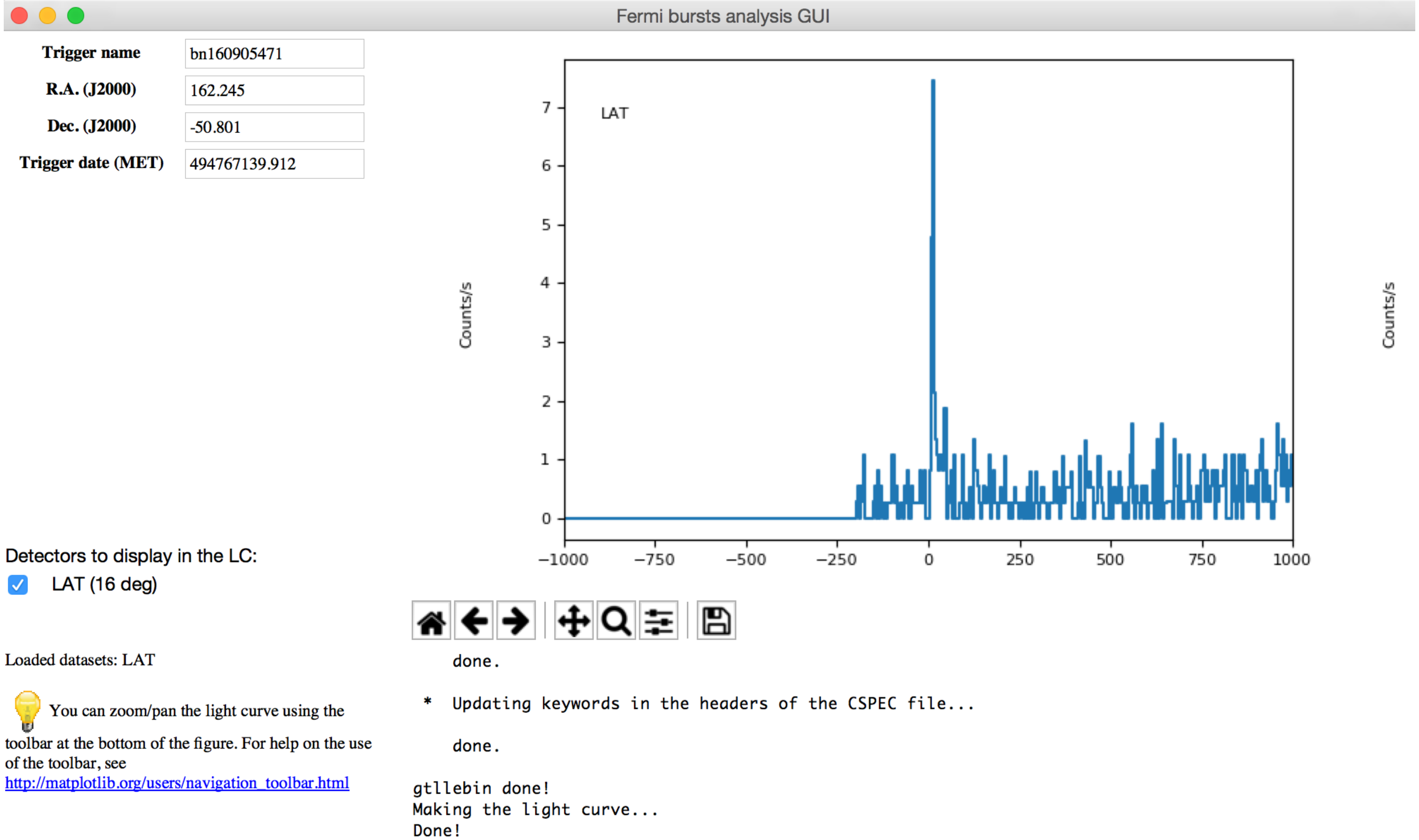

Select event class

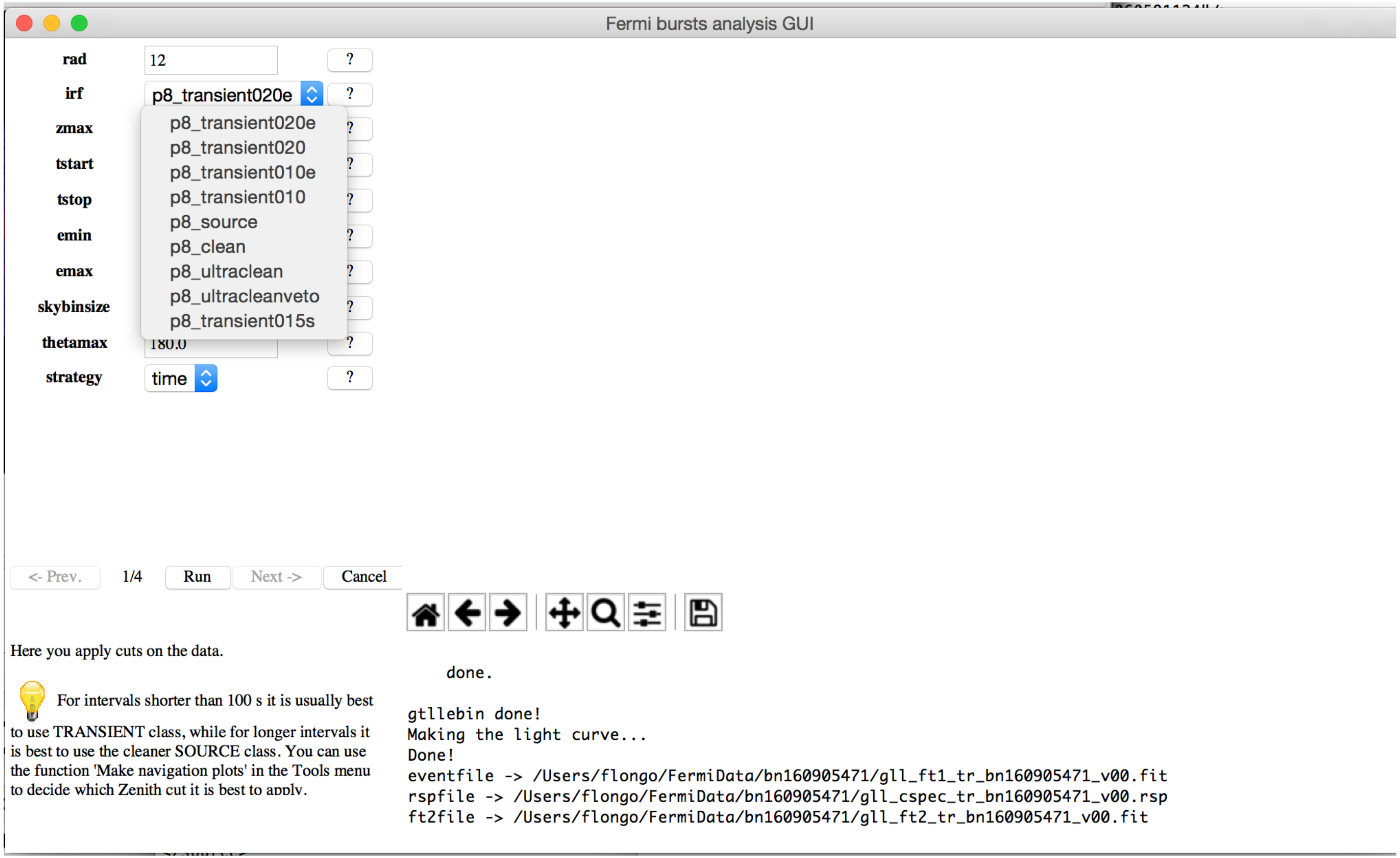

See count map and list of photons

rad	12	?
irf	p8_transient020e	?
zmax	100	?
tstart	0	?
tstop	100	?
emin	100	?
emax	100000	?
skybinsize	0.2	?
thetamax	180.0	?
strategy	time	?

<- Prev. 1/4 Run Next -> Cancel

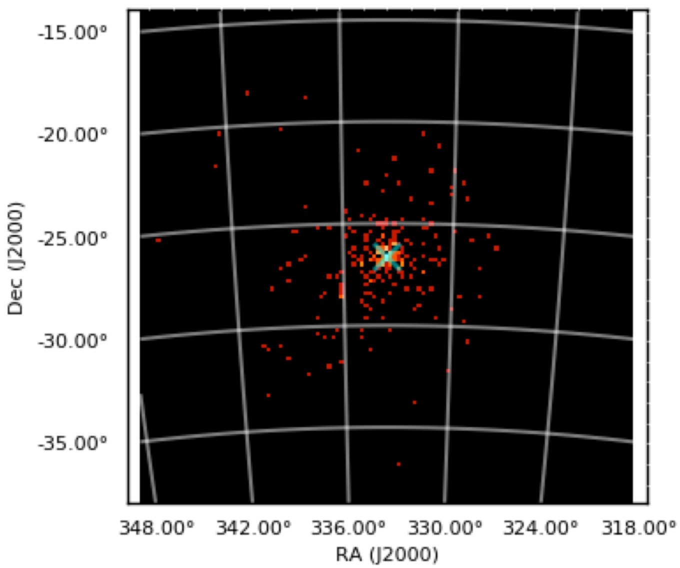

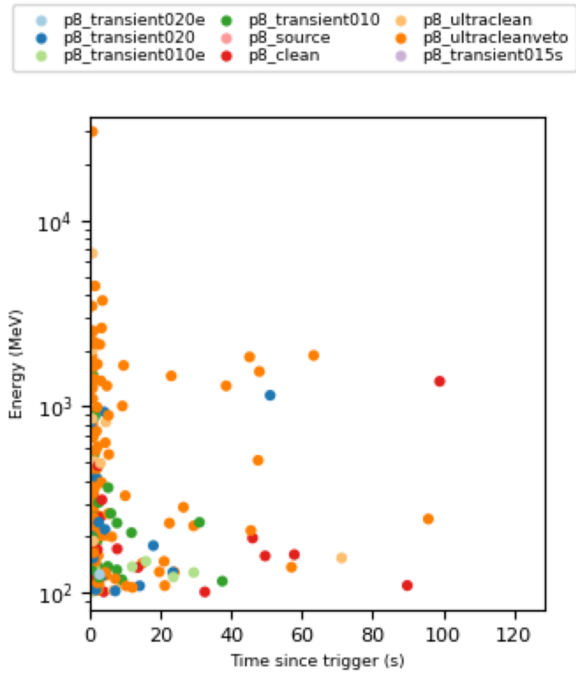

Here you apply cuts on the data.

For intervals shorter than 100 s it is usually best to use TRANSIENT class, while for longer intervals it is best to use the cleaner SOURCE class. You can use the function 'Make navigation plots' in the Tools menu to decide which Zenith cut it is best to apply.

```
Class p8_transient010 only:          47
Class p8_source only:                0
Class p8_clean only:                 32
Class p8_ultraclean only:            19
Class p8_ultracleanveto only:        123
Class p8_transient015s only:         0

============================================================
```

Create XML model

Select the parameters of the model

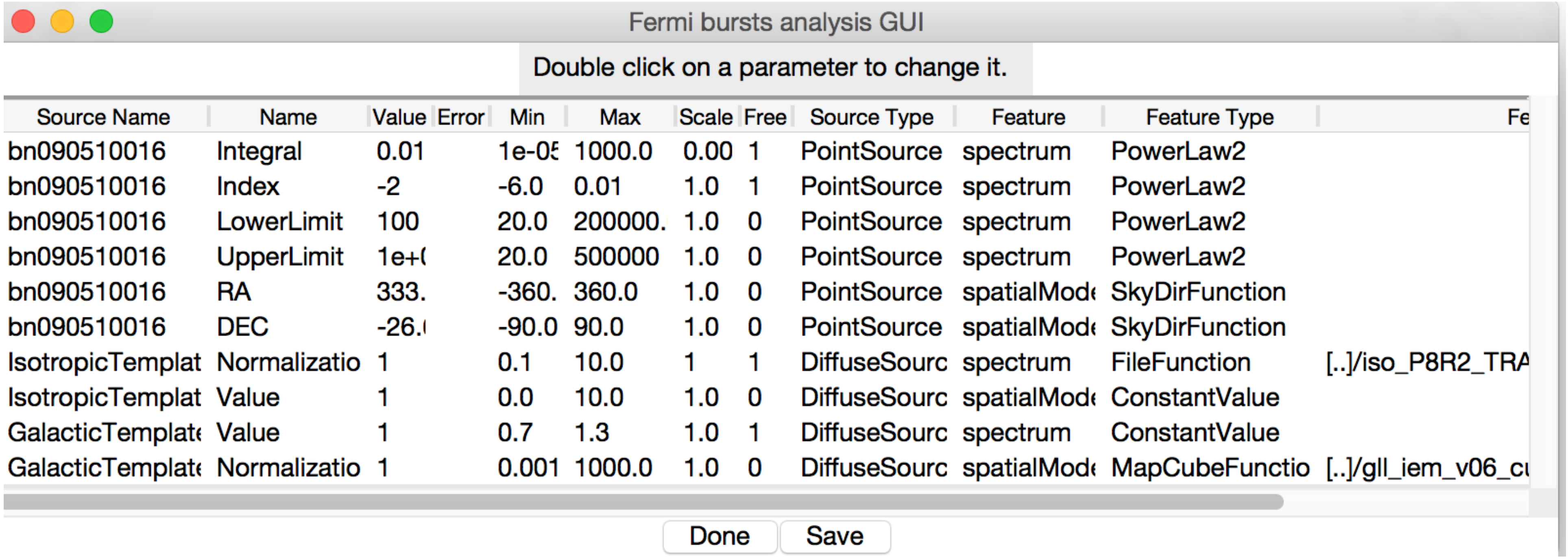

Source Name	Name	Value	Error	Min	Max	Scale	Free	Source Type	Feature	Feature Type	Fe
bn090510016	Integral	0.01		1e-05	1000.0	0.00	1	PointSource	spectrum	PowerLaw2	
bn090510016	Index	-2		-6.0	0.01	1.0	1	PointSource	spectrum	PowerLaw2	
bn090510016	LowerLimit	100		20.0	200000.	1.0	0	PointSource	spectrum	PowerLaw2	
bn090510016	UpperLimit	1e+(		20.0	500000	1.0	0	PointSource	spectrum	PowerLaw2	
bn090510016	RA	333.		-360.	360.0	1.0	0	PointSource	spatialMode	SkyDirFunction	
bn090510016	DEC	-26.(		-90.0	90.0	1.0	0	PointSource	spatialMode	SkyDirFunction	
IsotropicTemplat	Normalizatio	1		0.1	10.0	1	1	DiffuseSourc	spectrum	FileFunction	[..]/iso_P8R2_TRA
IsotropicTemplat	Value	1		0.0	10.0	1.0	0	DiffuseSourc	spatialMode	ConstantValue	
GalacticTemplate	Value	1		0.7	1.3	1.0	1	DiffuseSourc	spectrum	ConstantValue	
GalacticTemplate	Normalizatio	1		0.001	1000.0	1.0	0	DiffuseSourc	spatialMode	MapCubeFunctio	[..]/gll_iem_v06_cu

Fit plots

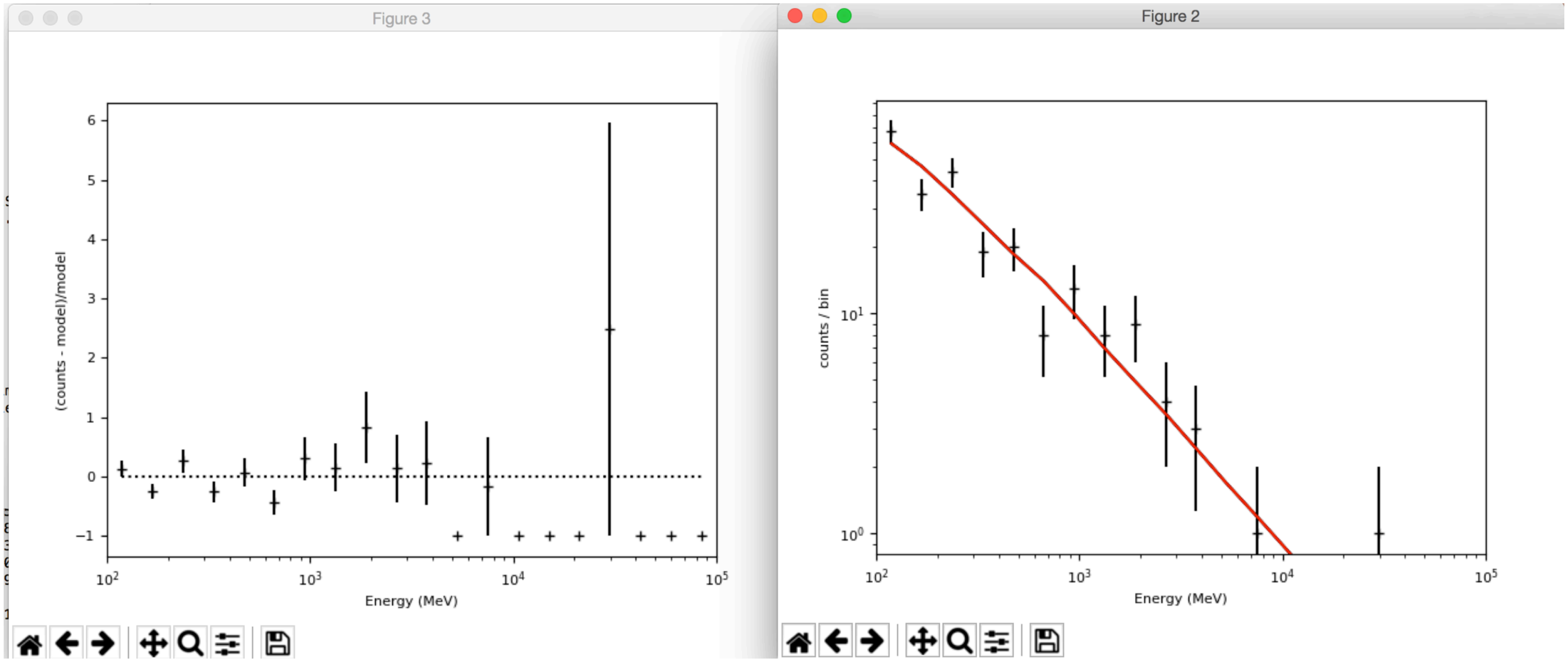

Figure 3
(counts - model)/model
Energy (MeV)
Figure 2
counts / bin
Energy (MeV)

Fit results

Likelihood results

Source name	Par. Name	Value	Error	Units	TS
GalacticTemplate					0
	Value	1	0.15	-	
	Energy flux	2.1e-07	3.14e-08	erg/cm2/s	
	Photon flux	0.000443	6.63e-05	ph./cm2/s	
IsotropicTemplate					1
	Normalization	0.426	1.32	-	
	Energy flux	4.75e-08	1.47e-07	erg/cm2/s	
	Photon flux	0.000134	0.000413	ph./cm2/s	
bn090510016					2056
	Integral	0.000363	2.31e-05	ph./cm2/s	
	Index	-2.03	0.0628	-	
	LowerLimit	100	n.a. (fixed)	MeV	
	UpperLimit	1e+05	n.a. (fixed)	MeV	
	Energy flux	1.33e-07	8.44e-09	erg/cm2/s	
	Photon flux	0.00033	2.2e-05	ph./cm2/s	

```
*** All fluxes and upper limits have been computed in the 100.0 - 1000.0 energy range.
*** Upper limits (if any) are computed assuming a photon index of -2.0, with the 95.0 % c.l.
Log(likelihood) = 769.199818608

New localization from gtfindsrc:

(R.A., Dec)                      = (333.567, -26.625)
68 % containment radius          =  0.028
90 % containment radius          =  0.040
Distance from initial position   =  0.039
```

Results of the last likelihood analysis. Select 'close' from the file menu to close this window.

Fit results

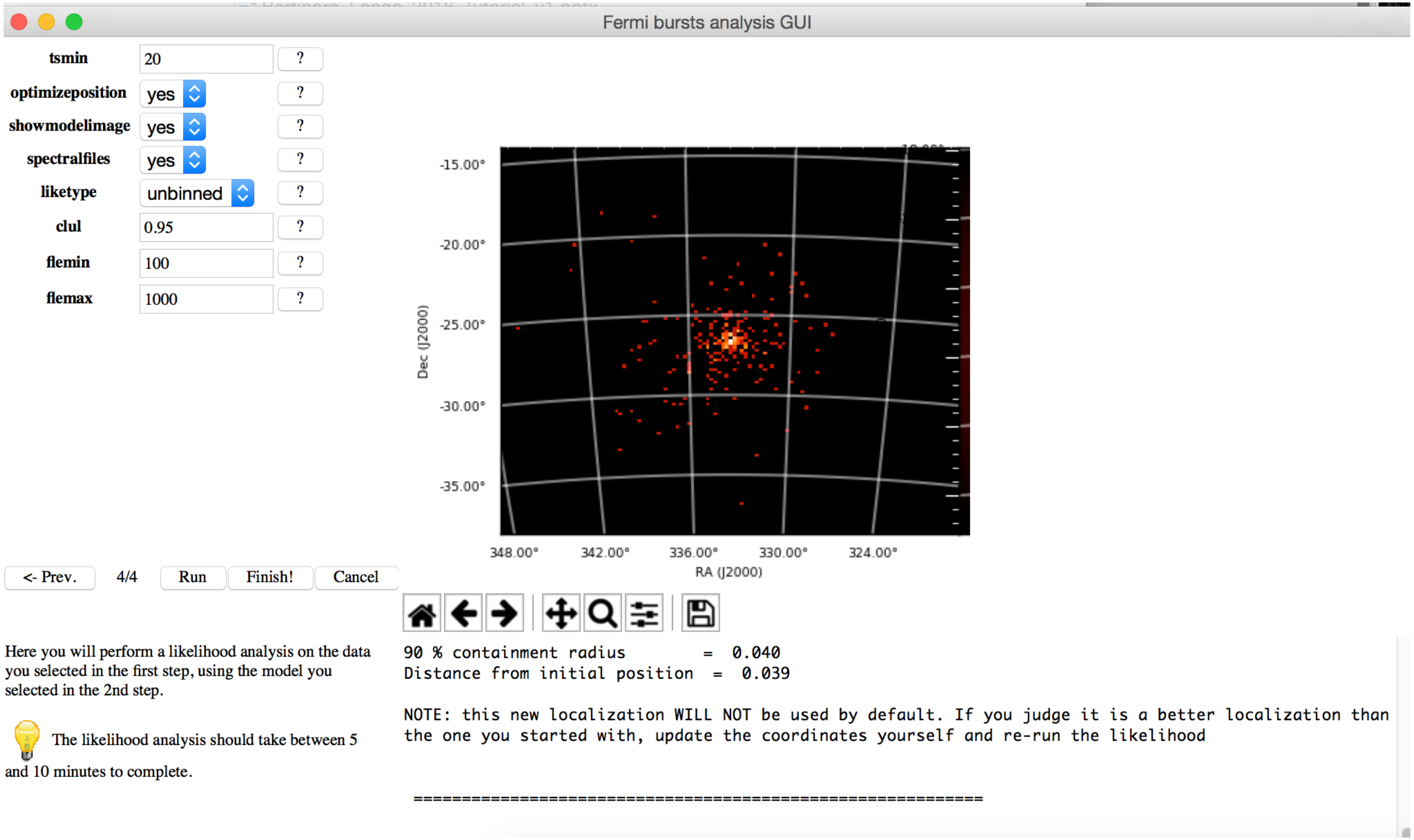
Fermi bursts analysis GUI
tsmin
20
optimizeposition
yes
showmodelimage
yes
spectralfiles
yes
liketype
unbinned
clul
0.95
flemin
100
flemax
1000
-15.00°
-20.00°
-25.00°
-30.00°
-35.00°
Dec (J2000)
348.00°
342.00°
336.00°
330.00°
324.00°
RA (J2000)
<- Prev.
4/4
Run
Finish!
Cancel
Here you will perform a likelihood analysis on the data you selected in the first step, using the model you selected in the 2nd step.
The likelihood analysis should take between 5 and 10 minutes to complete.
90 % containment radius = 0.040
Distance from initial position = 0.039
NOTE: this new localization WILL NOT be used by default. If you judge it is a better localization than the one you started with, update the coordinates yourself and re-run the likelihood
===

Astrofisica Nucleare e Subnucleare

Galactic GeV Sources

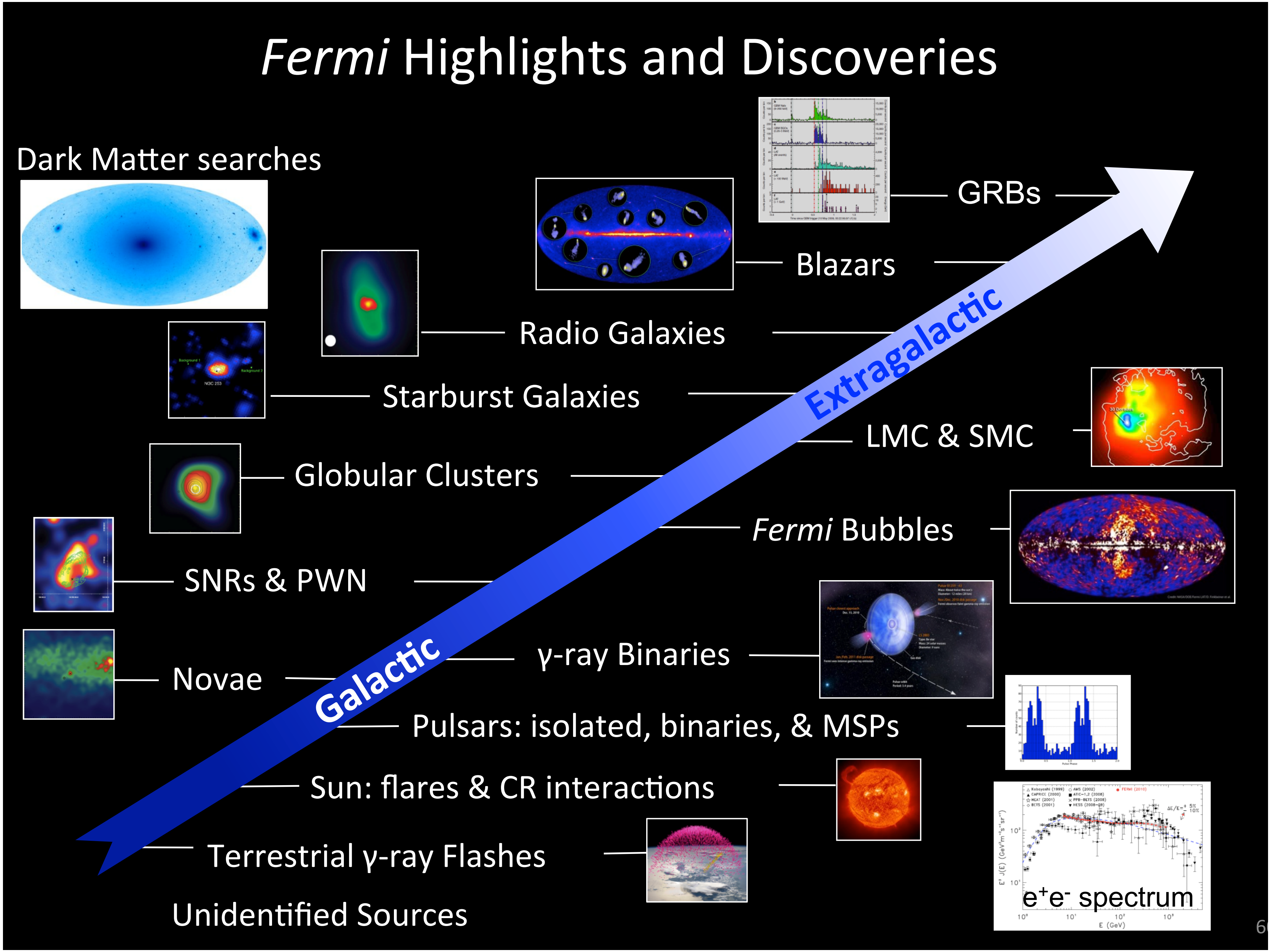

Fermi Highlights and Discoveries
Dark Matter searches
GRBs
Blazars
Radio Galaxies
Starburst Galaxies
Extragalactic
LMC & SMC
Globular Clusters
Fermi Bubbles
SNRs & PWN
γ-ray Binaries
Galactic
Novae
Pulsars: isolated, binaries, & MSPs
Sun: flares & CR interactions
Terrestrial γ-ray Flashes
Unidentified Sources
e+e- spectrum

Pulsars Dominate the GeV Galaxy

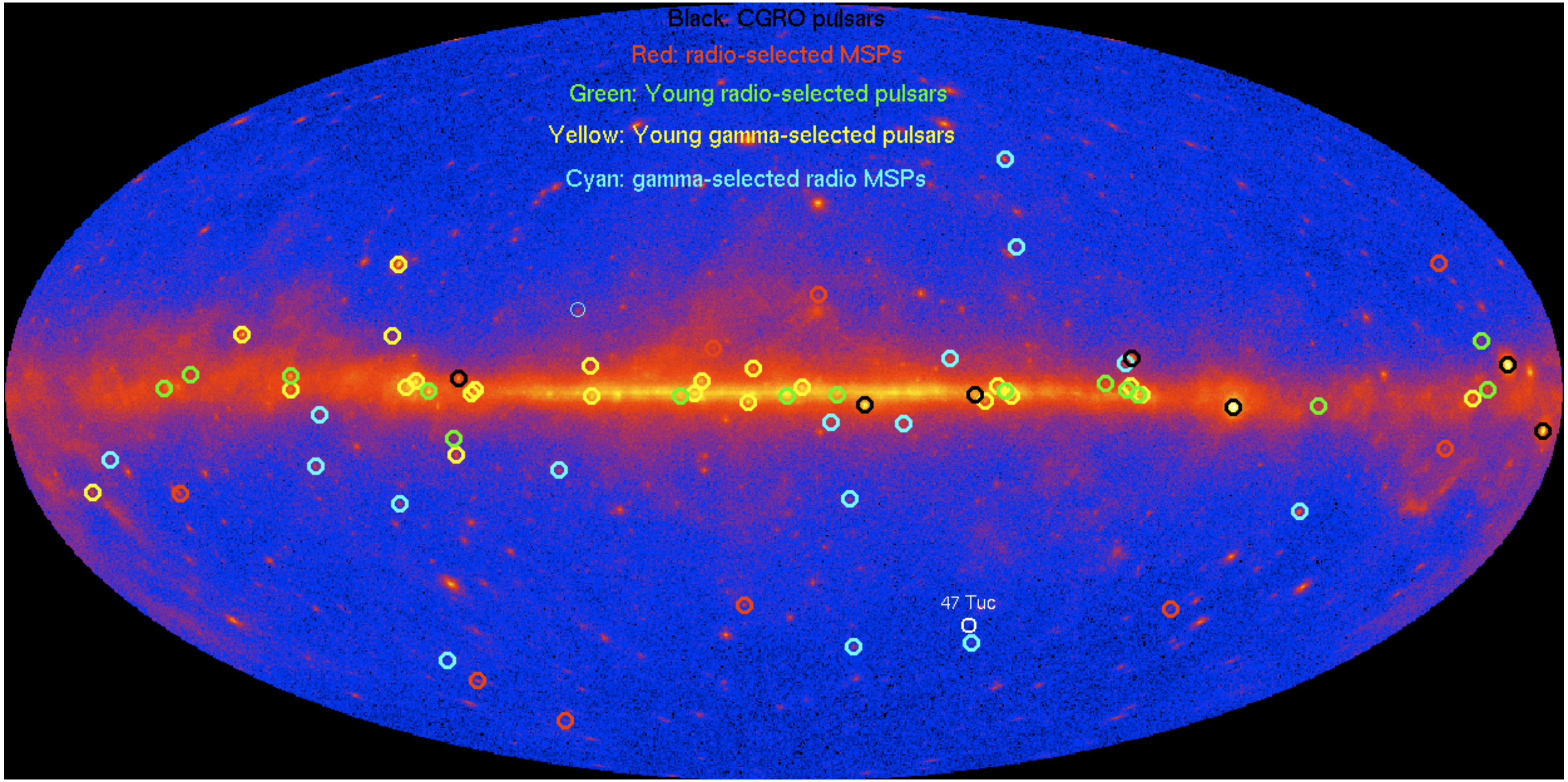

Abdo, A. A. et al. 2010, ApJS, 187, 460

Hays 2010

LAT Pulsars

LAT is producing a more complete sample of young, energetic, nearby pulsars

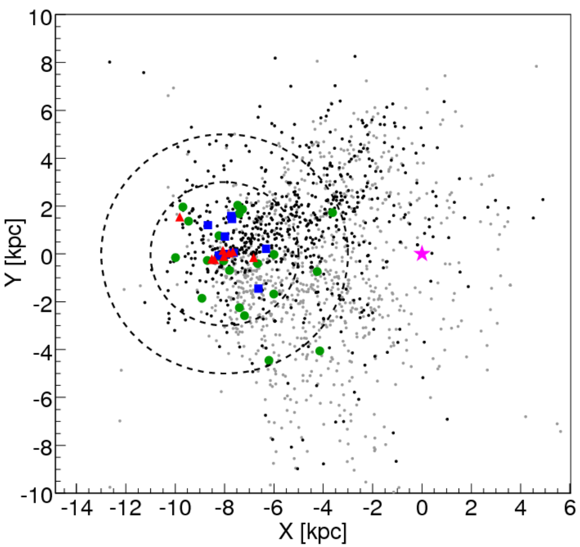

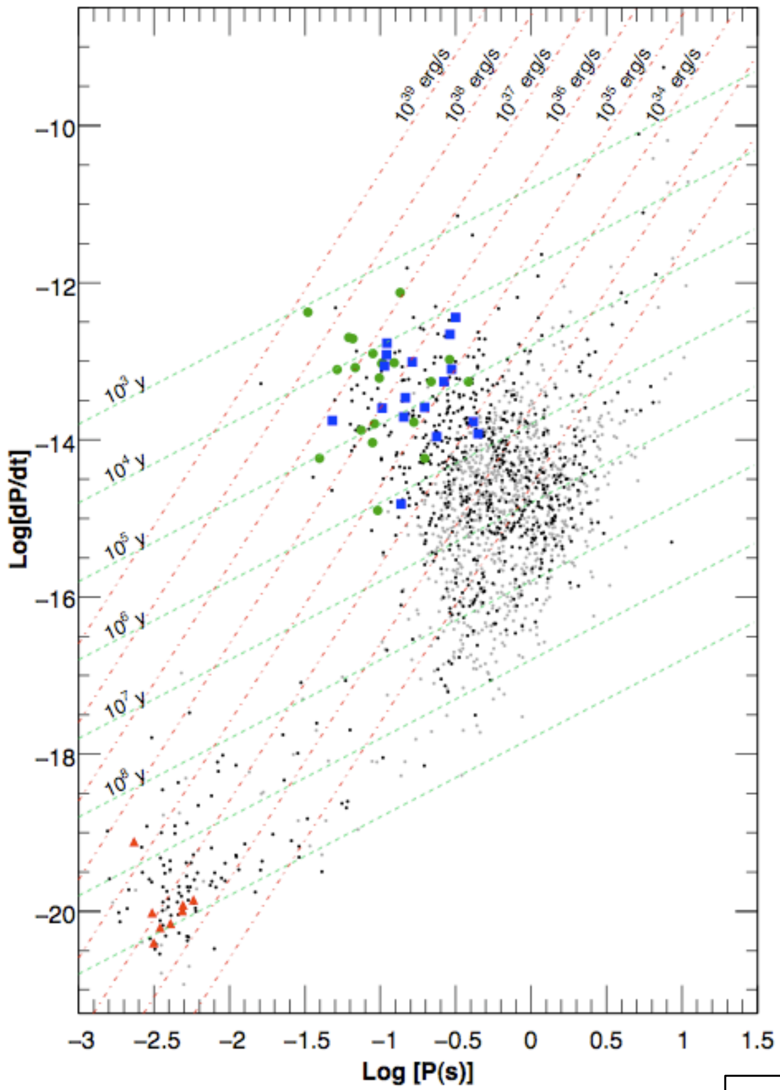

Hays 2010

How pulsars are interesting and/or useful:

Interesting in their own right. But also:

• Unresolved (distant) pulsars contribute to diffuse gamma emission. ~10%, increasing at higher energies.

- ➢ Diffuse model tests [(cosmic rays) ⊗ (dust, gas)] throughout Milky Way.
- ➢ Diffuse model allows deep, uniform (``complete'') population samples.
- ➢ Especially for faint things like, perhaps, Dark Matter signatures.

• On the origin of cosmic rays

- ➢ Pulsar Wind Nebulae (PWN) can be confused with supernova remnants (SNRs), probable proton etc accelerators. Identifying PSRs helps.
- ➢ Towards complete PWN models: pulsar wind and B field as inputs.
- ➢ PWNe dominate TeV sky. But there are UnId'd TeV sources too.
- ➢ Nearby pulsars contribute to the local e+ e- flux,
  - ➢ a foreground to other Dark Matter signatures.

• "Endpoint of stellar evolution" – pulsar census to cross-check massive star tallies & supernova rates.

•To get MSP population right, need to understand the young pulsars. GWs!

Smith 2016


14 August 2009 | $10
Science
Fermi
Detecting Gamma-Ray Pulsars
AAAS

2nd Pulsar Catalog: "2PC", ApJ Suppl. 208 17 (2013)

Smith 2016

Catalog contents online at http://fermi.gsfc.nasa.gov/ssc/data/access/lat/2nd_PSR_catalog/

Described in loving detail in Appendix B.

46 pulsars in *"1PC"* (6 months data),
Abdo et al., ApJS 187 460-494 (2010)

National Aeronautics and Space Administration
Goddard Space Flight Center

Search: Fermi GO

FSSC • HEASARC • Sciences and Exploration

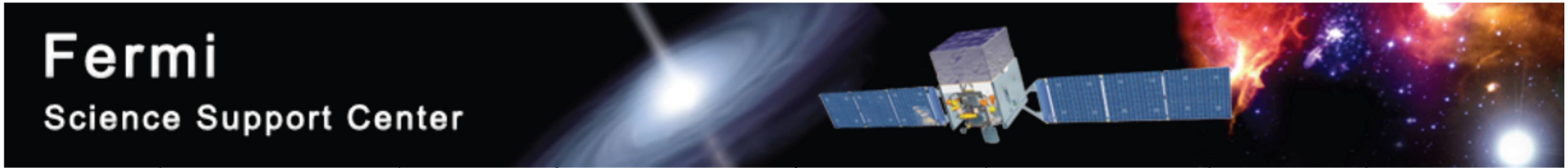

Home | Observations | Data | Proposals | Library | HEASARC | Help | Site Map

Data

- Data Policy
- **Data Access**
  - + LAT Data
  - + LAT Catalog
  - + LAT Data Queries
  - + LAT Query Results
  - + LAT Weekly Files
  - + GBM Data
- Data Analysis
- Caveats
- Newsletters
- FAQ

LAT Second Catalog of Gamma-ray Pulsars

The Fermi Gamma-ray Space Telescope (Fermi) Large Area Telescope (LAT) has discovered dozens of radio-quiet gamma-ray pulsars and dozens of millisecond pulsars (MSPs), establishing pulsars as the dominant GeV gamma-ray source class in the Milky Way. Here they present 117 gamma-ray pulsars unveiled in three years of on-orbit observations. They characterize the known gamma-ray pulsars as uniformly as feasible, and provide additional information from other wavebands where available. For a full explanation about the catalog and its construction see the LAT Second Pulsar Catalog Paper draft on arxiv.

LAT Catalog Data Products

The LAT Second Pulsar Catalog is currently available as a .tgz (tarred and zipped) archive file. The archive includes a main catalog FITS file with the data from the paper tables, images of the light curve and spectral energy distributions (SEDs) for each pulsar, FITS files containing the data points used in those images, and the timing parameters used in the analysis. A full description of the online archive is given in Appendix B of the preprint. Upon final publication, this catalog will also be generated as a BROWSE table that will be linked to this page.

The LAT Second Pulsar Catalog archive of electronic files is linked below. To extract the content of the file, save the file to the target destination on your system. Navigate that directory and use the following command on the command line:

Update of **2PC** Fig 2,

2nd Pulsar Catalog: ApJ Suppl. 208 17 (2013)

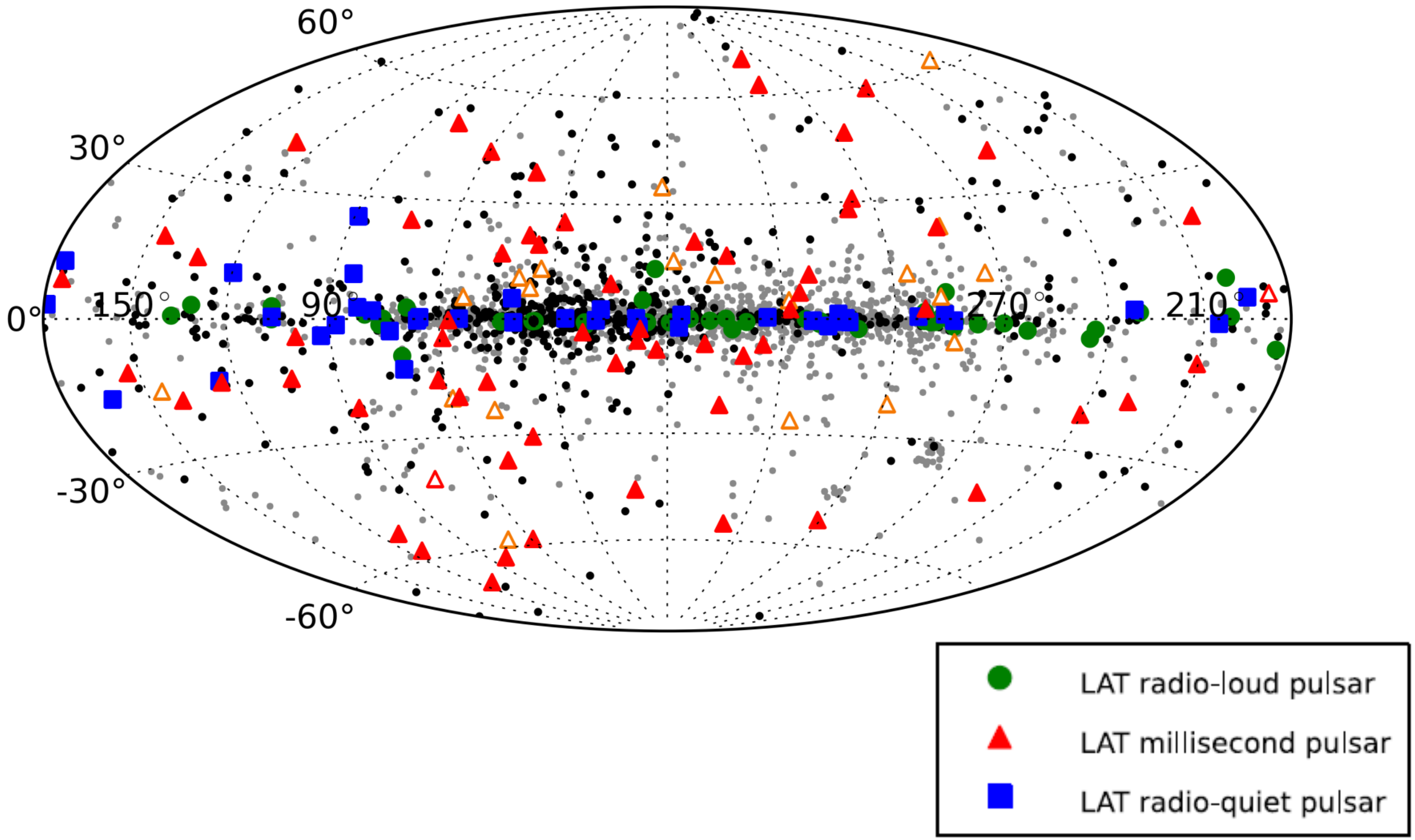

Smith 2016

``Anatomically correct'' Milky Way.
Reid et al, ApJ 700, 137 (2009)

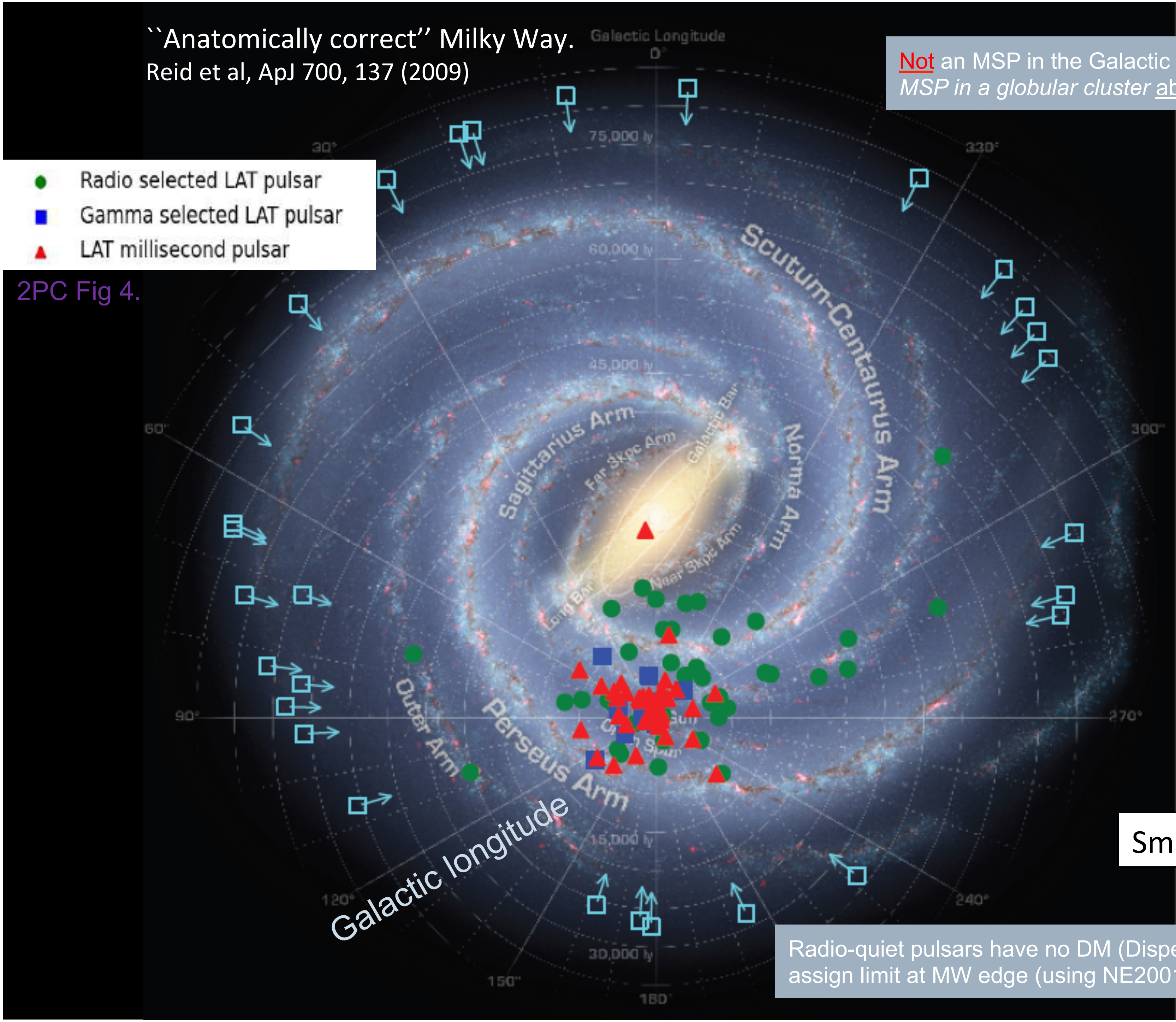

2PC Fig 4.

Not an MSP in the Galactic center.
MSP in a globular cluster above the center.

Smith 2016

Radio-quiet pulsars have no DM (Dispersion Measure): assign limit at MW edge (using NE2001).

Discovery of radio pulsars, 1967

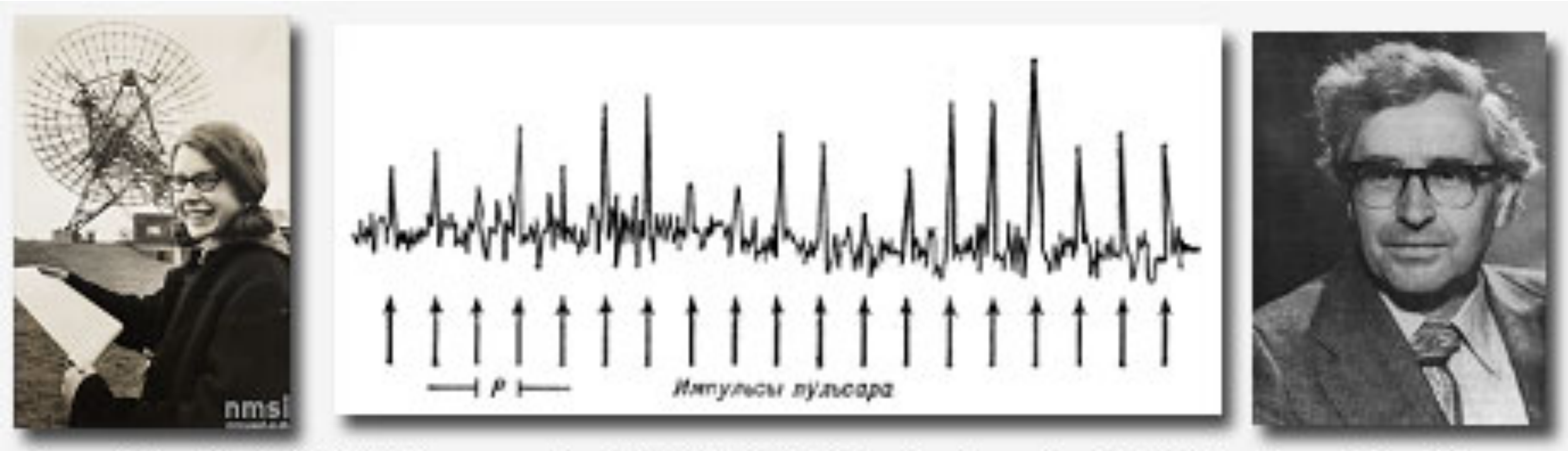

La période 1,33730113 seconde de PSR 1919+21 entre Jocelyn Bell et Anthony Hewish

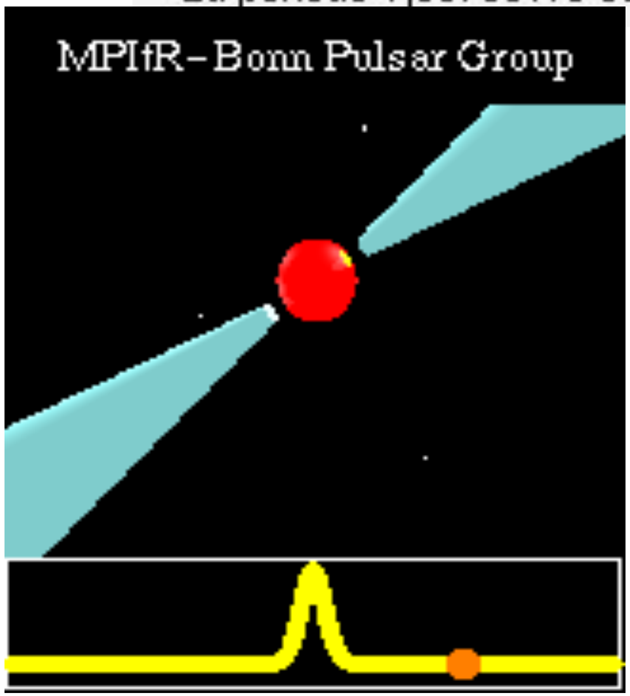

• To study interstellar scintillation & quasars, they used faster electronics.

• A big surprise --they hadn't thought about Baade & Zwicky's 1935 prediction of neutron stars, nor that Pacini (1967) had deduced that the spinning magnet would be like a lighthouse.

Smith 2016

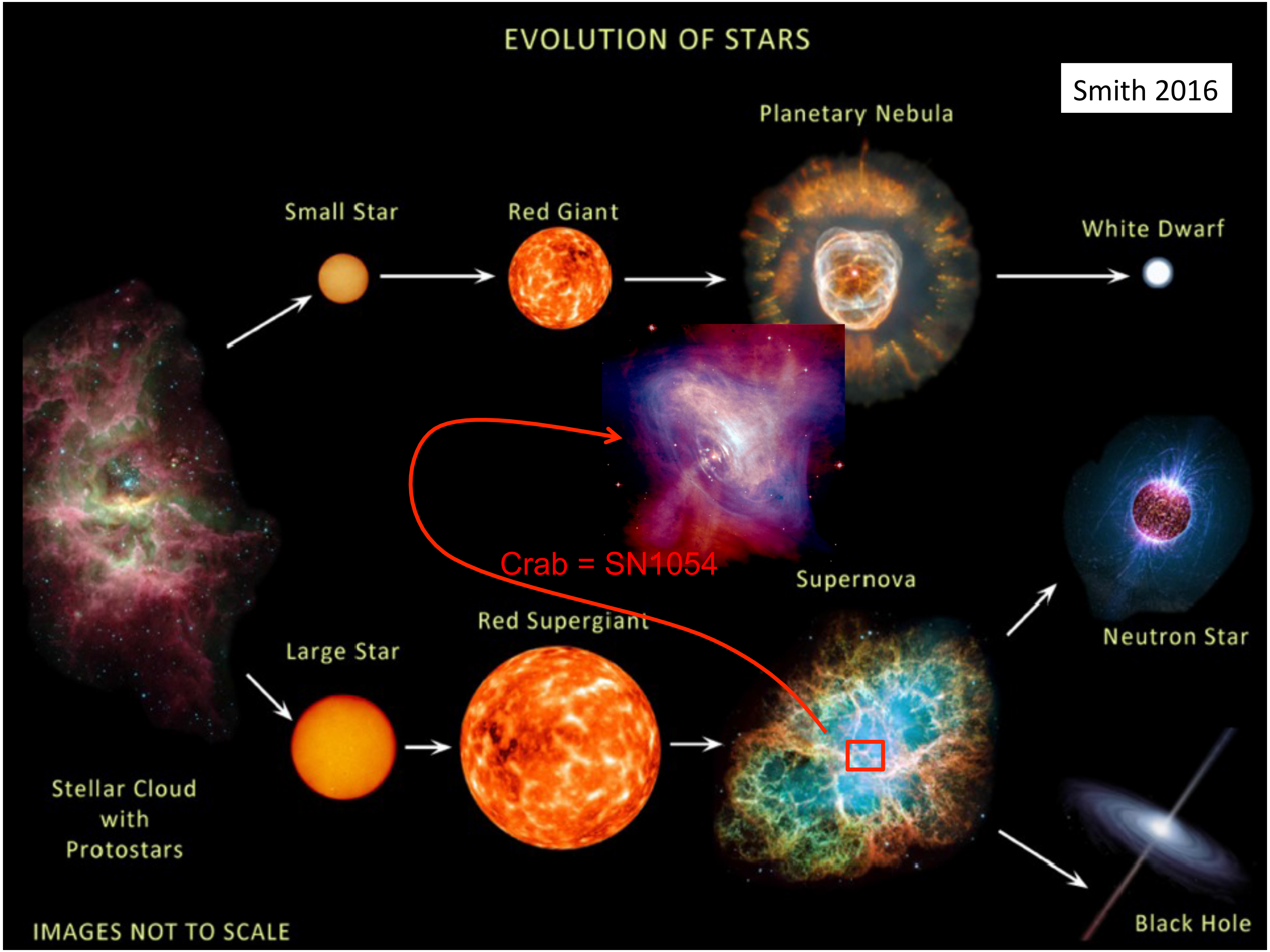
EVOLUTION OF STARS
Smith 2016
Planetary Nebula
Small Star
Red Giant
White Dwarf
Crab = SN1054
Supernova
Red Supergiant
Large Star
Neutron Star
Stellar Cloud
with
Protostars
Black Hole
IMAGES NOT TO SCALE

Rotating magnets make volts.

Ω x B x r

Dipole radiation converts to electron current, wind.

Current radiates radio (and gammas).

Neutron star looses rotational energy at rate

$$\dot{E} = I\dot{\Omega}\Omega$$

"spindown power"

where I ≡ 10^{45} gm-cm²
is the moment of inertia for an n.s. with
R=10 km and 1.4 $M_\odot$.

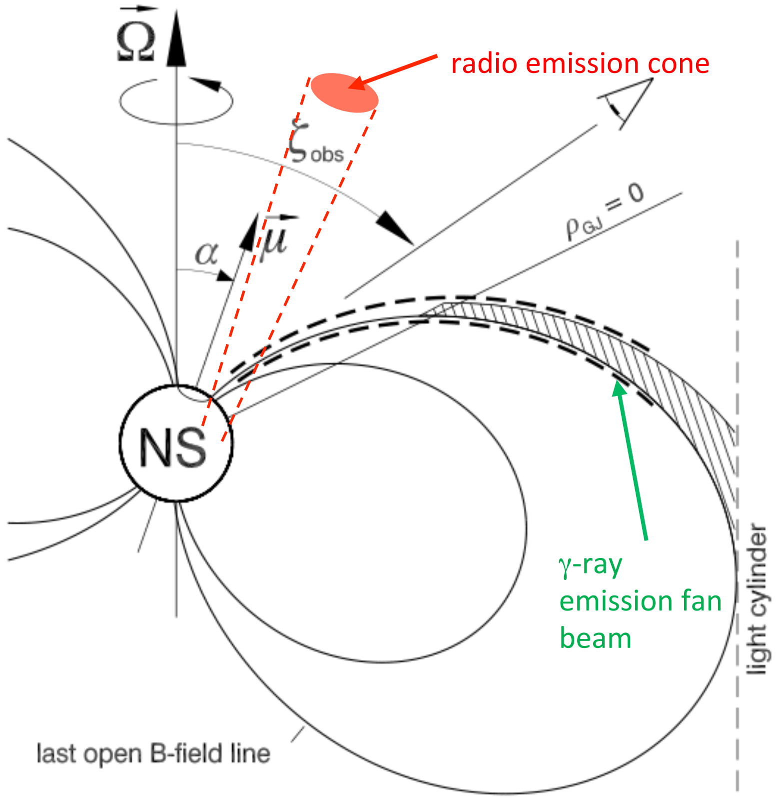

Smith 2016

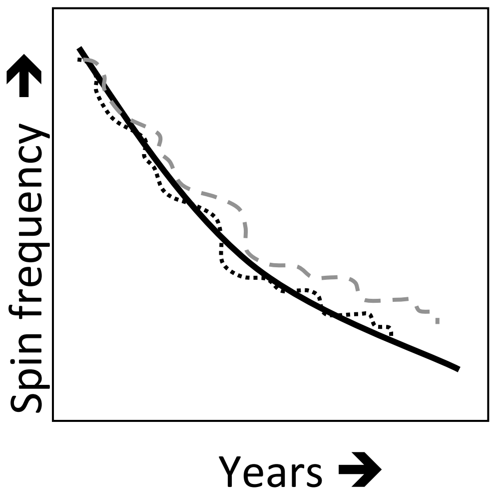

Young pulsars

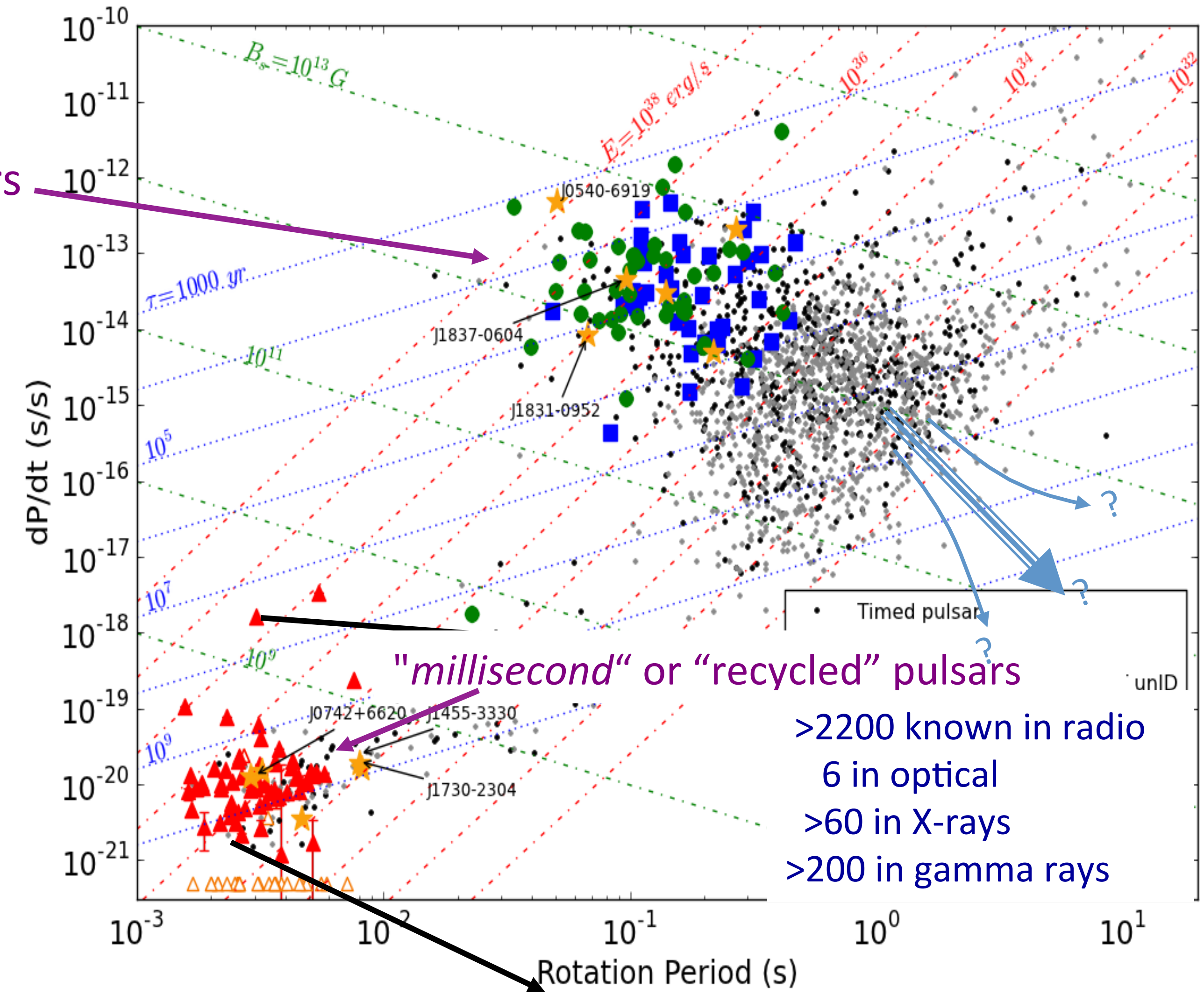

Slow-down Ṗ slows down(Ṗdot) .
Perfect dipole : parabola.

Real life: not parabola. Also "timing noise"
(starquakes? Wind changes?*)*

~1 supernova/century x ~10 Gyr = 10^8 ns's.

Graveyard after mega-years.

Smith 2016

Recycle old neutron stars into millisecond pulsars (=MSPs)

Smith 2016

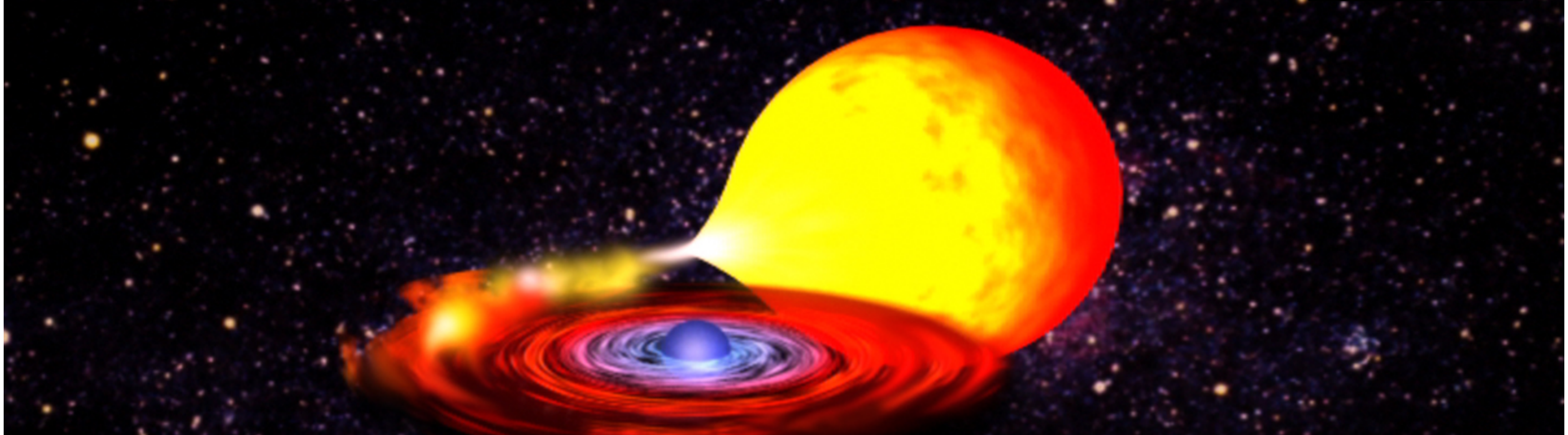

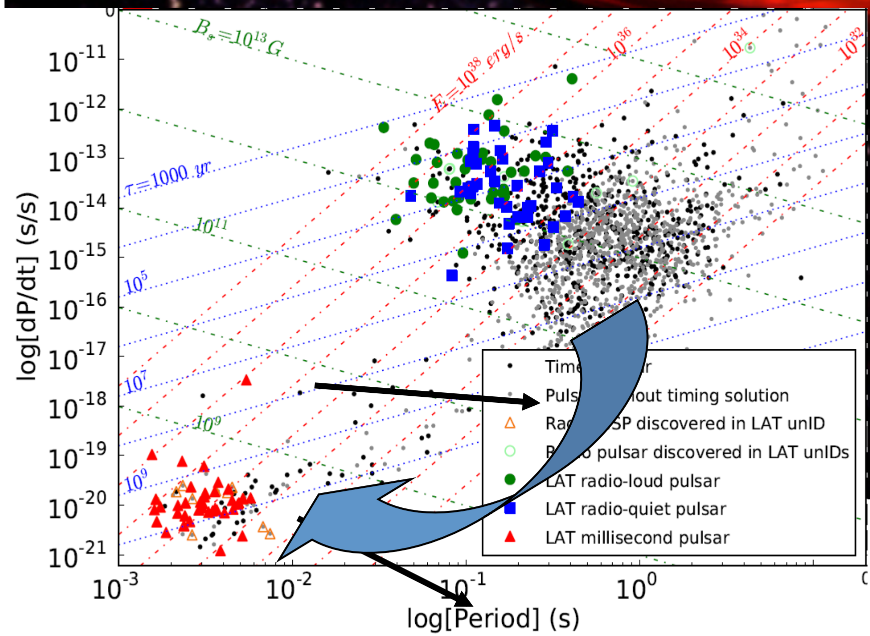

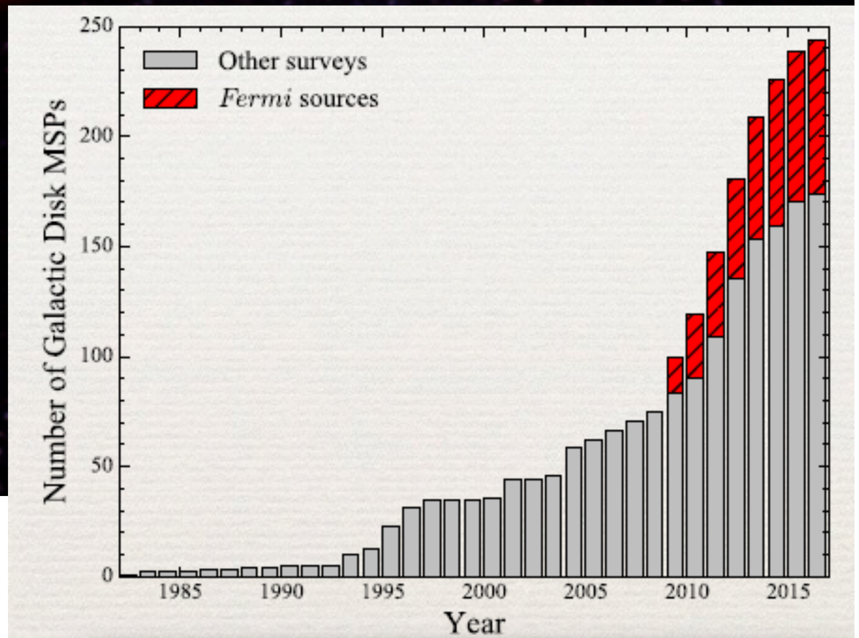

Gamma-ray beam: Curvature radiation in 'gaps'.

Long in latitude, thin in longitude.

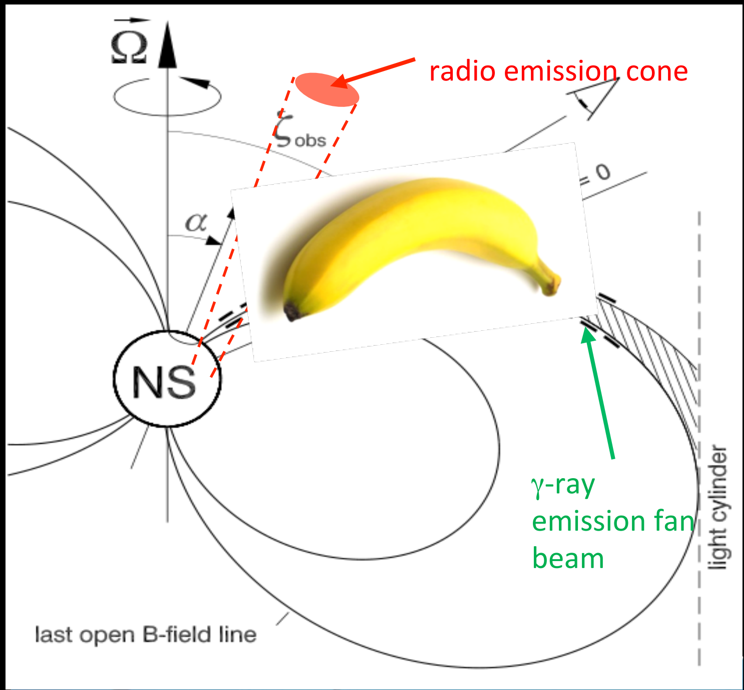

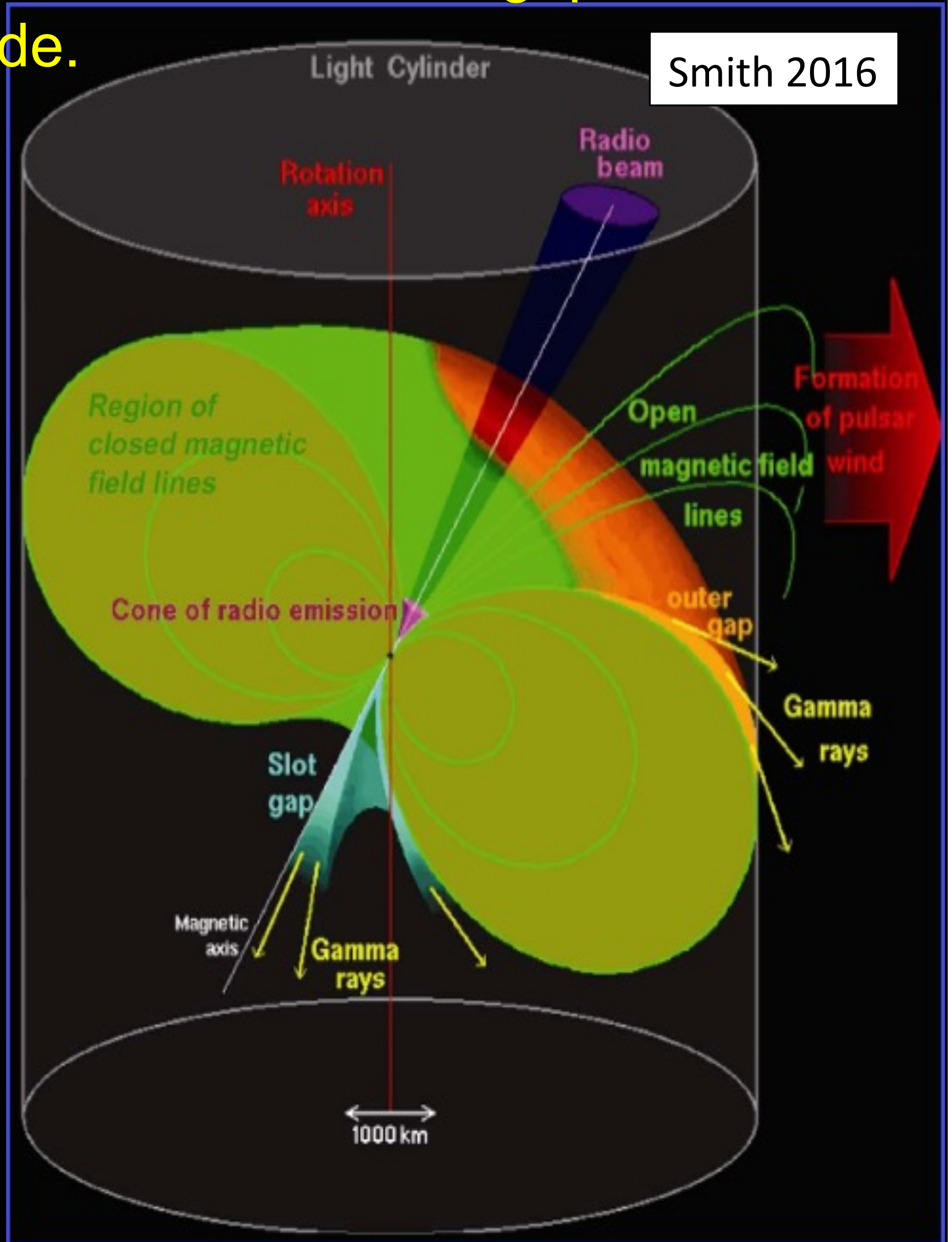

Gamma-ray pulse profiles

Smith 2016

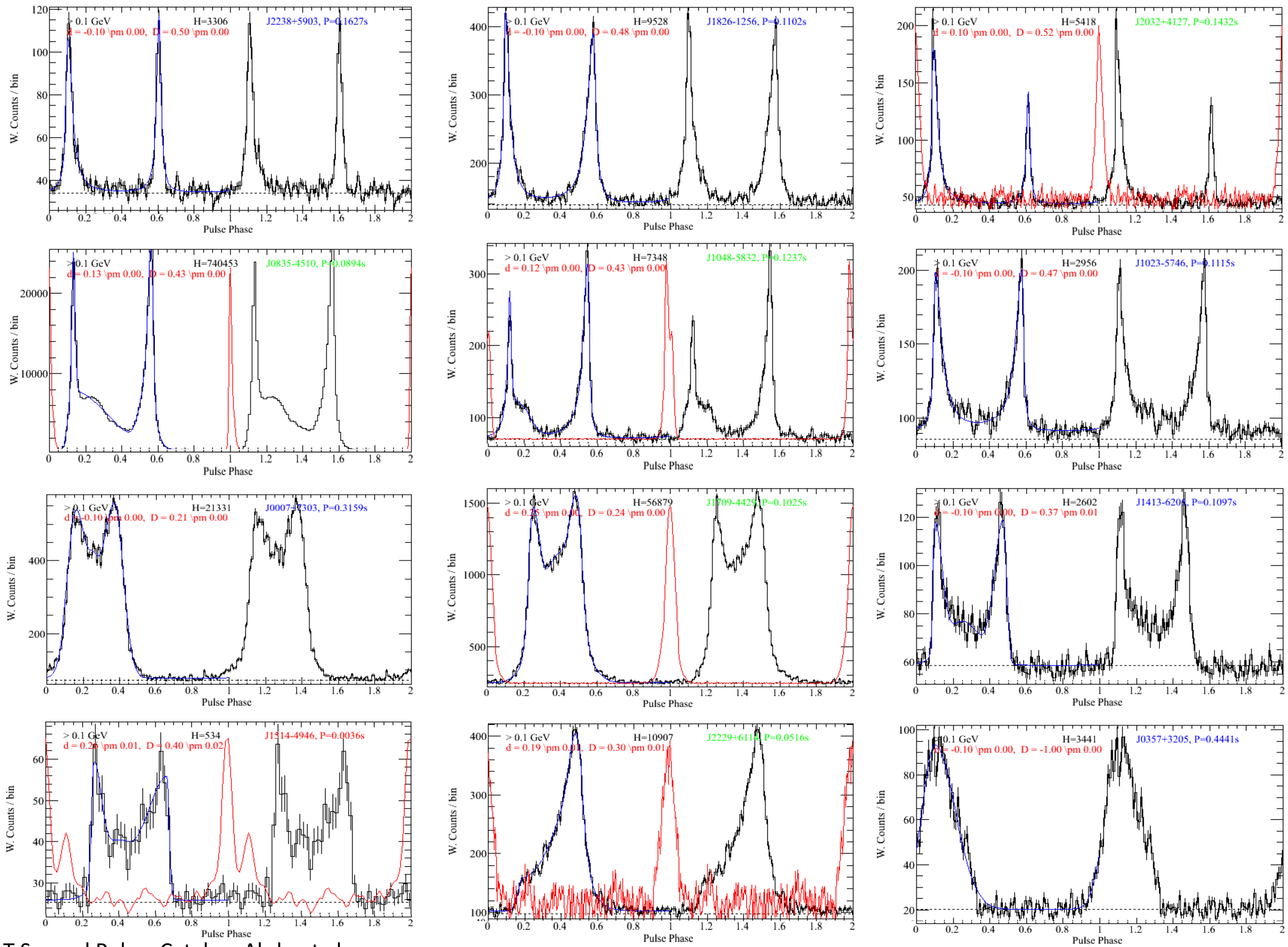

LAT Second Pulsar Catalog, Abdo et al.

Sky distribution of intensity

m dipole

Smith 2016

Profile shapes depend on P, $\dot{E}$, α, β.

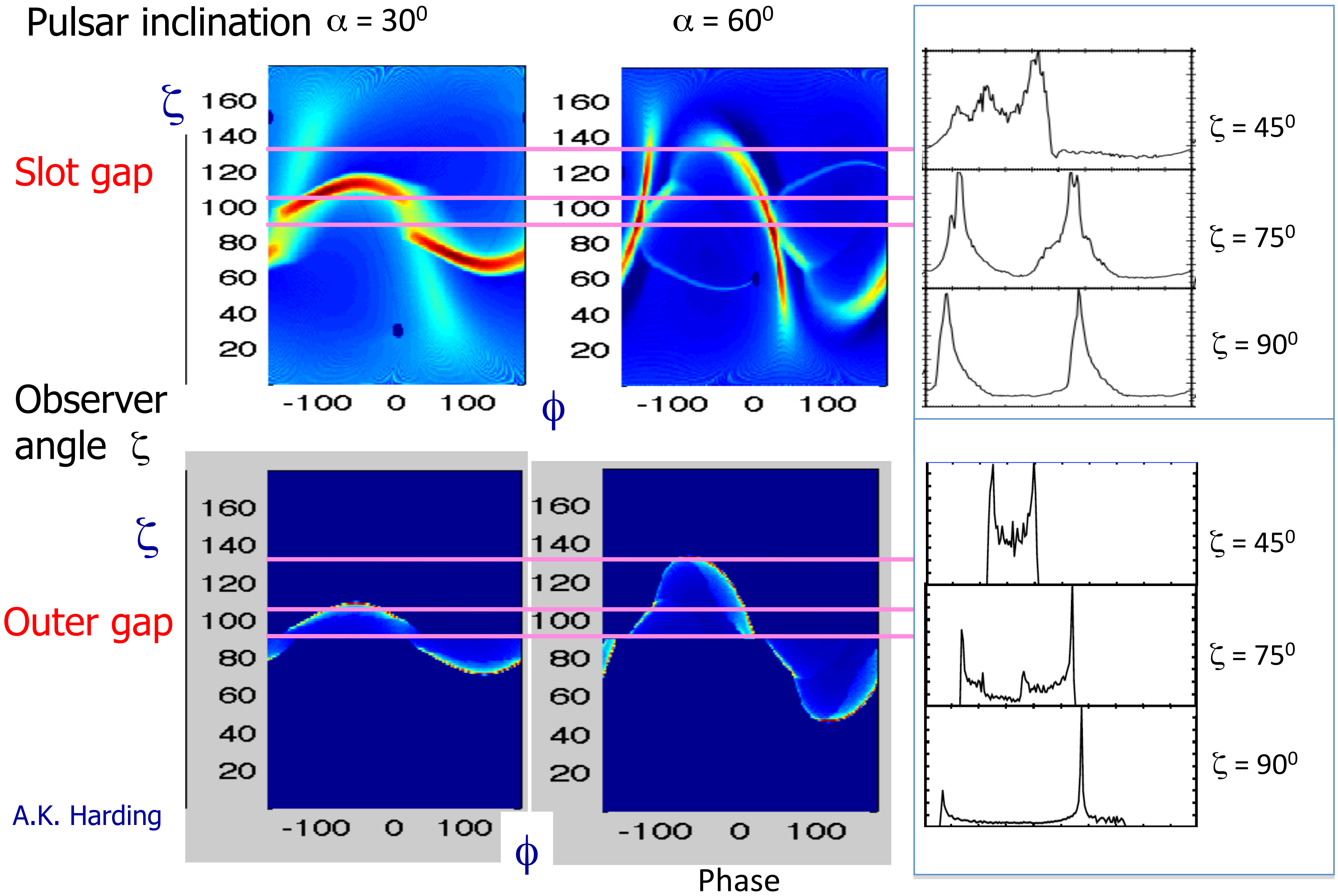

A.K. Harding

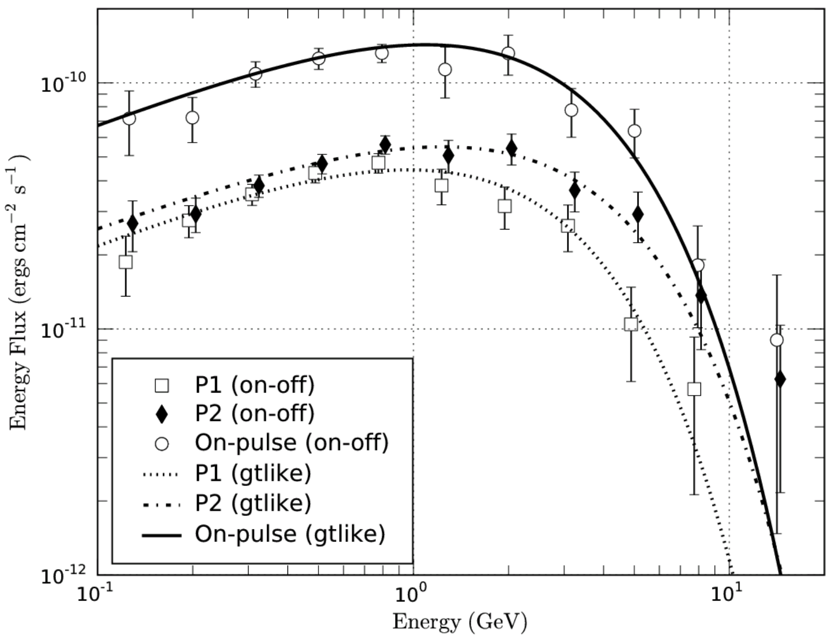

LAT spectra for PSR J2021+3651
Abdo et al. 2009, ApJ, 700, 1059

$$\frac{dN}{dE} = N_0 E^{-\Gamma} \exp\left(-\frac{E}{E_0}\right)^{b} \mathrm{cm}^{-2}\mathrm{s}^{-1}\mathrm{GeV}^{-1}$$

➔ b=1 ➔ high altitude curvature radiation.

(strong magnetic fields near surface "absorb" gammas.)

Spectral '<u>signature</u>' for pulsars.

(Most gamma sources, e.g. blazars, are power laws with little or no curvature.)

Smith 2016

Smith 2016

Most photon power in gammas (for known γ psr's) (i.e. high Edot pulsars) .
“Most of power in the electron wind” (but be careful to stay below Ė) .

Radio is smoke. Gammas is fire.

Power

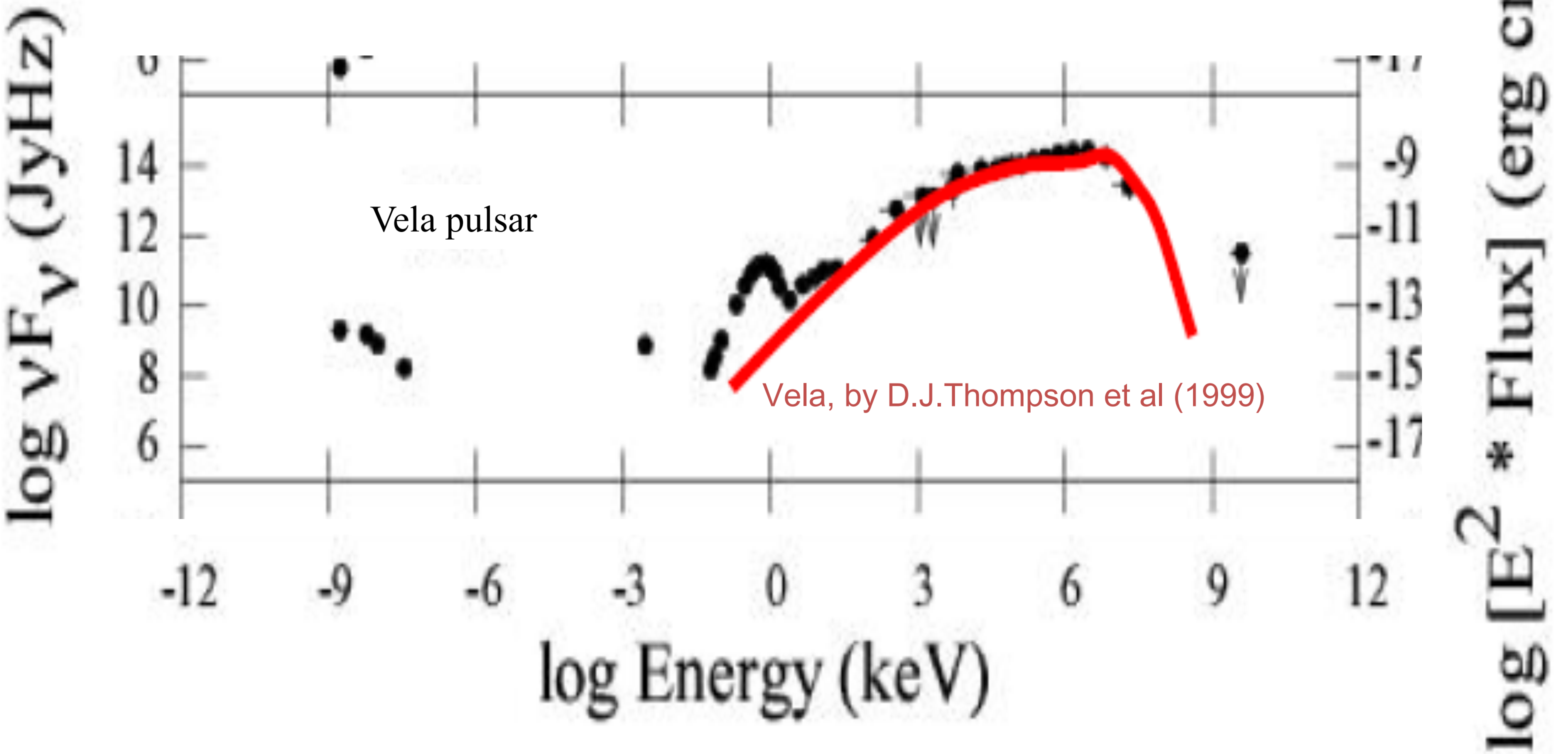

Gamma-ray luminosity versus spindown power

Smith 2016

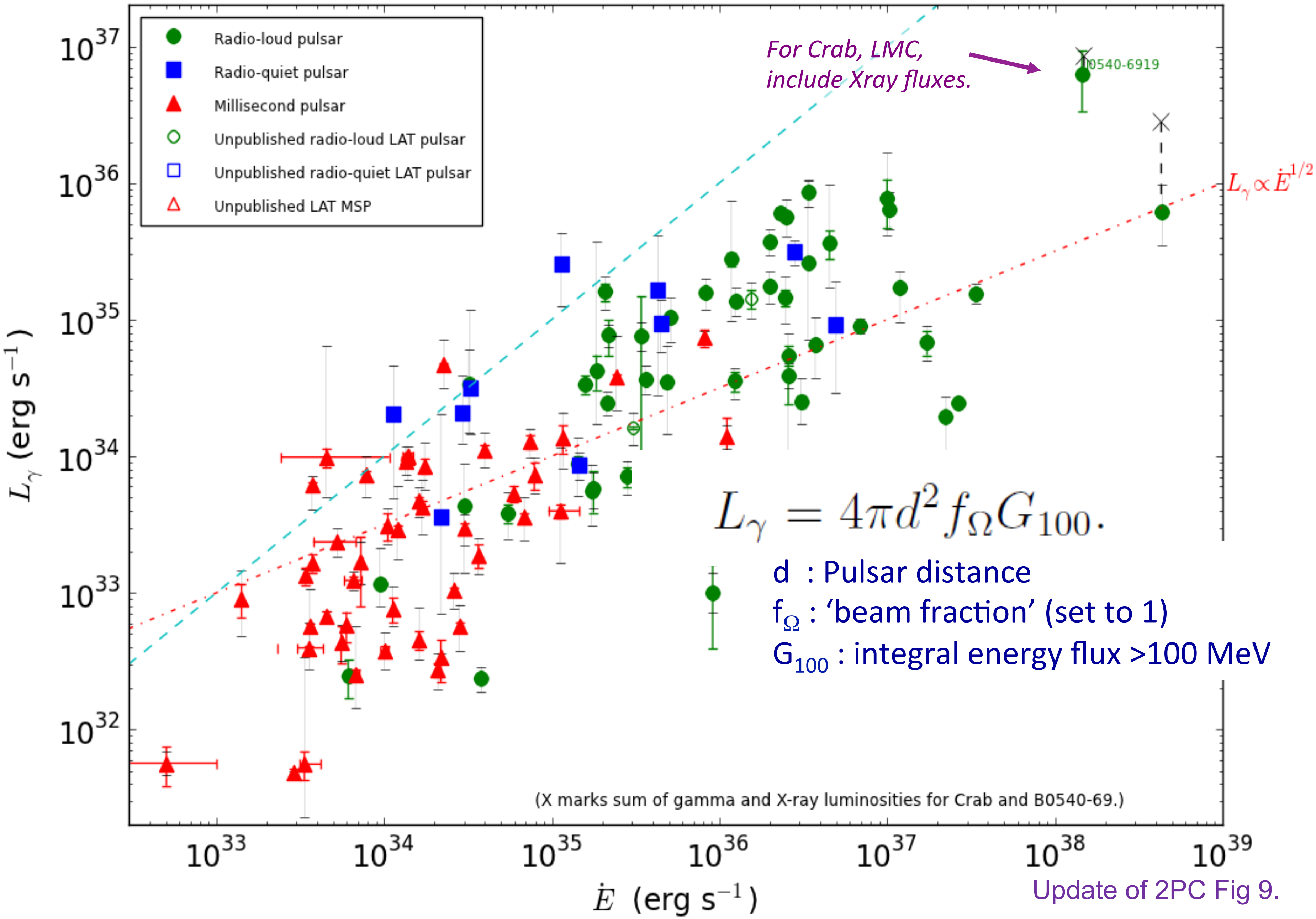

$$L_\gamma = 4\pi d^2 f_\Omega G_{100}.$$

d : Pulsar distance

f_Ω : 'beam fraction' (set to 1)

G_{100} : integral energy flux >100 MeV

Update of 2PC Fig 9.

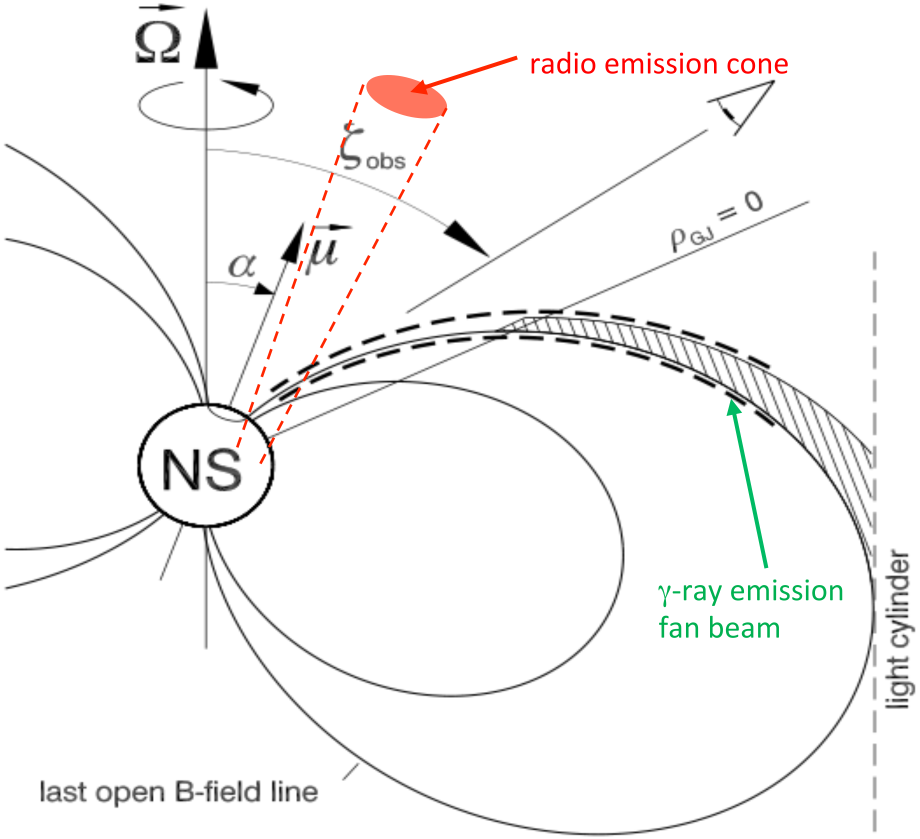

Radio pulsars have a limited range of magnetic (α) and overall (ζ) inclinations: the radio beam must sweep the Earth.

LAT shows, γ-ray beams are mostly *wide*: Many (⅔?) young, **radio-quiet** pulsars.

MSPs have a smaller light-cylinder. The magnetic field lines are cut close in, making broader radio beams.

No radio-quiet MSPs yet. Expect few or none.

Before *Fermi*, 'Geminga' was the only radio-quiet pulsar.

Einstein@Home (Pletsch & Clark in Hannover, and Wu in Bonn): 10 kyrs of CPU!

Smith 2016

Detection of Pulsed Gamma Rays Above 100 GeV from the Crab Pulsar

VERITAS Collaboration: E. Aliu et al Science 334, 69-72 (2011)

Crab – the exception to many rules… Vela pulsar also seen by H.E.S.S.

Smith 2016

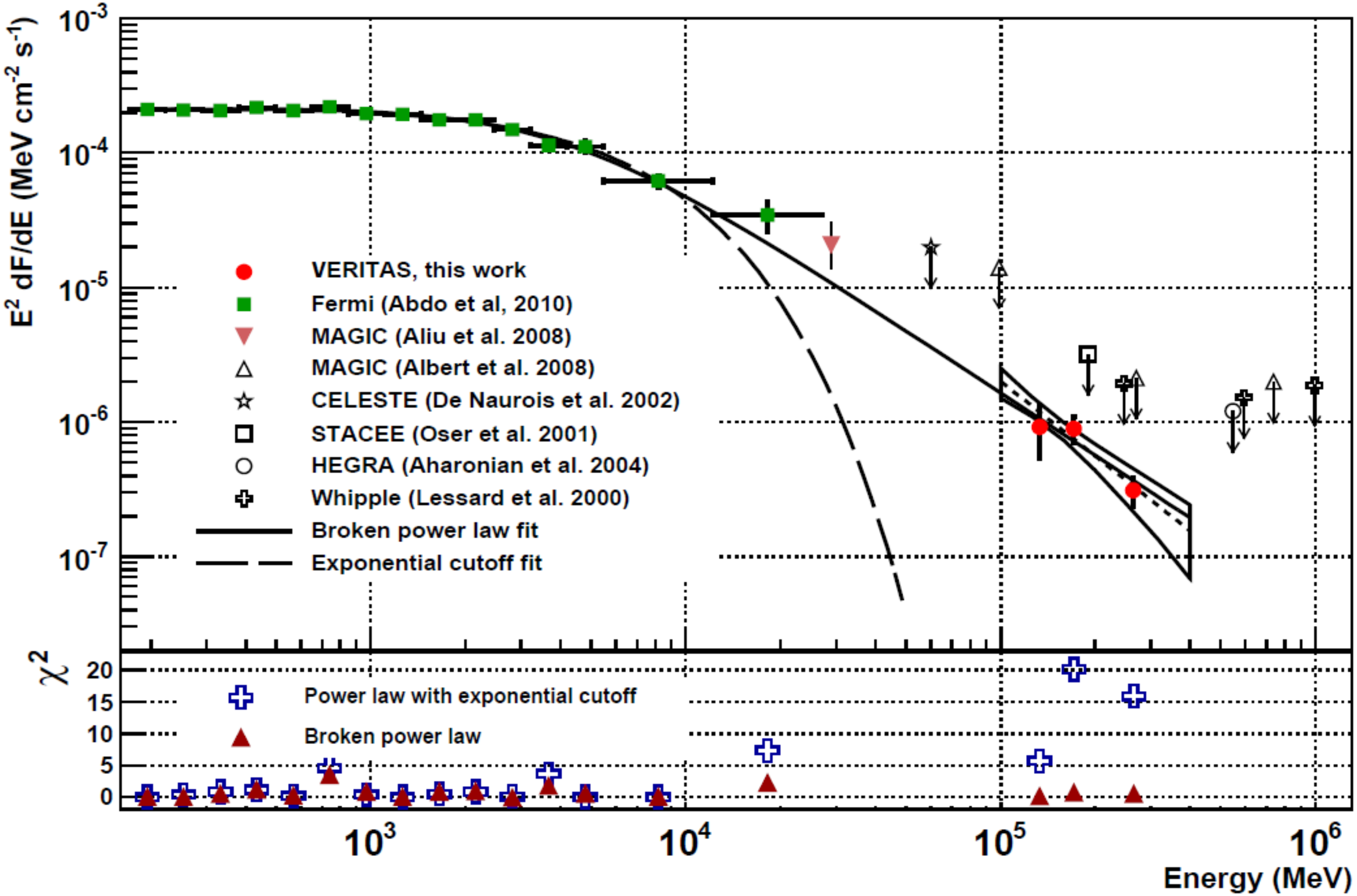

MSPs found in *Fermi* sources are faster than MSPs from radio surveys.

Most *Fermi* MSPs are 'spiders'.
Only 3 before *Fermi*, ~misunderstood.

Spiders:
pulsar wind 'eats' companion star.

Black Widows: $M_2 \leq 0.1 M_{\odot}$
Redbacks : $0.1 \leq M_2 \leq 0.4 M_{\odot}$

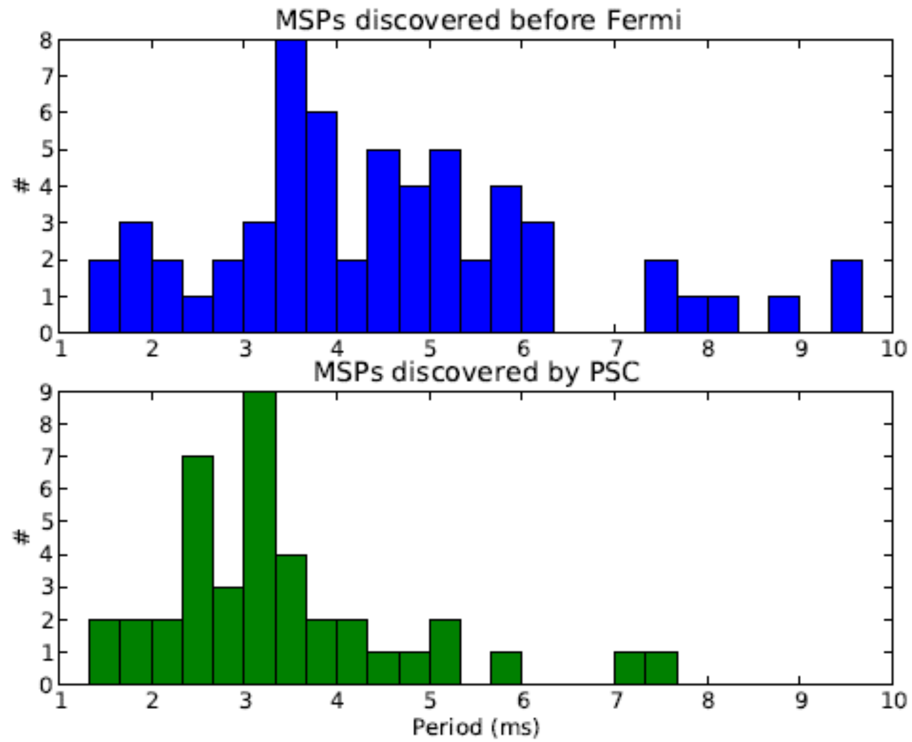

Ray et al. 2012, arXiv:1205.3089

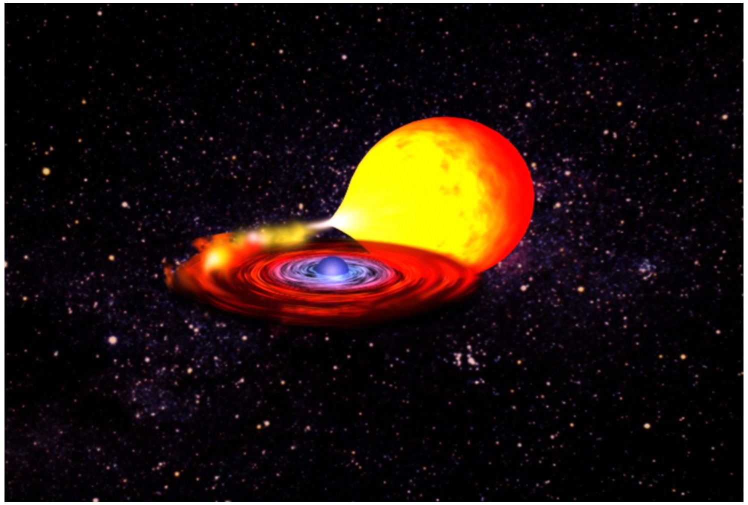

Key observations to better understand MSP creation in particular and binary evolution in general.

Binaries give GRBs, FRBs, and GWs ➔ important!*

* Nature 530, 453 (25 February 2016)
Nature 531, 202 (10 March 2016)

Smith 2016

Update of 2PC Fig 2.

Smith 2016

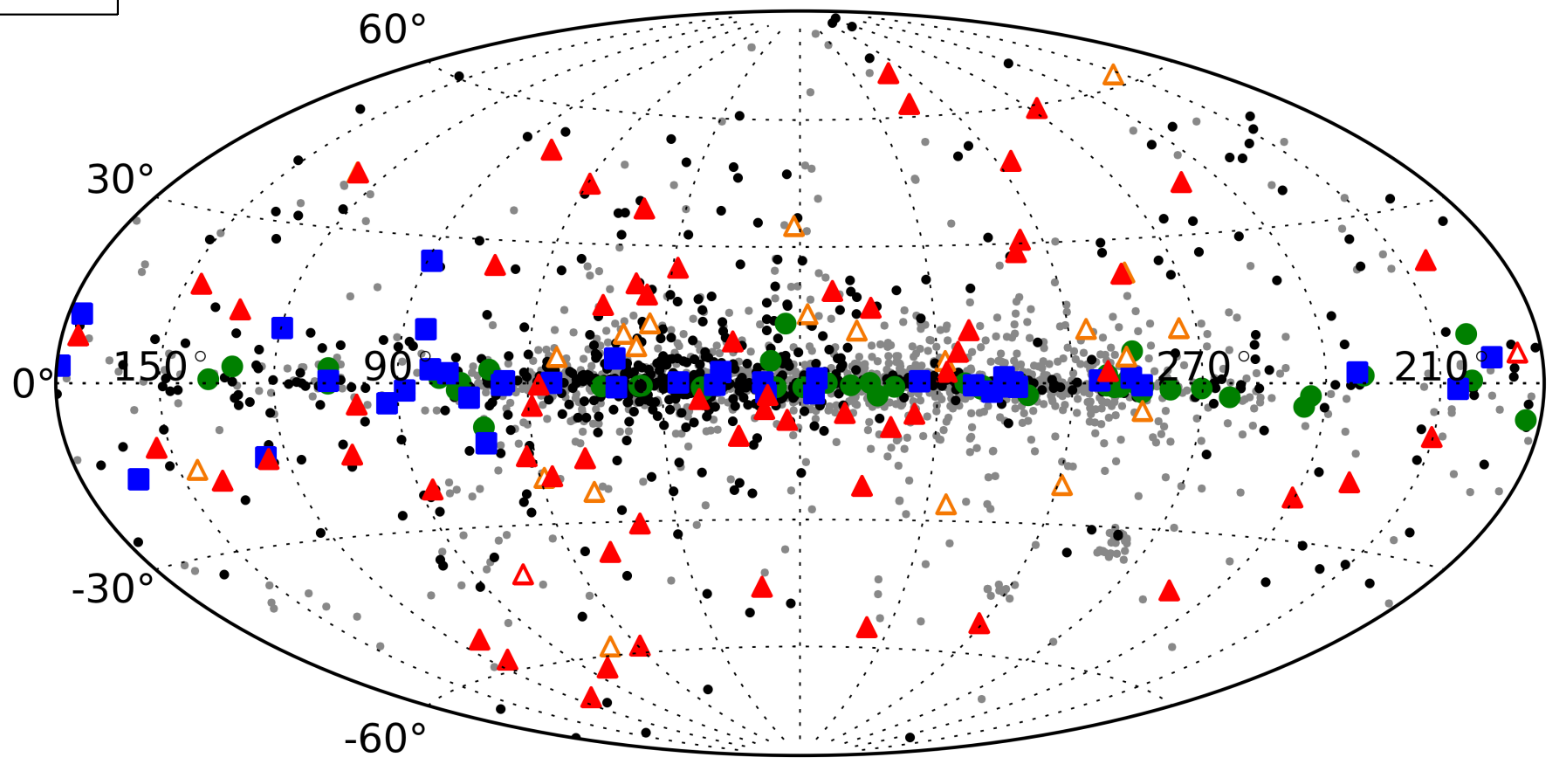

- The MSPs are faint:
  low $\dot{E}$ → low L_γ → nearby → big latitude spread. *(larger scale height, too.)*

- The *Fermi* "treasure map" allows deeper, repeated (scintillation! eclipsing!) radio searches than radio surveys.
- Some new radio MSPs 'good timers' suitable for gravity wave searches.

Smith 2016

Detected pulsars versus time

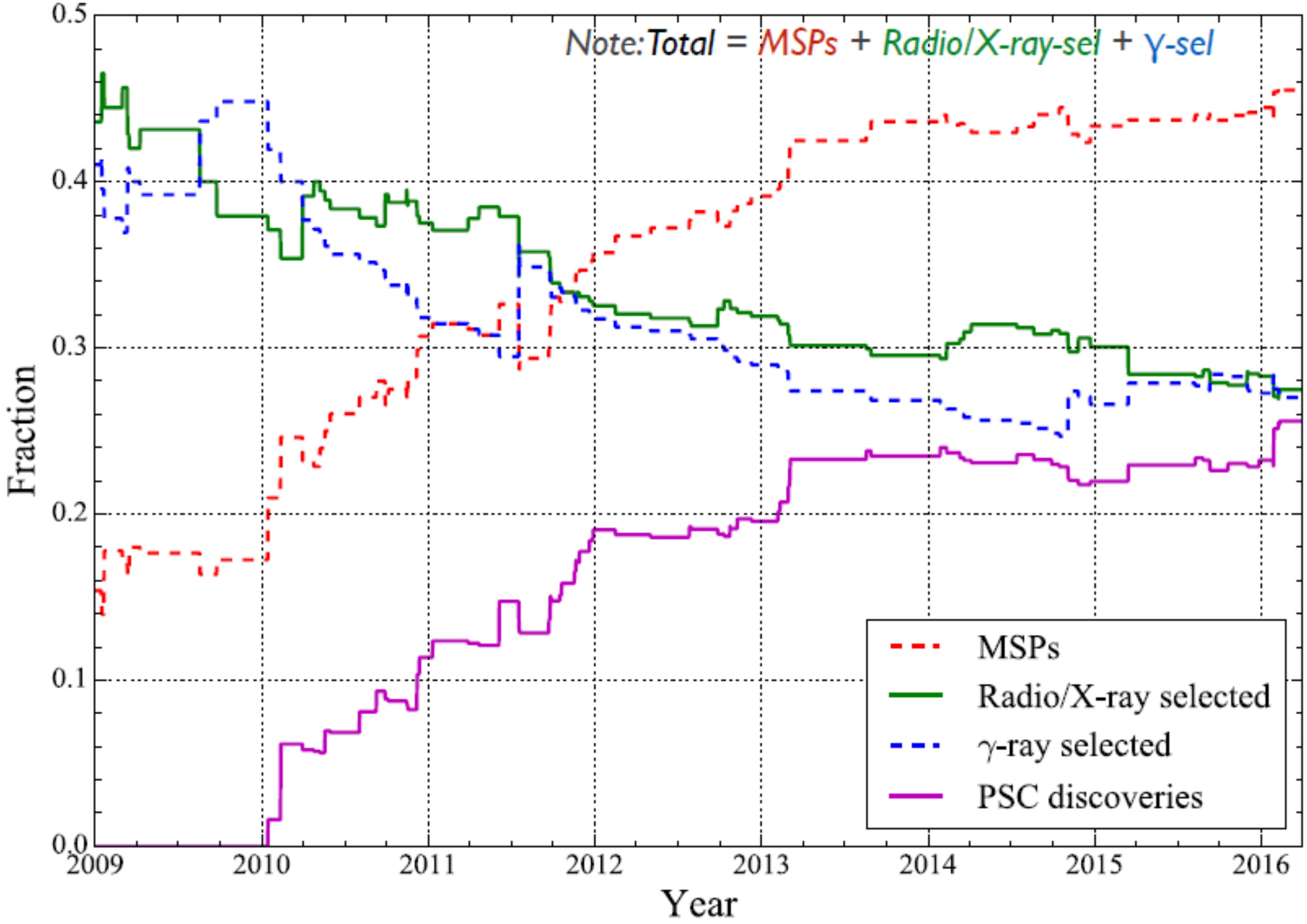

Lucas Guillemot, 2016

Some folks think the LAT excess is particle Dark Matter (e.g. neutralinos).

Smith 2016

PHYSICAL REVIEW D **88**, 083009 (2013)

Millisecond pulsars cannot account for the inner Galaxy's GeV excess

Dan Hooper,[1,2] Ilias Cholis,[1] Tim Linden,[3] Jennifer M. Siegal-Gaskins,[4] and Tracy R. Slatyer[5]

[1]*Center for Particle Astrophysics, Fermi National Accelerator Laboratory, Batavia, Illinois 60510, USA*

[2]*Department of Astronomy and Astrophysics, University of Chicago, 5640 S Ellis Avenue, Chicago, Illinois 60637, USA*

[3]*Department of Physics, University of California, Santa Cruz, 1156 High Street, Santa Cruz, California 95064, USA*

[4]*California Institute of Technology, 1200 East California Boulevard, Pasadena, California 91125, USA*

[5]*School of Natural Sciences, Institute for Advanced Study, Princeton, New Jersey 08540, USA*

(Received 7 June 2013; published 18 October 2013)

Using data from the Fermi Gamma-Ray Space Telescope, a spatially extended component of gamma rays has been identified from the direction of the Galactic center, peaking at energies of ~2–3 GeV. More recently, it has been shown that this signal is not confined to the innermost hundreds of parsecs of the Galaxy, but instead extends to at least ~3 kpc from the Galactic center. While the spectrum, intensity, and angular distribution of this signal is in good agreement with predictions from annihilating dark matter, it has also been suggested that a population of unresolved millisecond pulsars could be responsible for this excess GeV emission from the inner Galaxy. In this paper, we consider this later possibility in detail.

But

a) large uncertainties on diffuse gamma spectrum of central galaxy,

Fermi-LAT Observations of High-Energy Gamma-Ray Emission Toward the Galactic Center

Ajello, M. et al. 2016, ApJ, 819, 44

and

b) Surely more unresolved gamma PSRs and MSPs than once thought.

Young pulsars bright but short-lived. MSPs dim but last ~forever.

Determining pulsar luminosities and the pulsar population requires finding as broad a variety of gamma-ray pulsars as possible.

Probing the dark corners of parameter space…

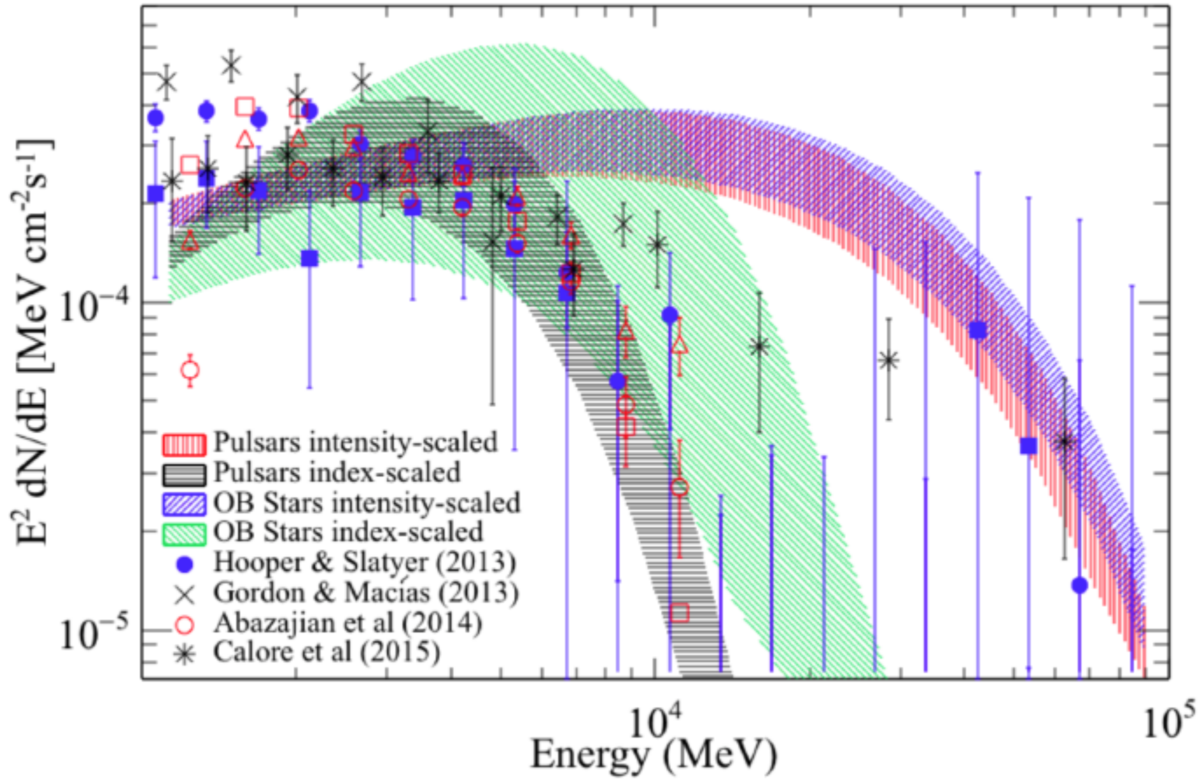

Fermi-LAT Observations of High-Energy Gamma-Ray Emission Toward the Galactic Center

Ajello, M. et al. 2016, ApJ, 819, 44

See also *Fermi*-LAT Dark Matter "white paper", submitted to Phys. Reports (E. Charles *et al.*)

Smith 2016

Transitional Millisecond Pulsars

Smith 2016

Gamma-ray Transition of PSR J1023+0038

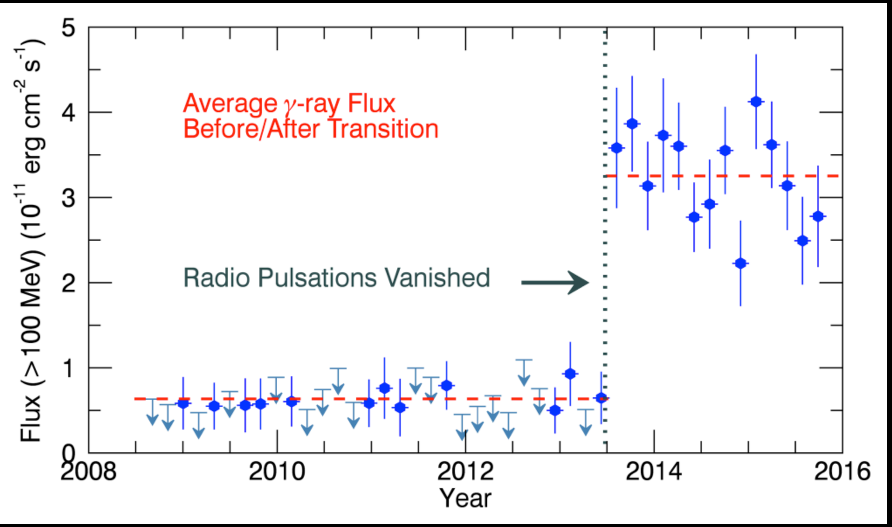

X-ray and U Band Light Curves of 3FGL J1544.6-1125

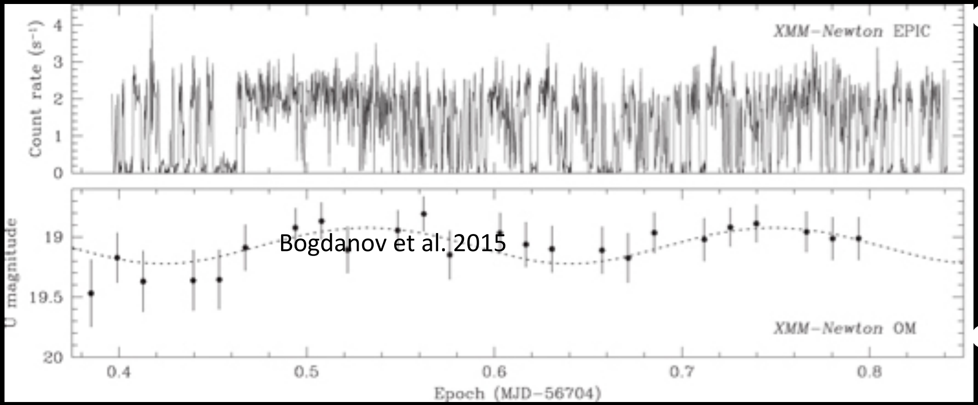

- 40% of MSPs discovered in searches of LAT sources are interacting binaries (`black widows' and `redbacks')
- Prior to *Fermi* only 1 redback and ~6 black widows were known outside of globular clusters (now ~12 and 24)
- More expected - LAT already detected two transitions between accreting and radio MSP states
- γ-ray emission brighter in the accreting state – a mystery since accreting sources are *not* typical γ-ray emitters. What is the mechanism?
- Optical searches of LAT sources have revealed new candidates

A new area of study for *Fermi*

25-Year Period Pulsar Binary

Smith 2016

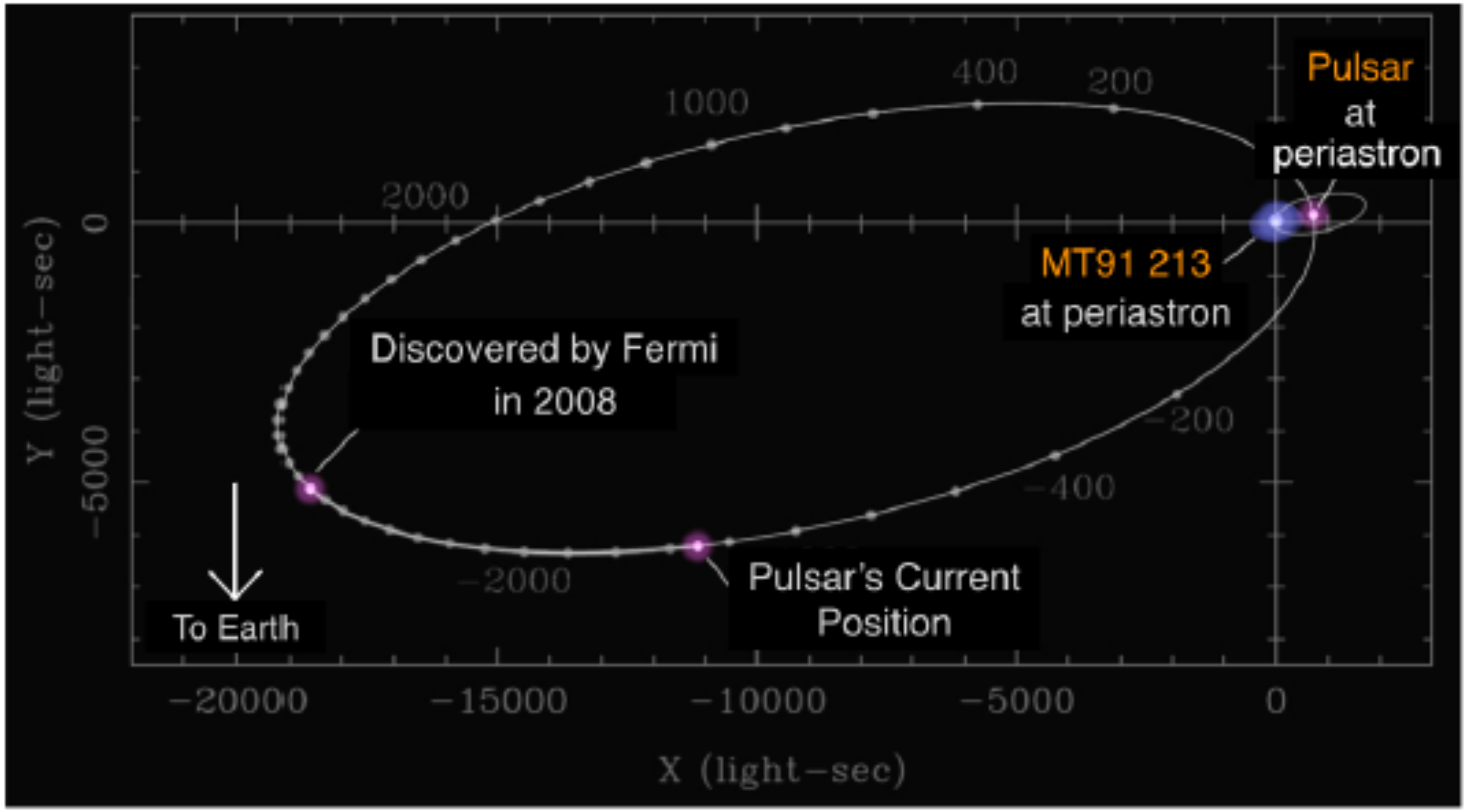

Figure 6: In 2018 *Fermi* will provide critical observations of the periastron passage of the 25-year binary system MT91 213/PSR J2032+4127 [31].

[31] Lyne, A. G. et al. *MNRAS* 451, 581, 2015

Smith 2016

LAT Pulsars

- Pulsars are the end-point of stellar evolution. Gamma-rays key to understand how they convert rotational energy into radiation.
- *Fermi* LAT sees a broad variety of high-power pulsars in a variety of environments.
- The pulsars play a central role in a range of topics.
- We continue to detect about 30 per year.

Two excellent recent reviews:

Gamma-Ray Pulsar Revolution, P. Caraveo, Annual Review of Astronomy and Astrophysics 52, 2014.
Gamma-ray pulsars: A gold mine, I. Grenier & A.K. Harding, Compte rendus Physique 16, 2015

Pulsars in LMC

Spectral model allowed weighted gamma folding of LMC's two Ė>1E38 erg/s pulsars.

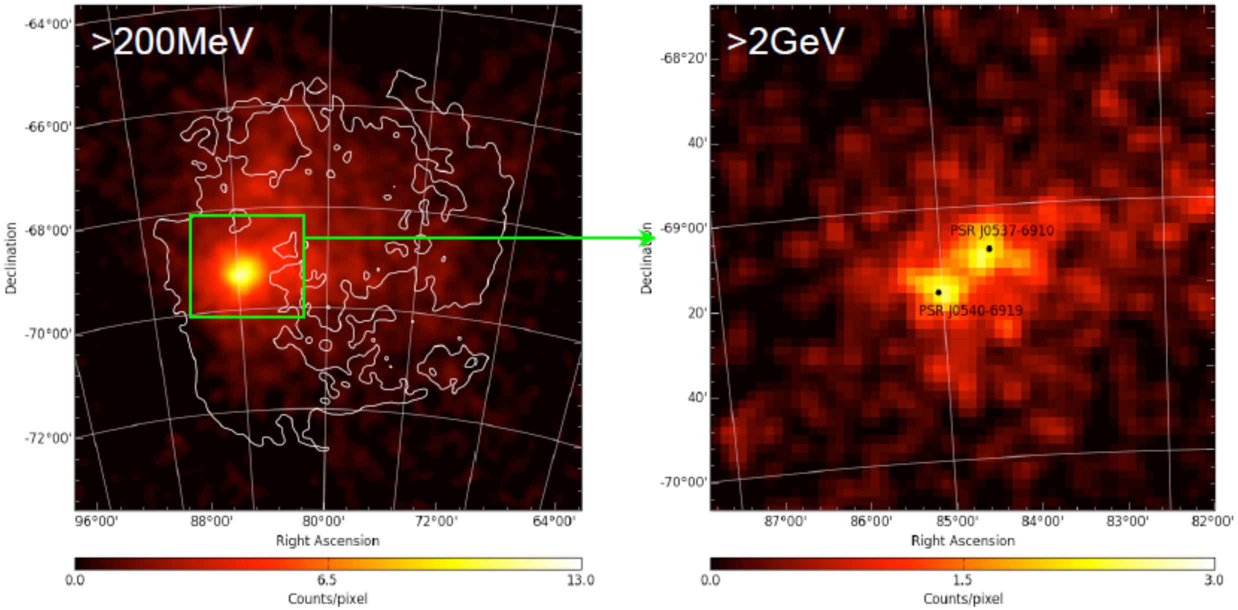

Weekly Analysis Meeting - 22 May 2015

The brightest gamma-ray pulsar seen in the LMC

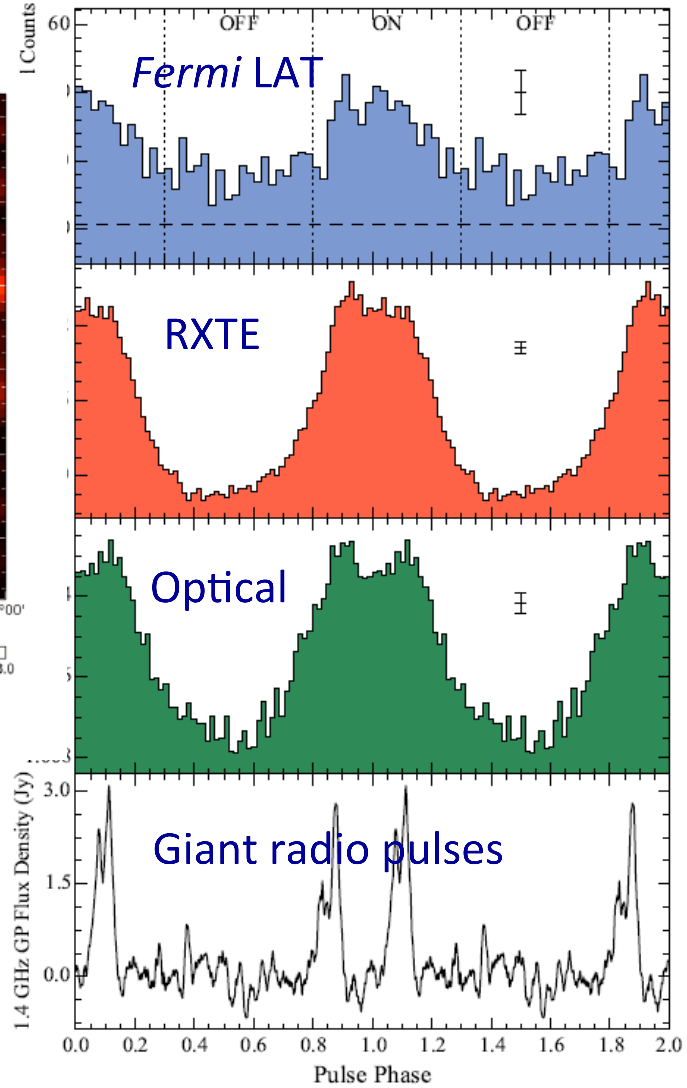

Smith 2016

High voltage from $\Omega \times B \times r$:
extracts electrons from crust.
e^+ from e^- scattering off B or photons.

Electrons stream along field lines.
Cone-like radio beam from polar cap.
(Return current heats cap ➔ X-rays)
Plasma filled « magnetosphere ».

Electron wind escapes from *open* lines.

Feeds nebula and cosmic rays.

Two principal acceleration zones:

- (Near the polar cap)
- Far, near the 'light cylinder', for a broad, thin 'fan-like' gamma beam.

Observed profile depends partly on overall inclination.

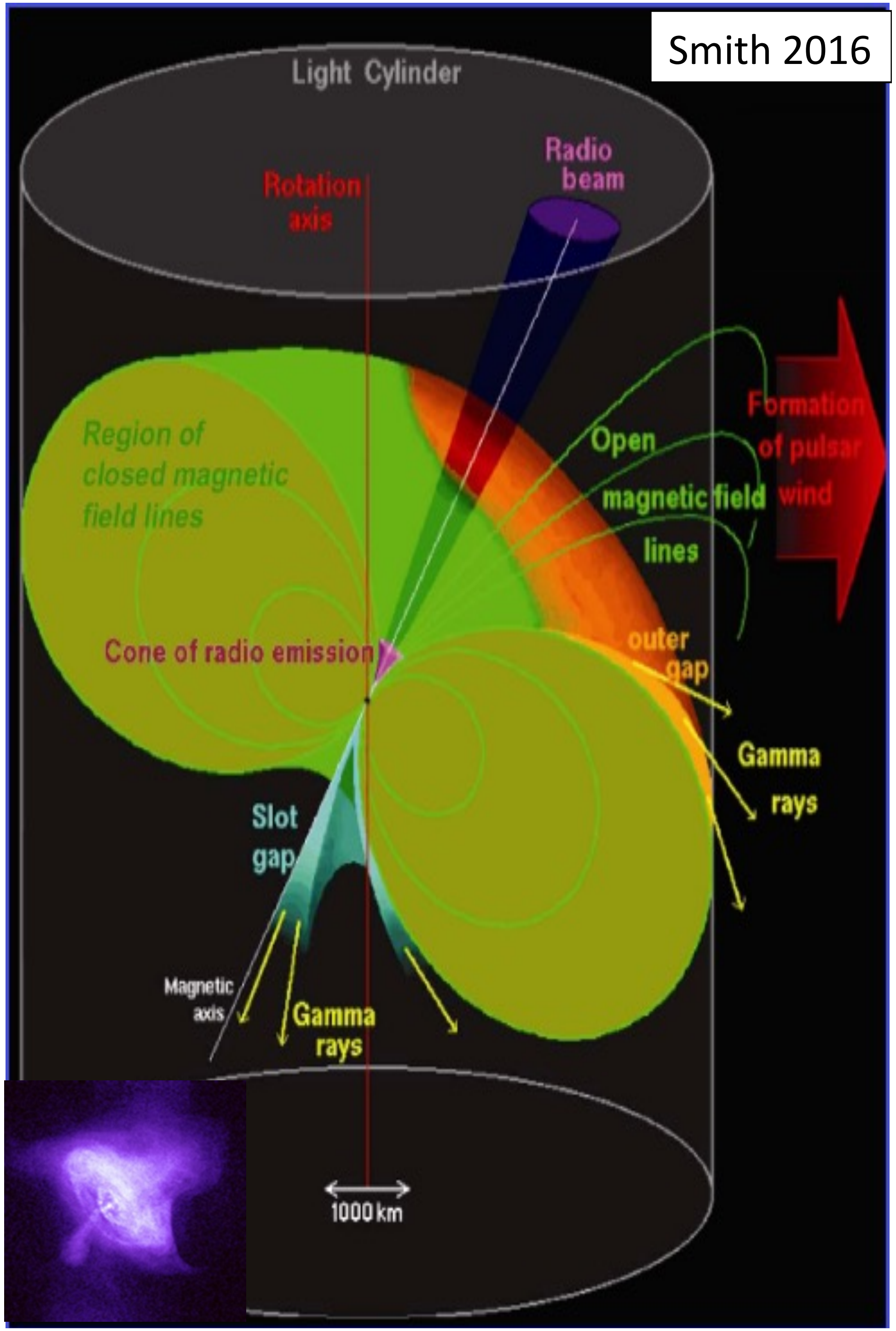

Chandra X-ray image of Crab pulsar wind nebula ➔

Pulsar winds

In France: Jérôme Pétri, Strasbourg.

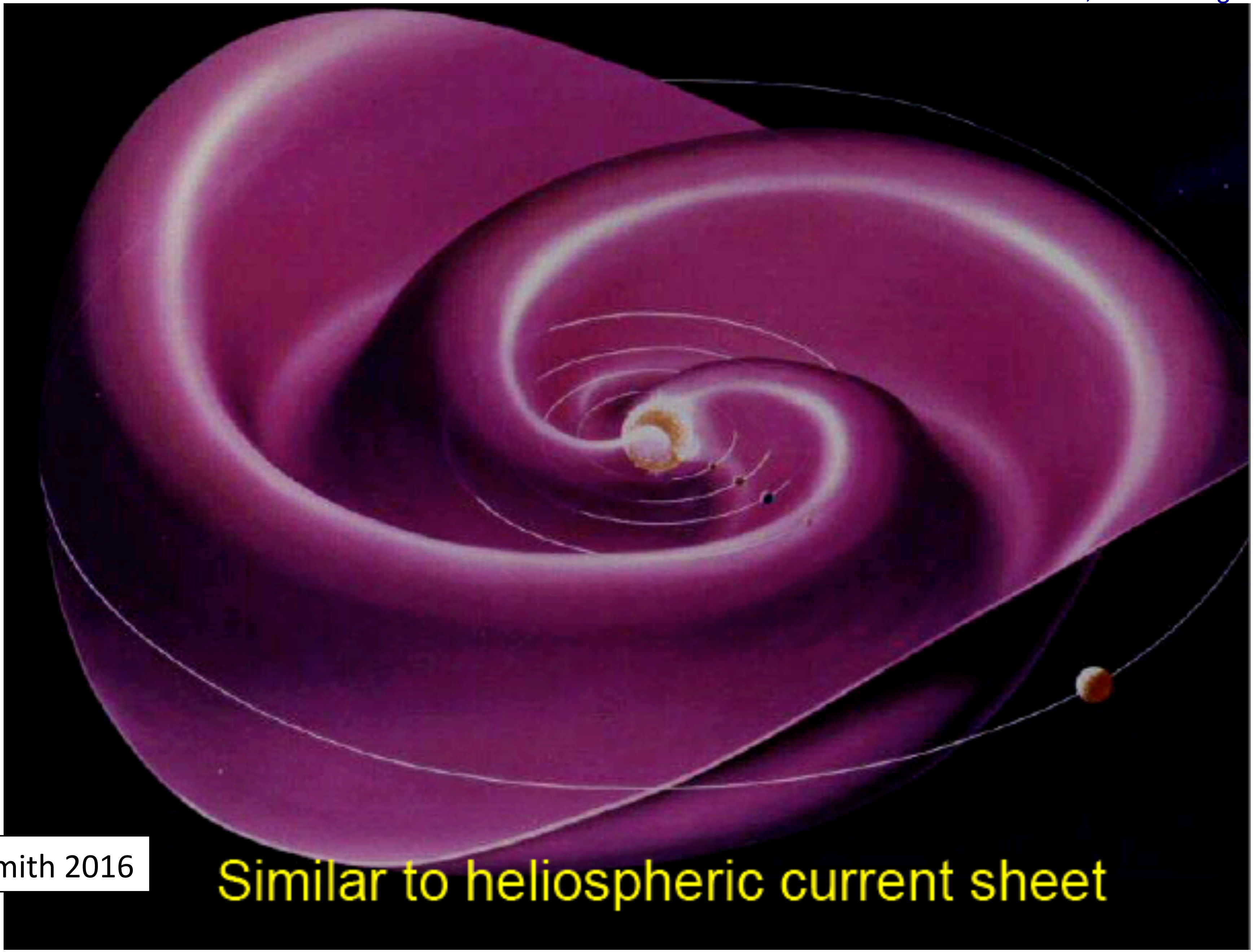

Smith 2016

GeV PWN - where to look?

- Known high-energy PWNe
  - From X-ray and TeV observations
  - For example, Crab, Vela X, MSH 15-52
- Gamma-ray pulsars
  - PWN Catalog based on off-pulse searches from LAT team underway
- Young, energetic radio pulsars
- TeV nebula candidates

Hays 2010

Crab Pulsar and Nebula

Pulsar 100 MeV to 20 GeV

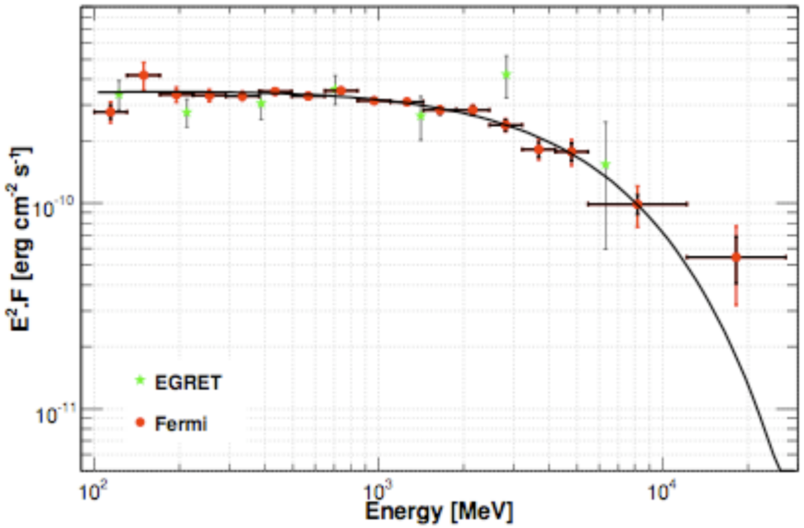

Hyper-exponential cutoff excluded at ~5 sigma.
Consistent with emission well above the neutron star surface

Nebula from MeV to TeV

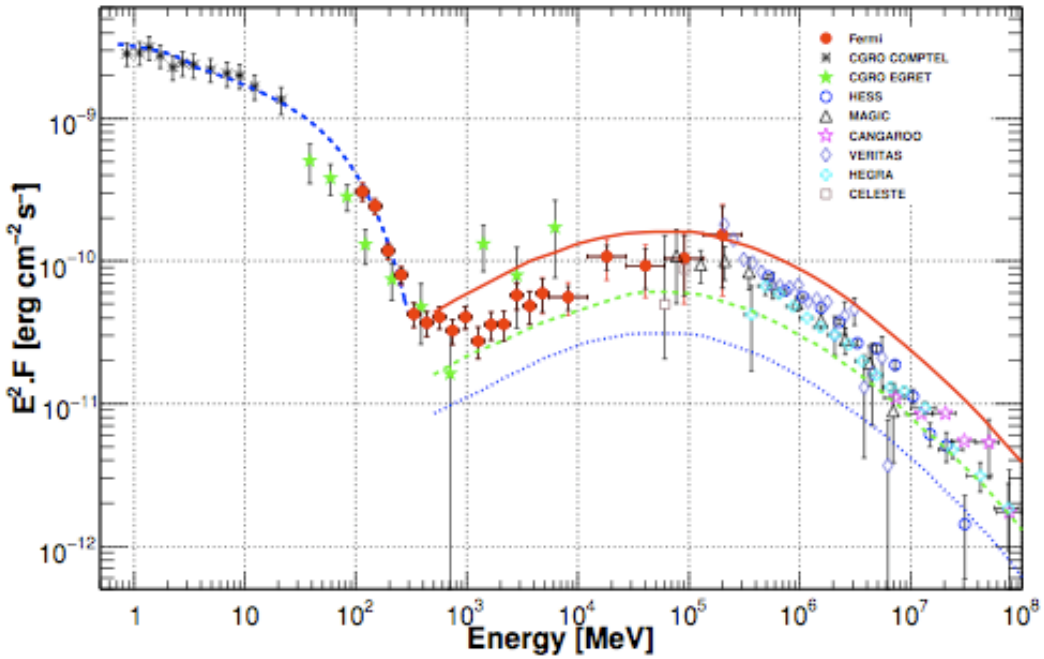

Inverse Compton emission consistent with mean magnetic field in nebula 100 μG < B < 200 μG

Hays 2010

Abdo, A. A. et al. 2010, ApJ, 708, 1254

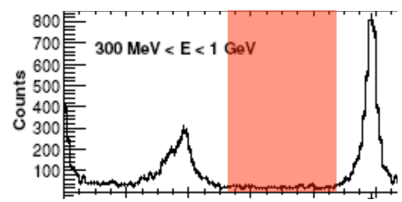

Vela X Nebula of Vela Pulsar

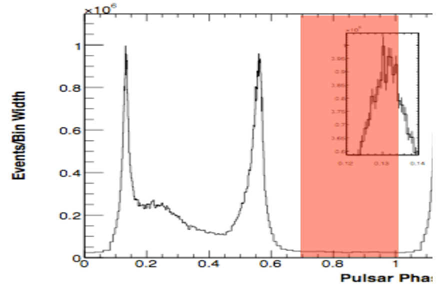

LAT Test Statistic Map

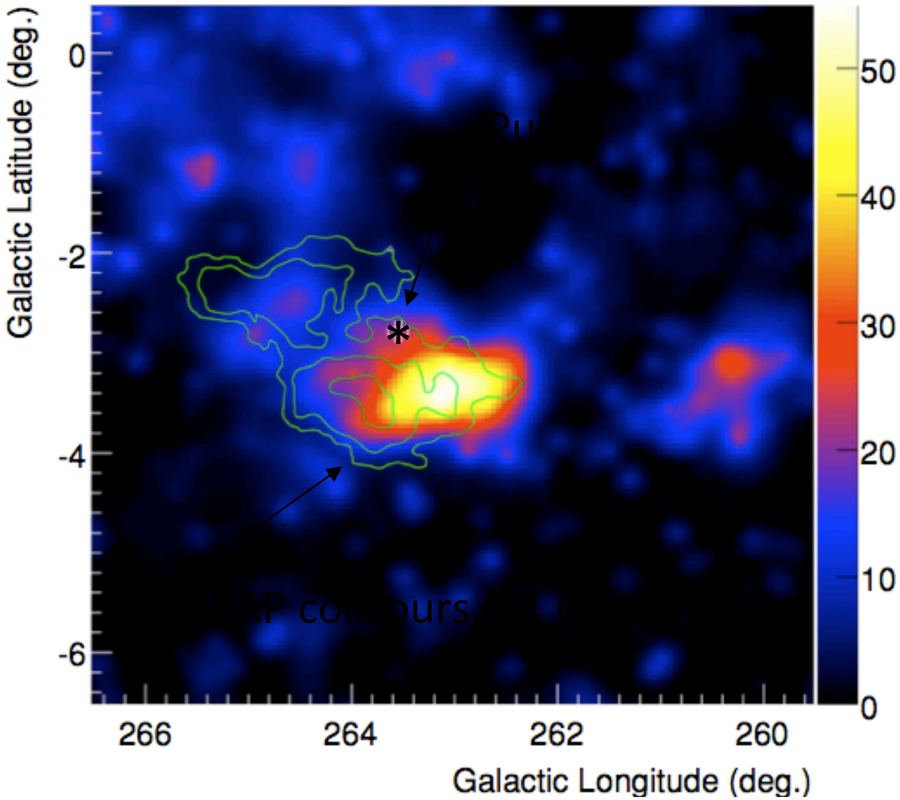

Radial Profile above 800 MeV

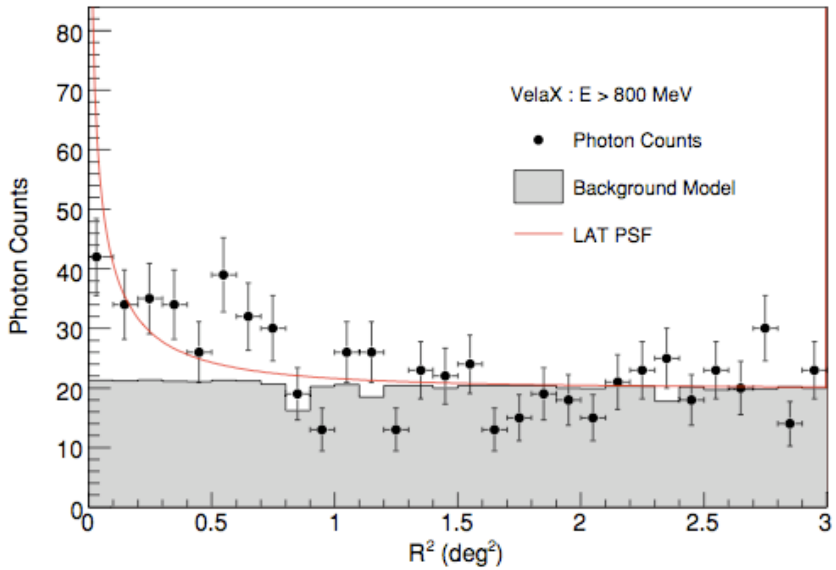

GeV significantly extended

Disk radius = 0.88° +/- 0.12

Better match to radio than TeV

Abdo, A. A. et al. 2010, ApJ, 713, 146

Hays 2010

Supernova Remnants

- Which remnants are GeV emitters?
- Where are the emission regions?
- What is producing the gamma rays?

Hays 2010

Supernova remnants (SNRs) seen with *Fermi* LAT

- GeV, TeV SNR studies are pinpointing the cosmic ray accelerators.
- Detailed shape studies in highly confused regions.
- Pulsar detections lead to an improved diffuse emission model.

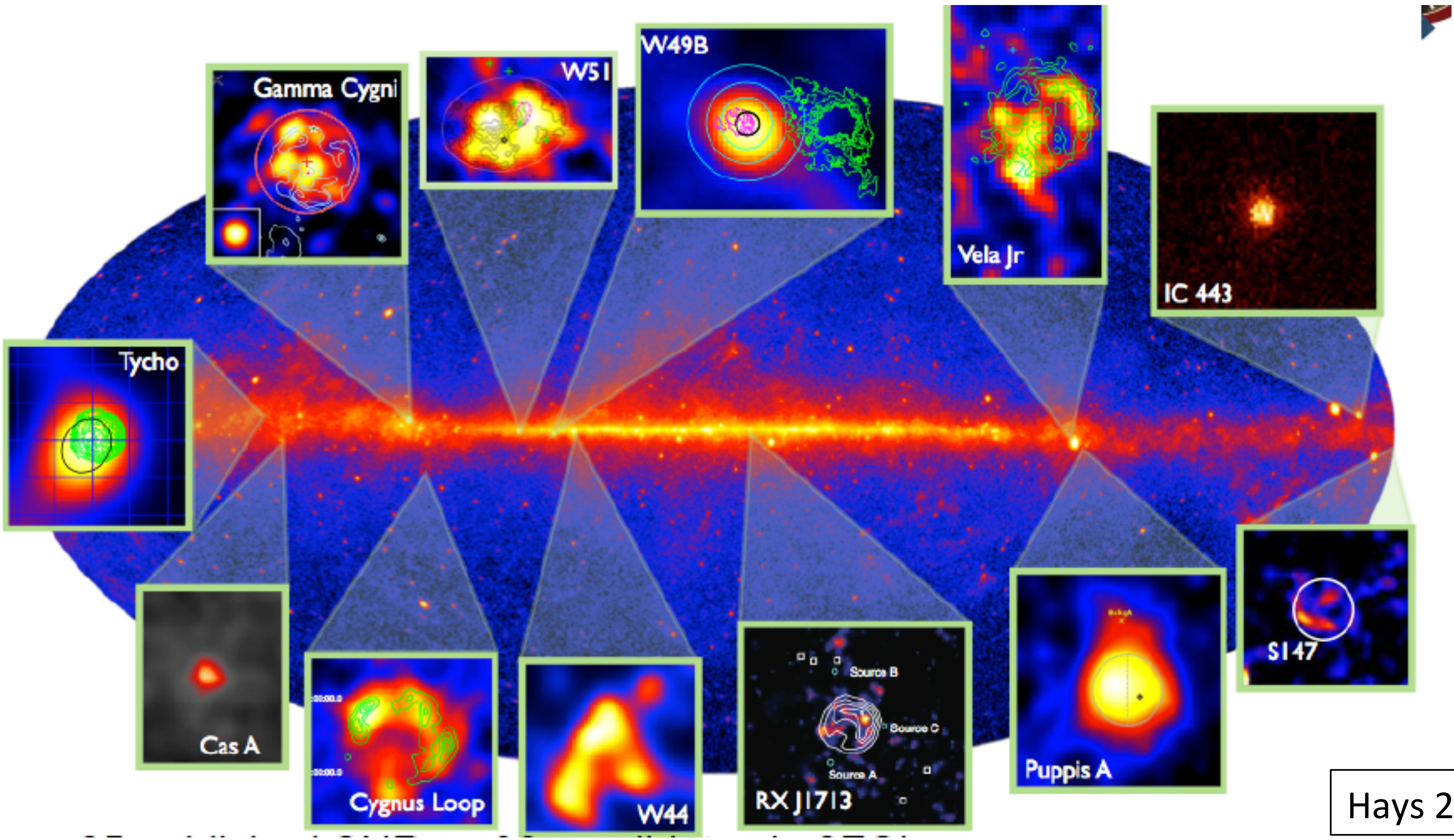

Hays 2010

SNR: GeV Morphology

SNRs W51C, W44, IC 443, W28 North source resolved by LAT. Cas A unresolved. Good agreement with shell structures.

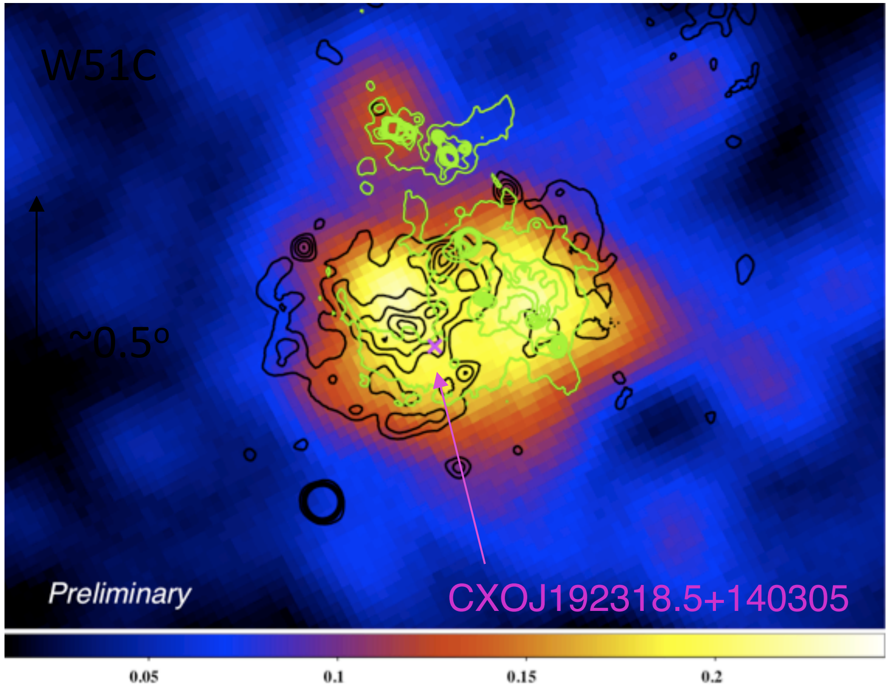

LAT counts map (2-8 GeV)
X-ray (0.1-2.4 keV, black) and radio (1.4 GHz, green) contours

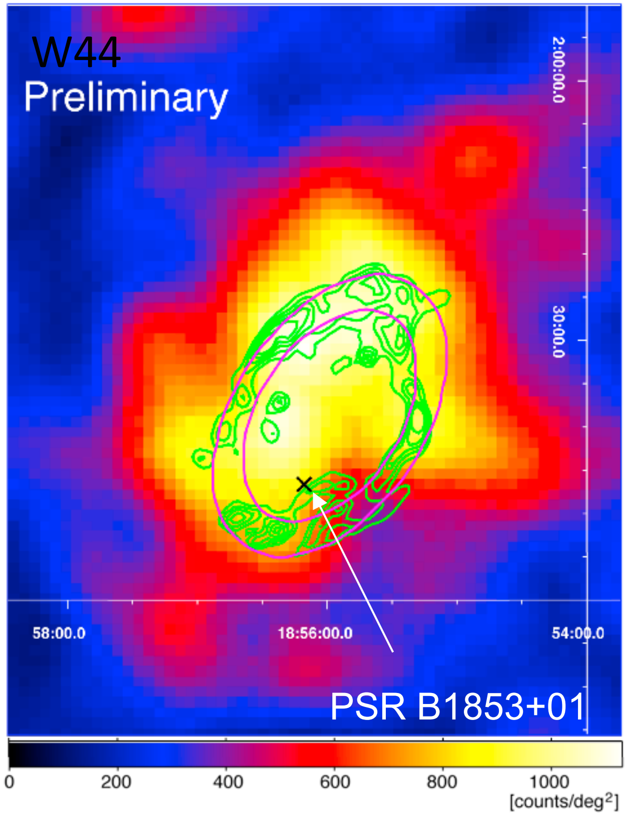

LAT counts (2-10 GeV)
Infrared contours (4.5 um)

Hays 2010

SNR: Molecular Connection

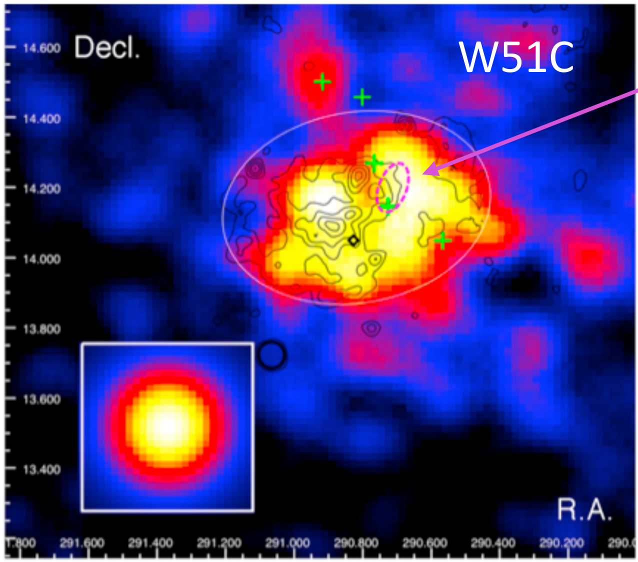

Shocked CO

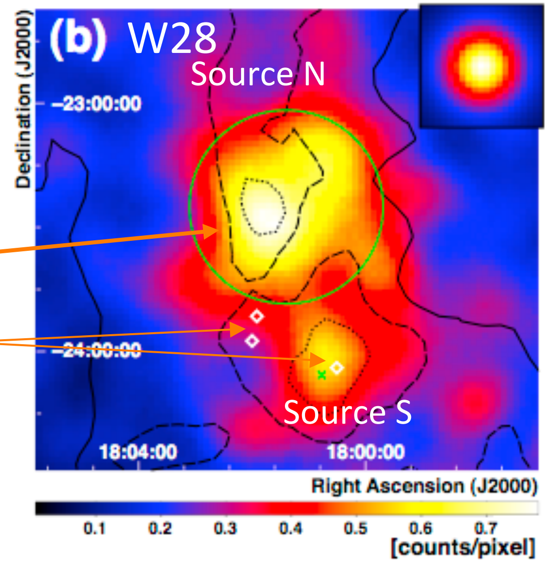

CO (J=1-0) contours
NANTEN

H II regions

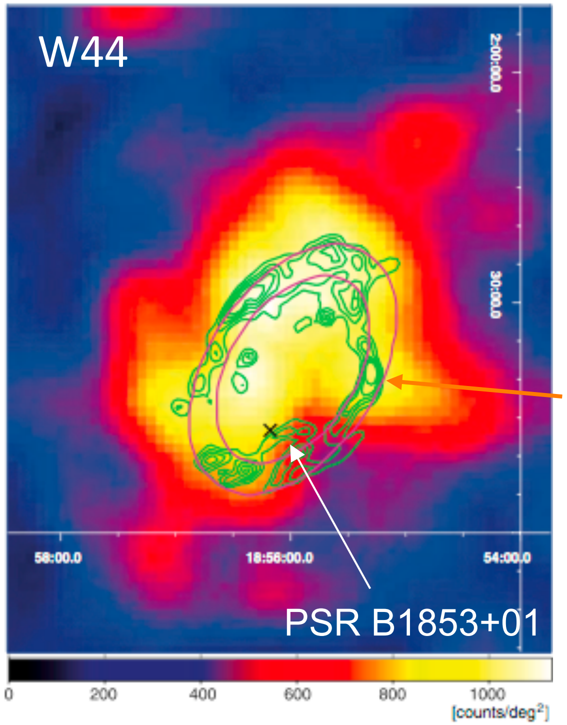

W44

Shocked H2

GeV emission from SNRs interacting with molecular clouds
IC 443, W51C, W44, W28…

Hays 2010

SNR: GeV Breaks

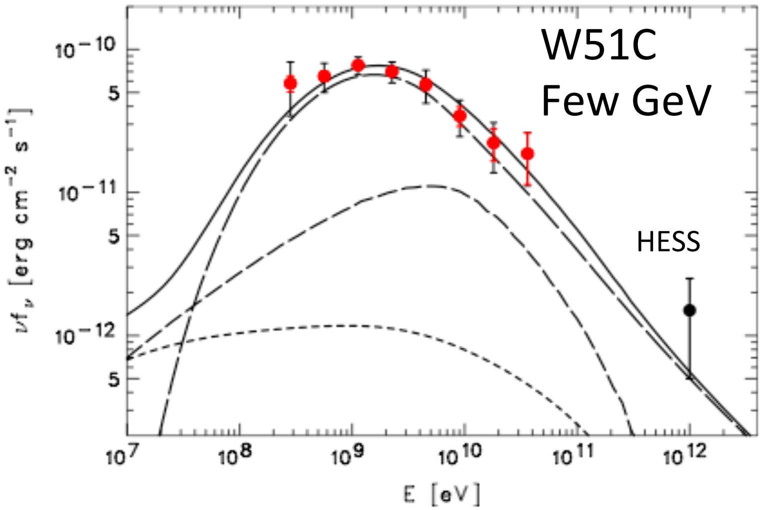

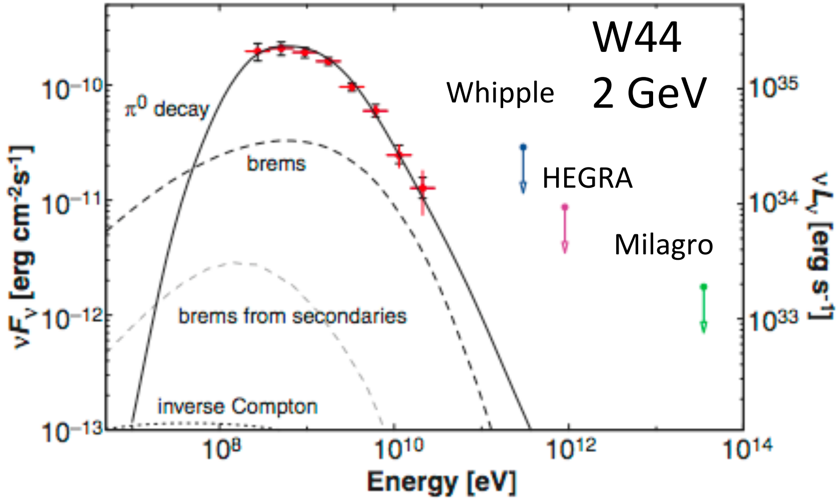

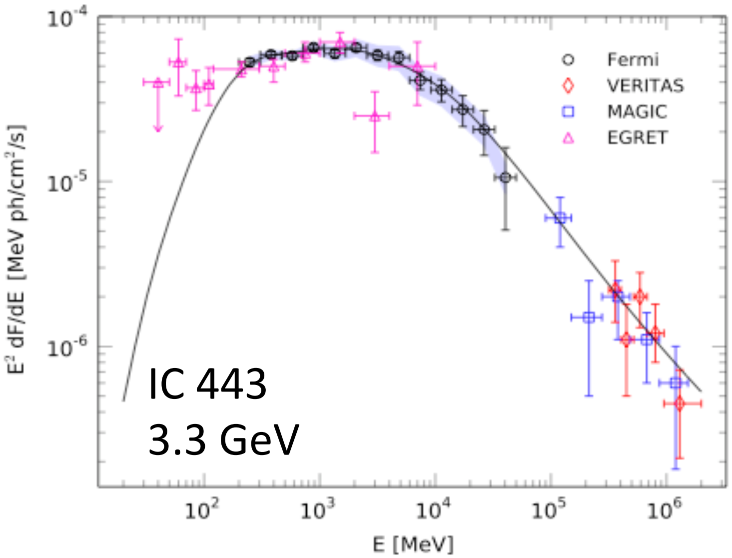

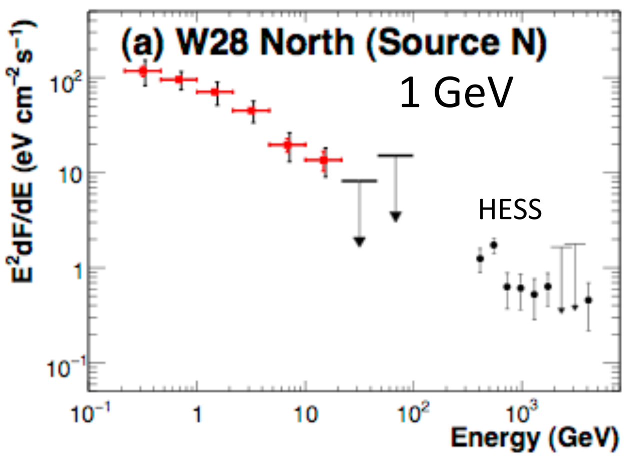

Hays 2010

SNR: Young vs. Old

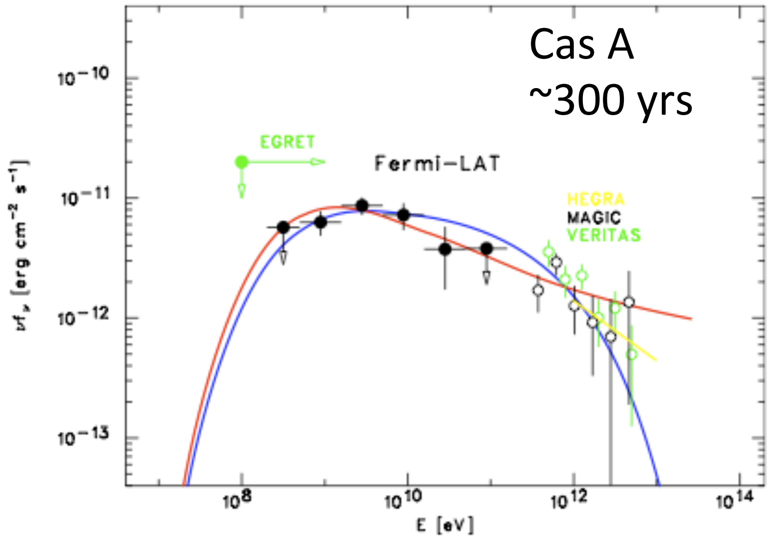

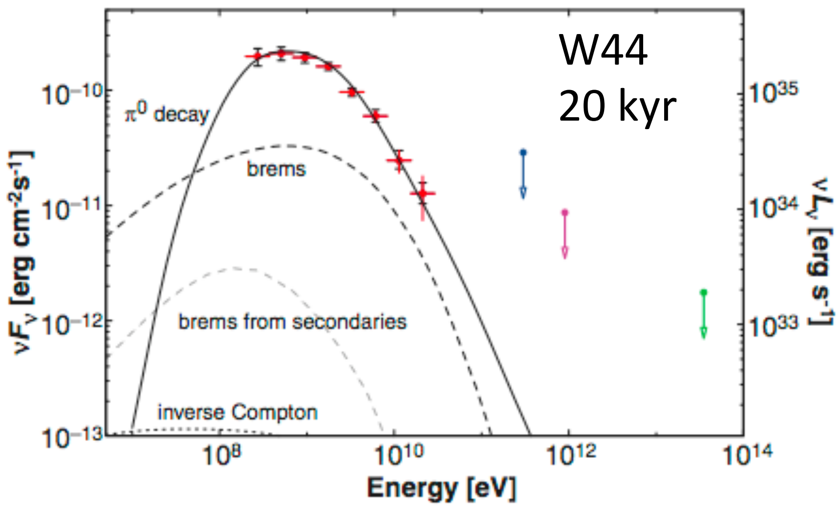

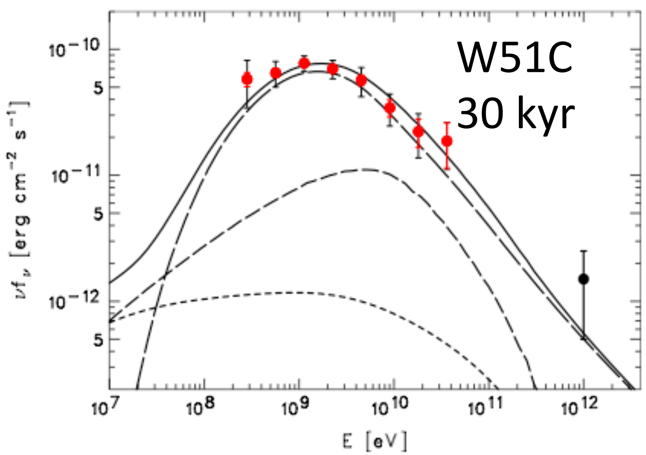

Hays 2010

Supernova Remnants

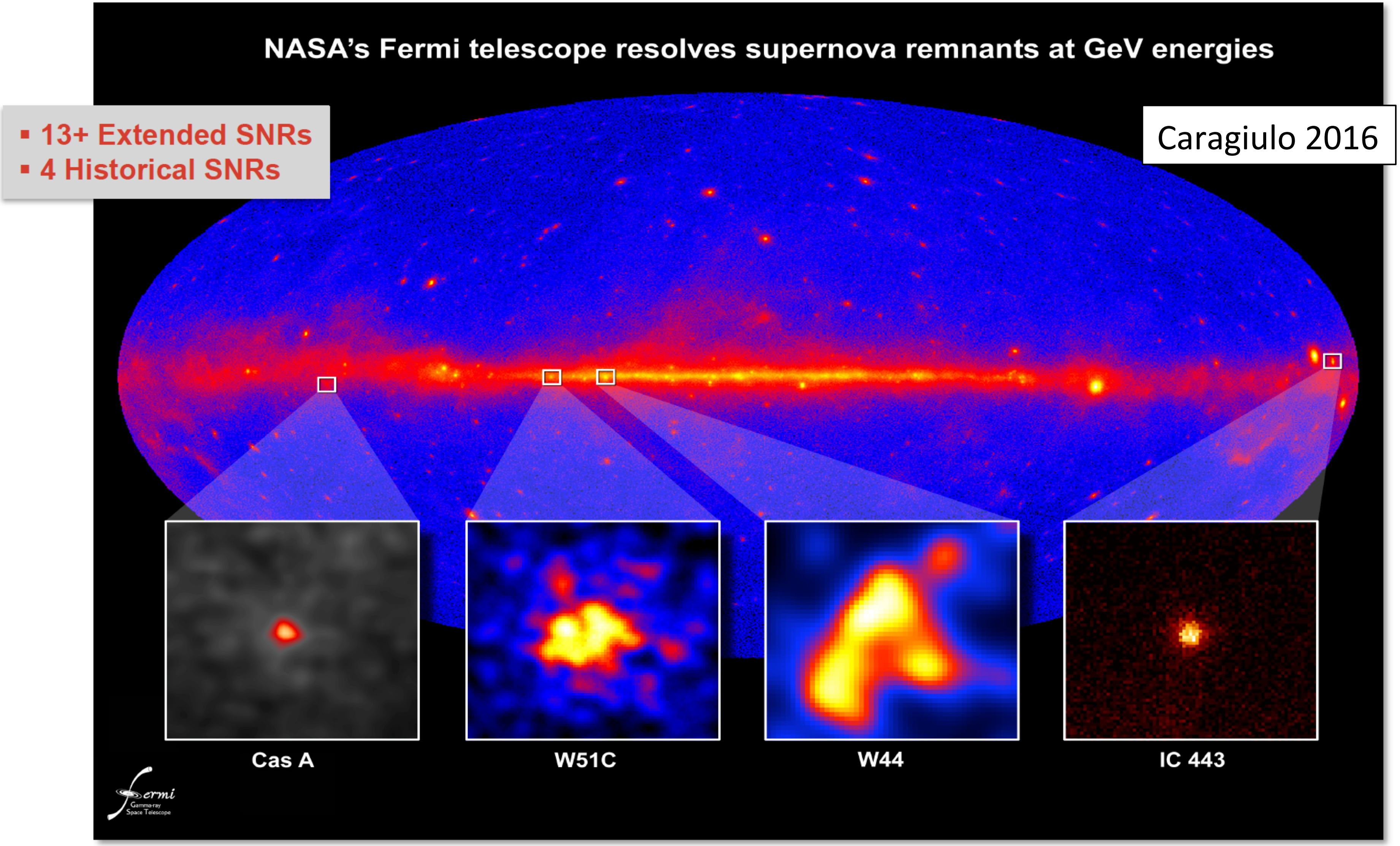

Supernova Remnants

Thought to be cosmic ray sources:

γ-ray flux originates from the interaction of accelerated particles with the SNR environment:

SNR paradigm for CRs

Caragiulo 2016

Radio to X-ray range:

- **Synchrotron radiation**

Three competitor processes for GeV-TeV energy range

- **Inverse Compton scattering**
- Bremsstrahlung radiation
- Hadronic interaction

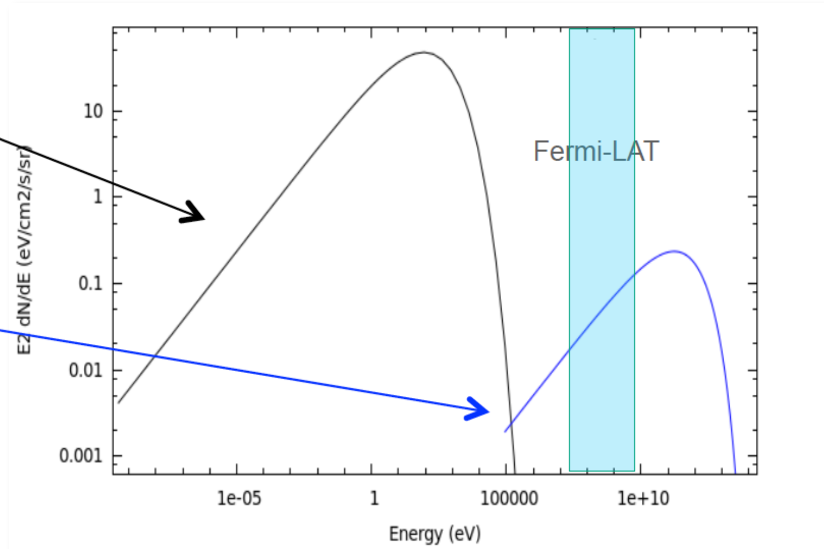

Supernova Remnants

Caragiulo 2016

Thought to be cosmic ray sources:
γ-ray flux originates from the interaction of accelerated particles with the SNR environment:
SNR paradigm for CRs

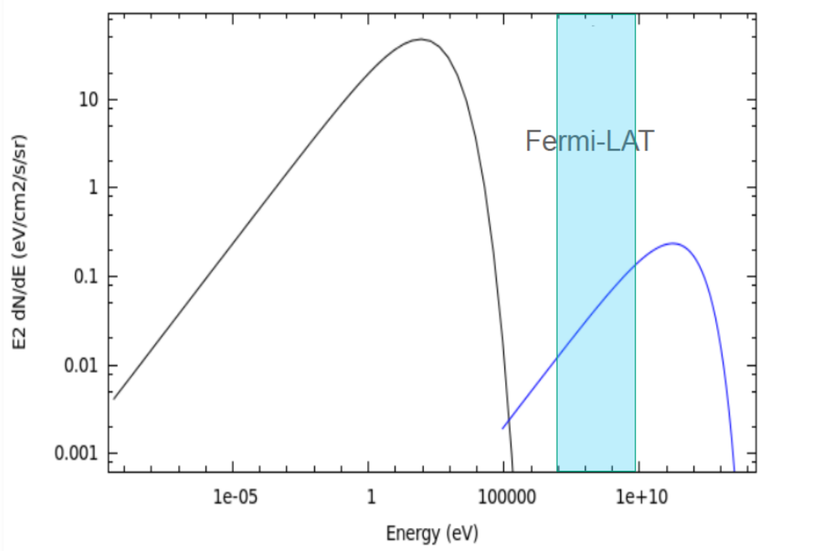

Radio to X-ray range:
- Synchrotron radiation

Three competitor processes for GeV-TeV energy range
- Inverse Compton scattering
- Bremsstrahlung radiation
- **Hadronic interaction**

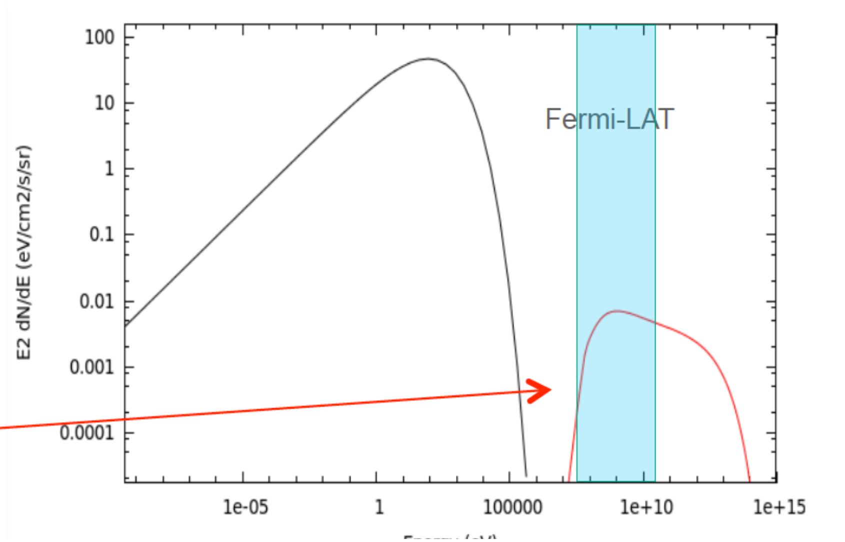

Supernova Remnants

Caragiulo 2016

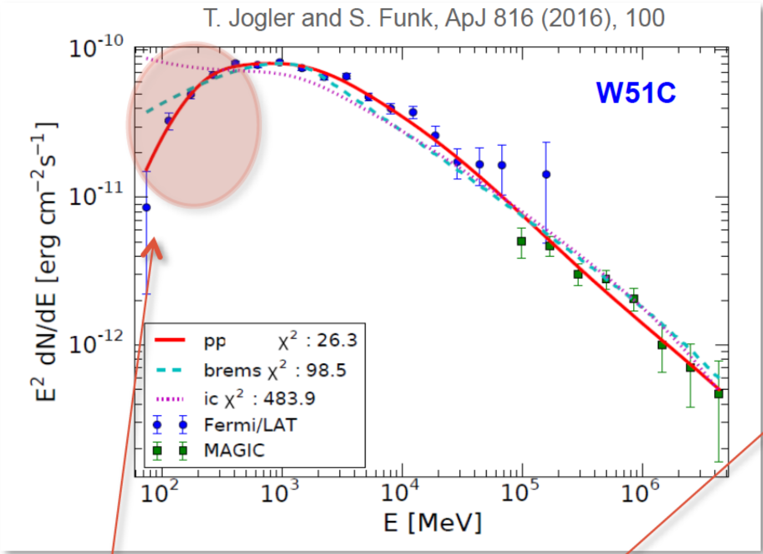

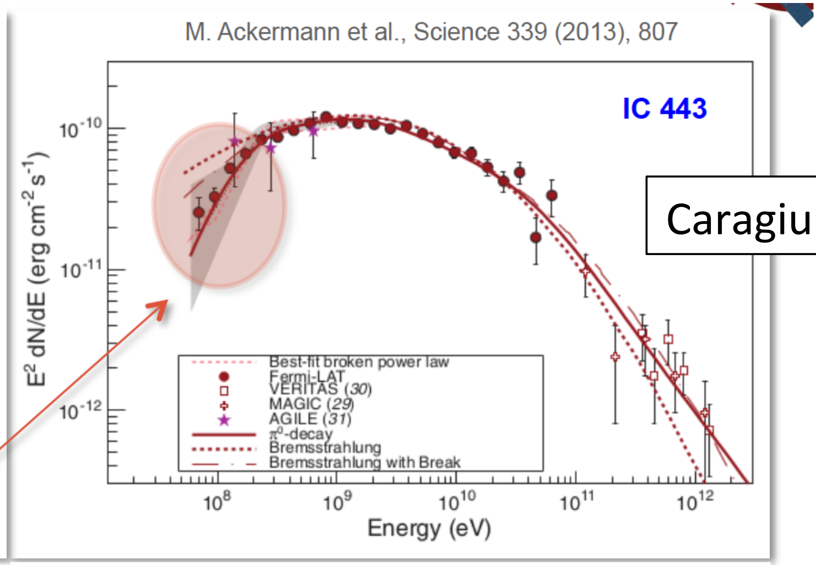

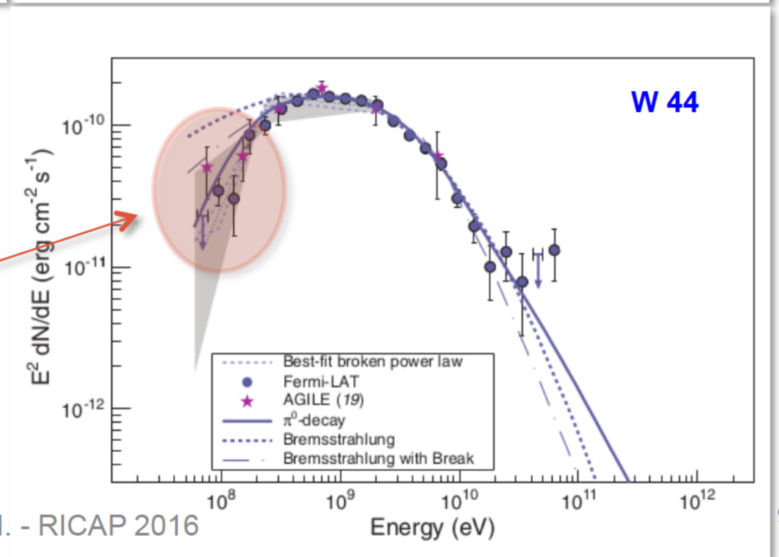

π^0–decay cut-off
'smoking gun' for accelerated protons

Supernova Remnants

Caragiulo 2016

Leptonic Scenario

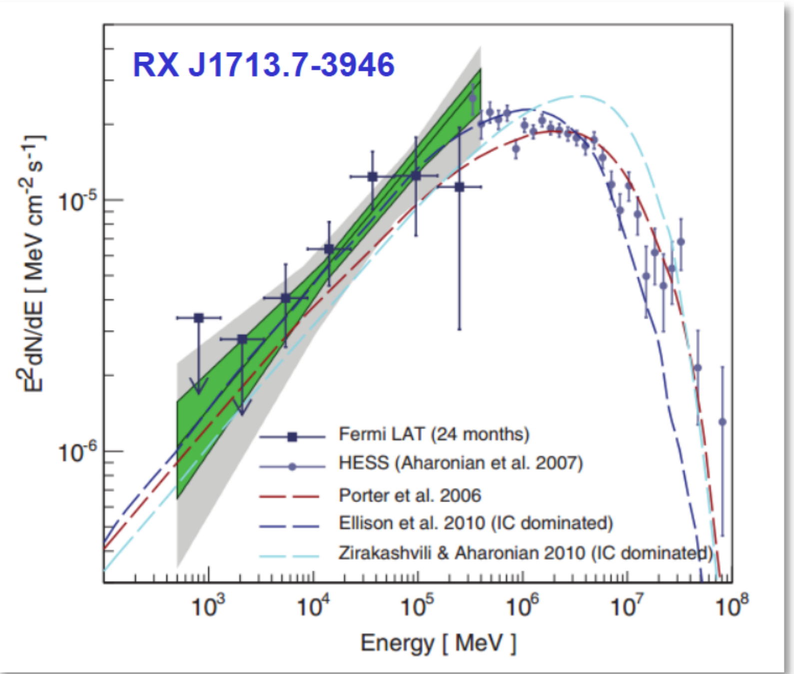

A. A. Abdo et al., ApJ 734 (2010), 28

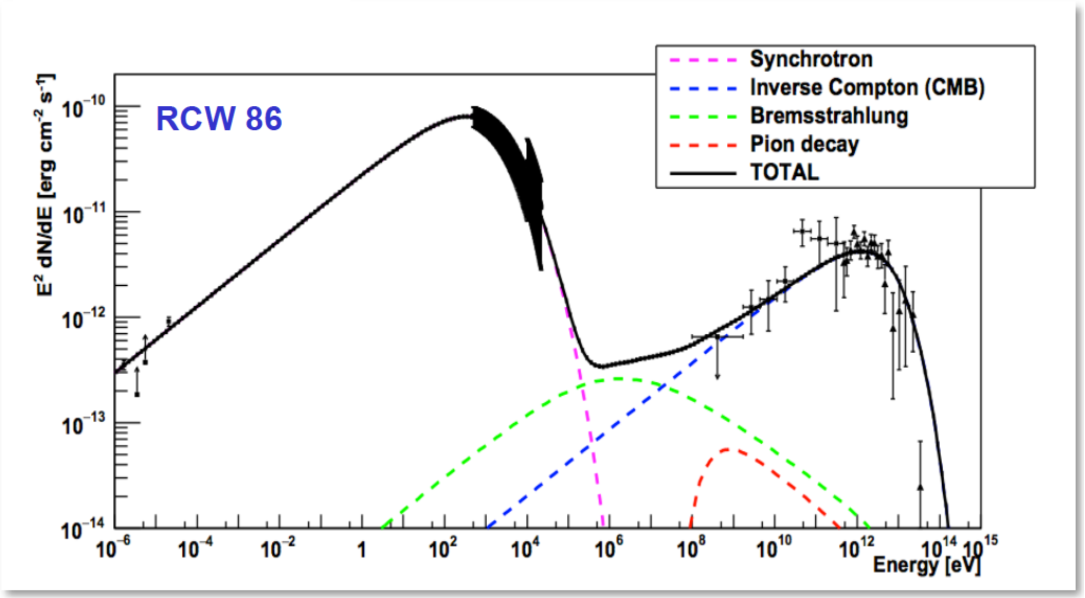

M. Ajello et al., ApJ 819 (2016) 98

The γ-rays emission is due to the **IC scattering** of high energy leptons **on** local photon fields, namely only **CMB**.

The **absence of γ-rays from π^0-decay** does not rule out the possibility of an efficiently accelerated of CRs in this remnant, but **might be due to a low gas density** around the source.

Supernova Remnants

Caragiulo 2016

Hadronic Scenario

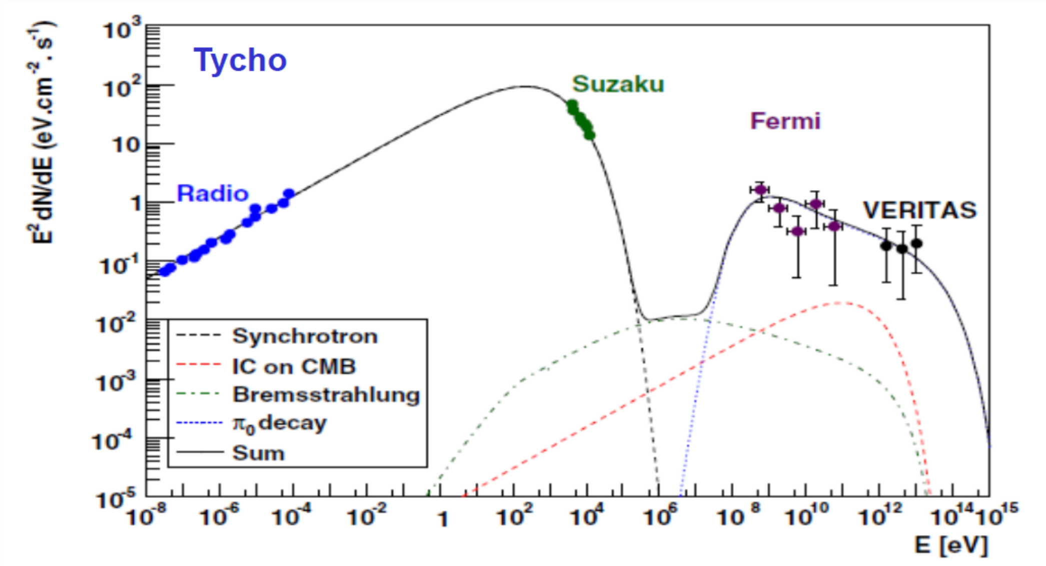

F. Giordano et al., ApJL 744 (2012) L2

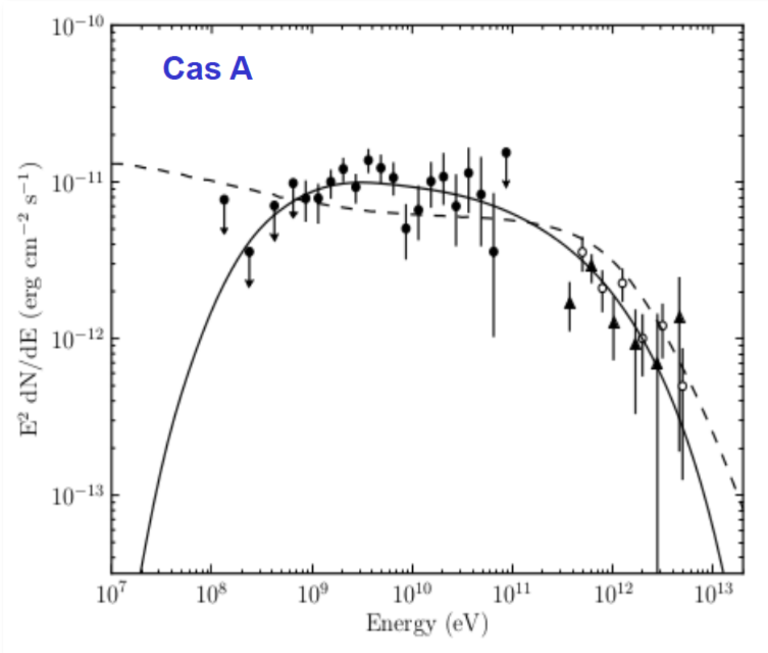

Y. Yuan et al., ApJ 779 (2013), 117

The γ-rays spectrum seems to be compatible only with the **π^0-decay** produced in nuclear collisions between relativistic nuclei and the background gas.

Furthermore, multiwavelength modeling of **Tycho** SED (G. Morlino and D. Caprioli, Astron. Astrophys. (2012) 538, A81) infer a **maximum proton energy** around **500 TeV**, which is very **close to the *knee*** of the CR spectrum.

Supernova Remnants

Caragiulo 2016

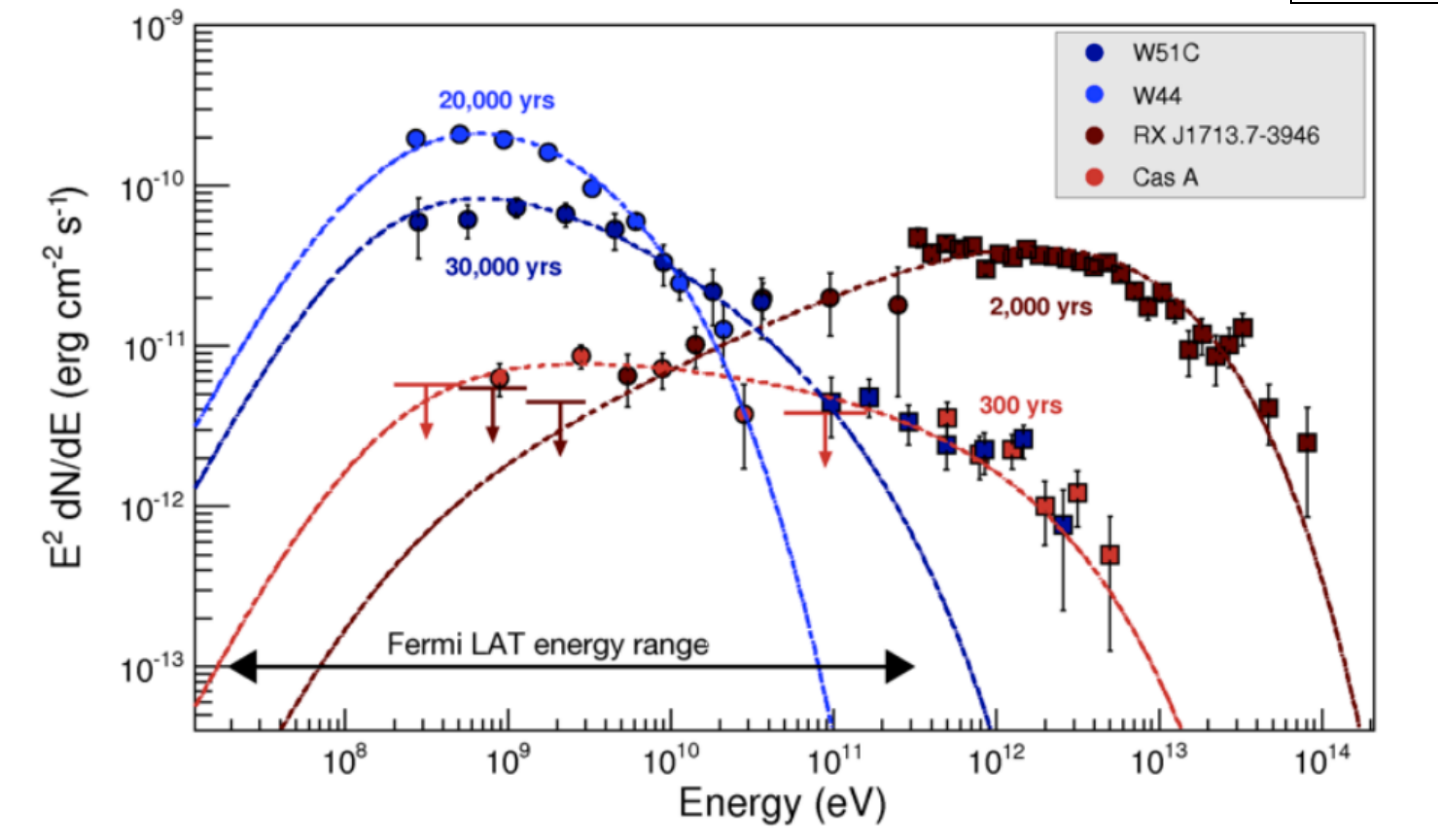

- ✓ Young SNRs have hard spectra, extend to ~ $10^{13\text{-}15}$ TeV
- ✓ Older SNRs are brighter (due to large target) but show a clear break in their spectrum at ~ few GeV

Supernova Remnants

Caragiulo 2016

- Search of known SNRs in 3 years of Fermi-LAT data
- 36 SNR candidates with spatial association with radio counterparts
  - **17 extended sources: 4 new**
  - **13 point-like sources: 10 new**

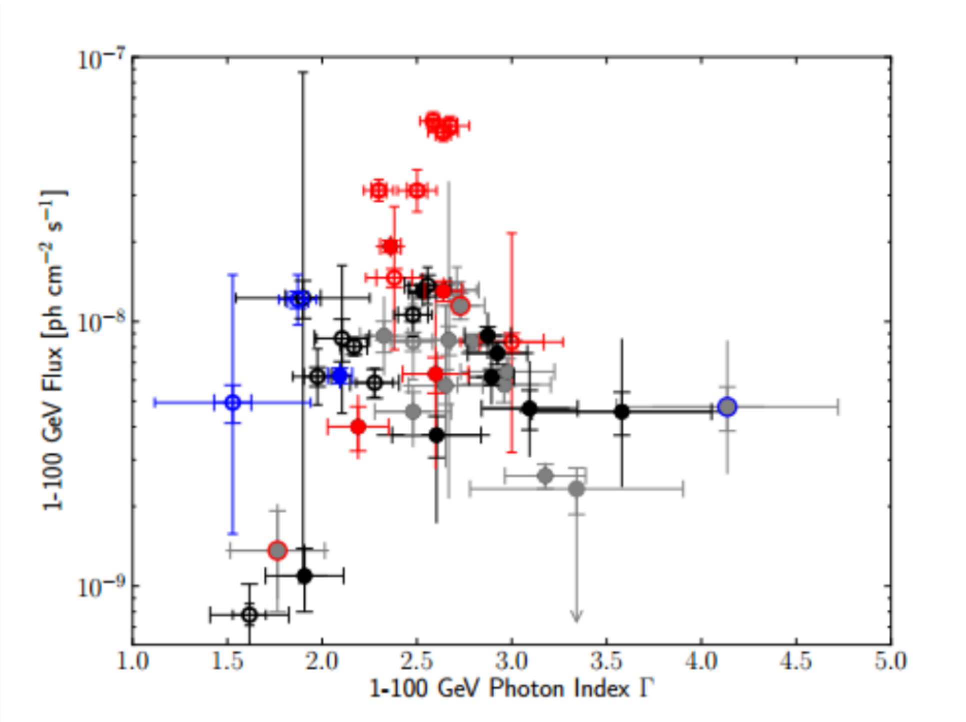

- **Interacting SNRs**
- **Young SNRs**

- **Classified candidates**
- **Marginal candidates**

- **Point-like sources**
- **Extended sources**

F. Acero et al., arXiv:1511.06778

Supernova Remnants

De Palma 2015

The radio and GeV diameters seems well correlated.

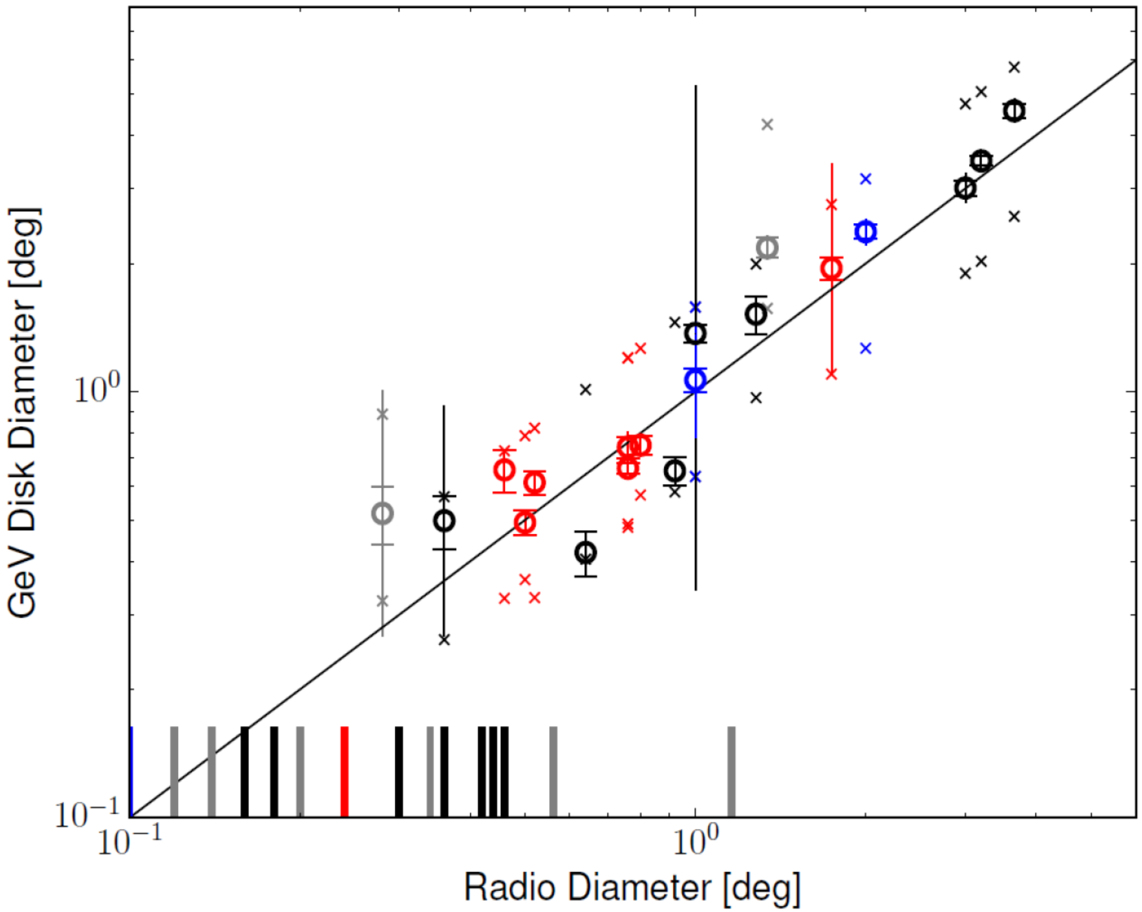

- Interacting SNRs
- Young SNRs
- Classified candidates
- Marginal candidates

x Min and max extension of the source needed to remain in the same class.

Supernova Remnants

Radio synchrotron emission indicates the presence of relativistic leptons.
LAT-detected SNRs tend to be radio-bright:

De Palma 2015

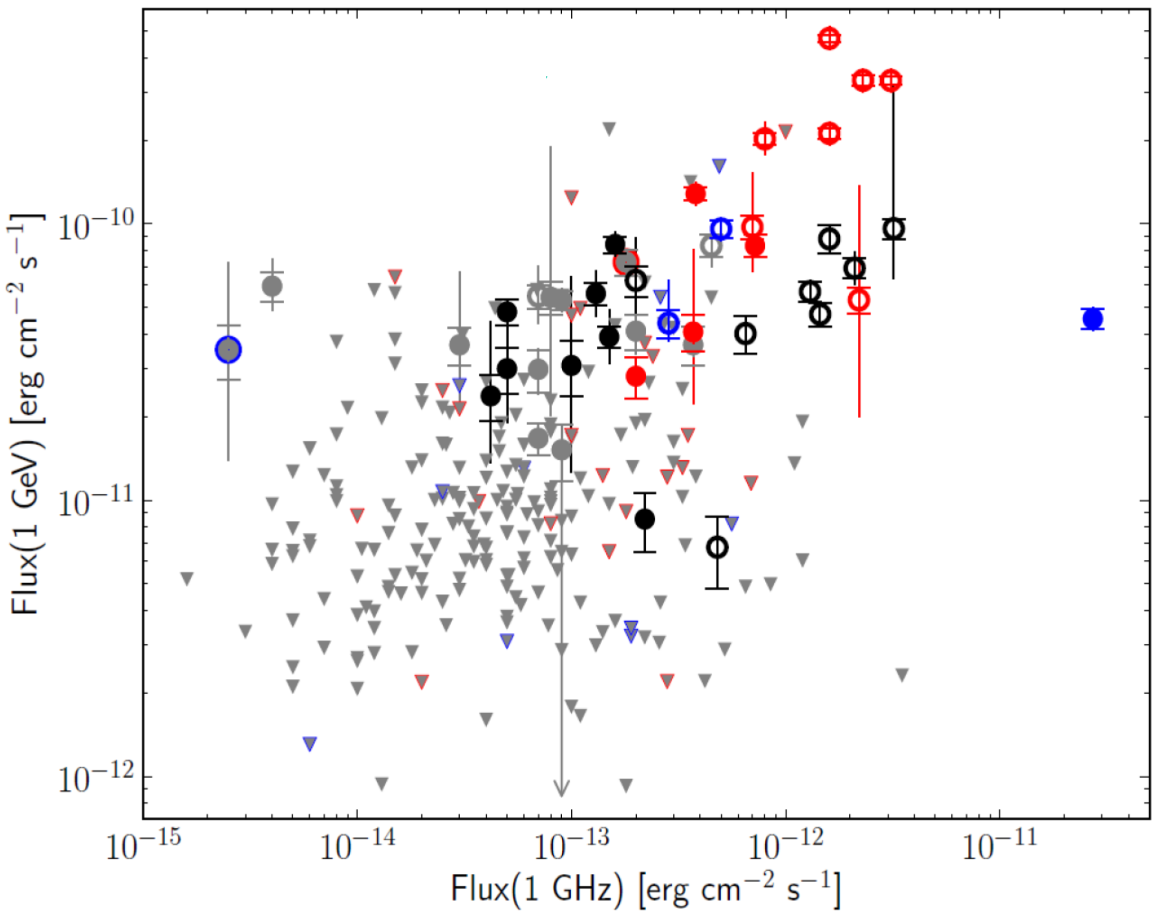

- Interacting SNRs: general correlation suggests a physical link
- Young SNRs show more scatter

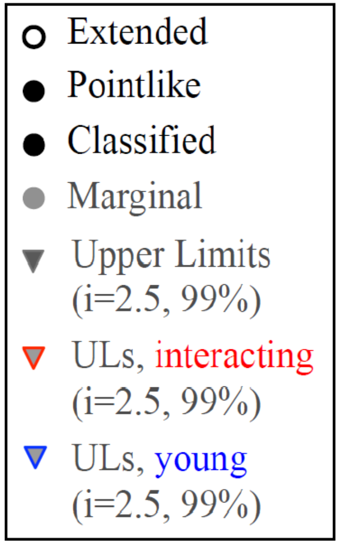

Supernova Remnants

De Palma 2015

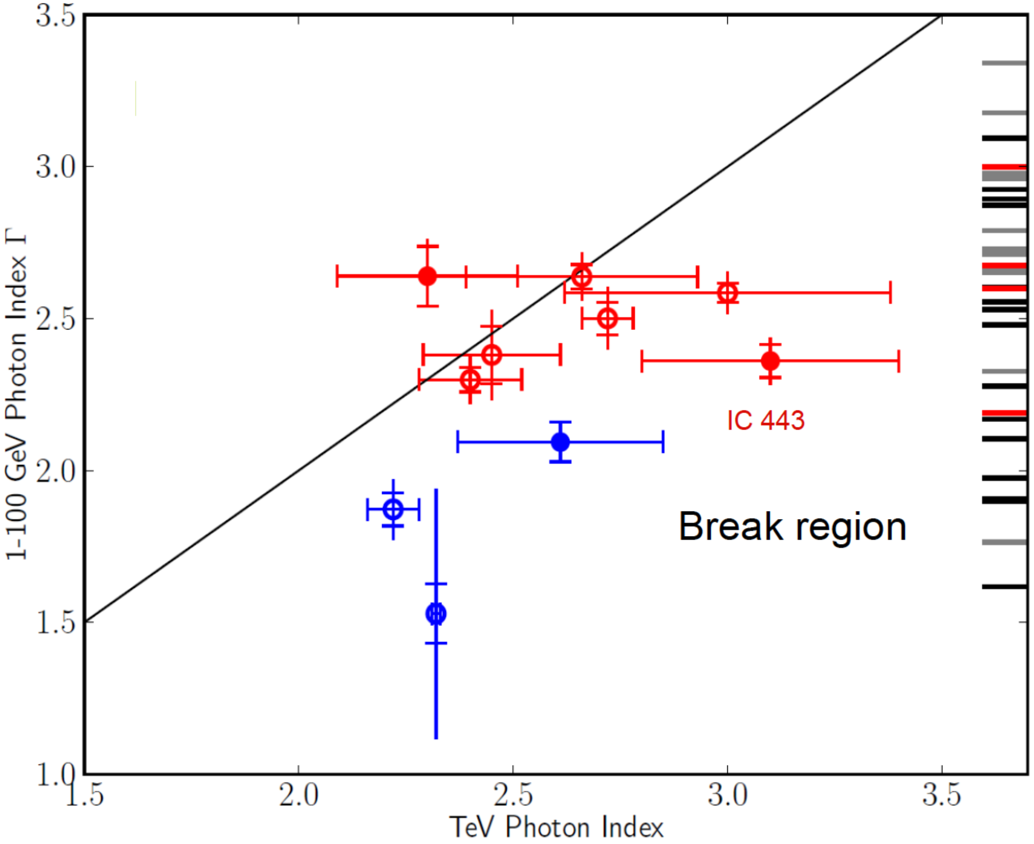

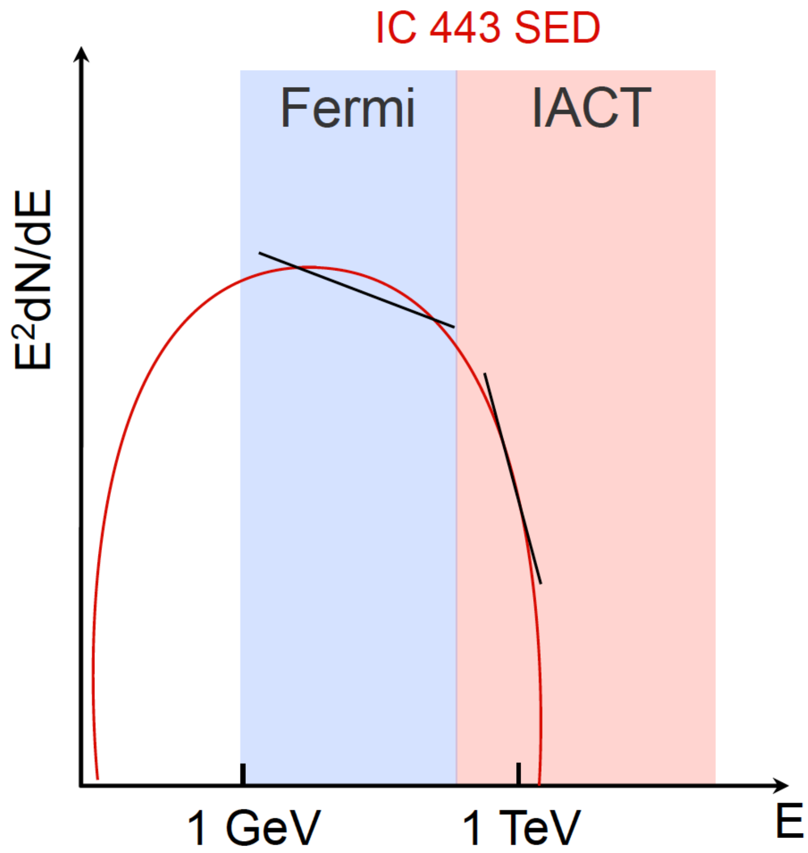

- Indication of break at TeV energies
- Caveat: TeV sources are not uniformly surveyed.

Supernova Remnants

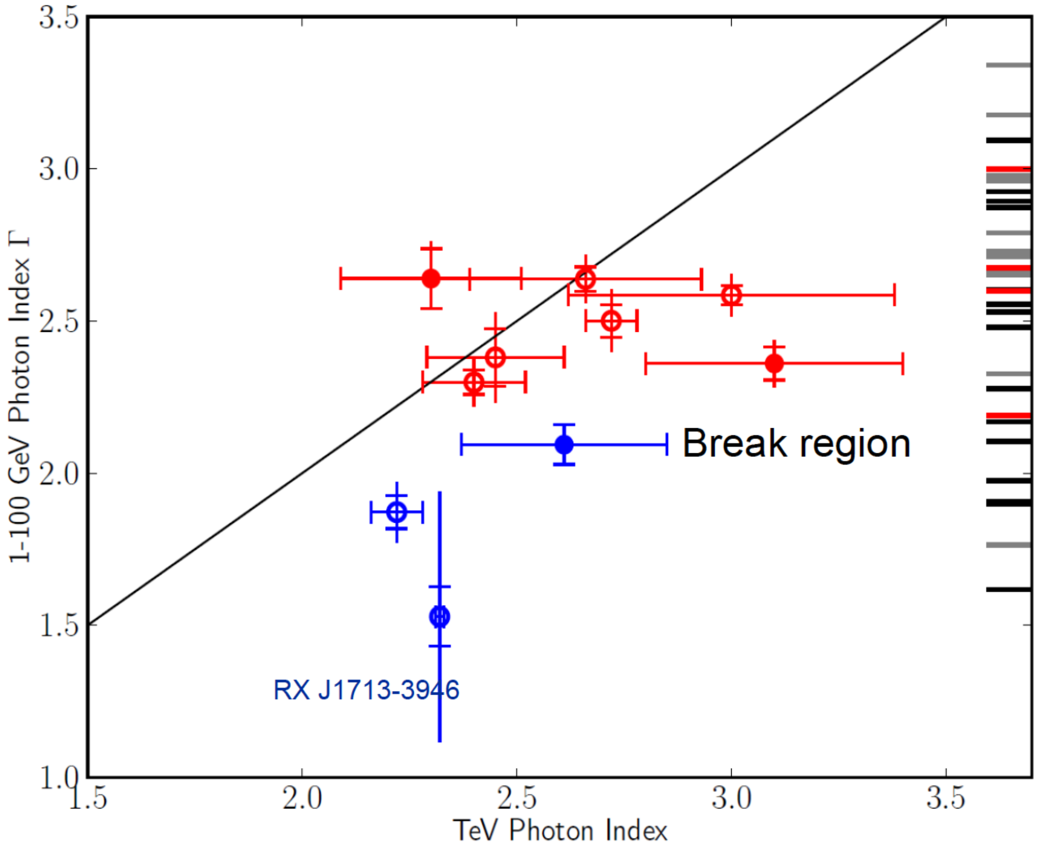

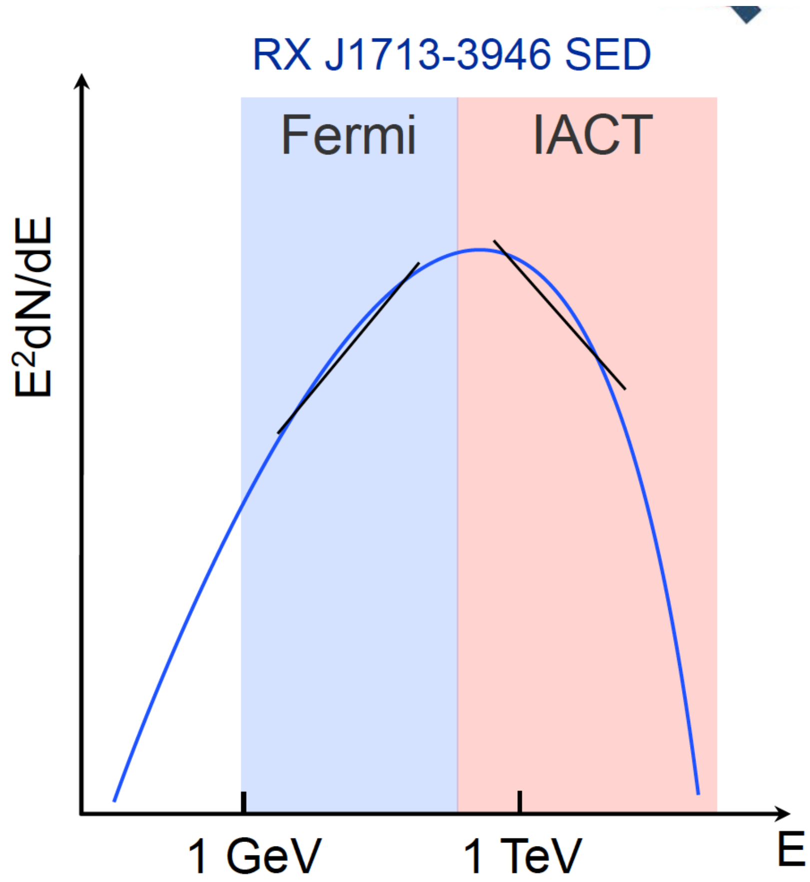

De Palma 2015

- Indication of break at TeV energies
- Caveat: TeV sources are not uniformly surveyed.

Supernova Remnants

Interacting SNRs tend to be more luminous than young SNRs.

Young SNRs:

- Low $L_\gamma \rightarrow$ evolving into low density medium?

Interacting SNRs:

- Higher $L_\gamma \rightarrow$ encountering higher densities?

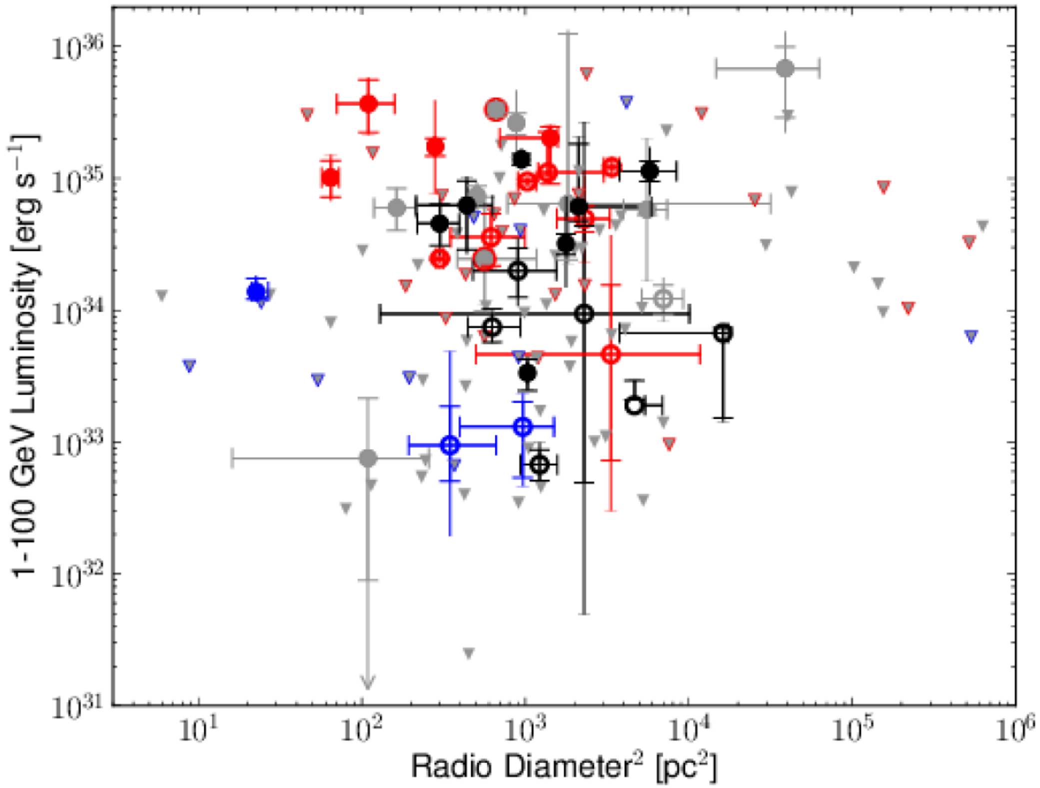

De Palma 2015

Gamma-ray Binaries

Tanaka et al 2012

Gamma-ray emitting X-ray binaries
First discovered by air Cherenkov telescopes

LS 5039

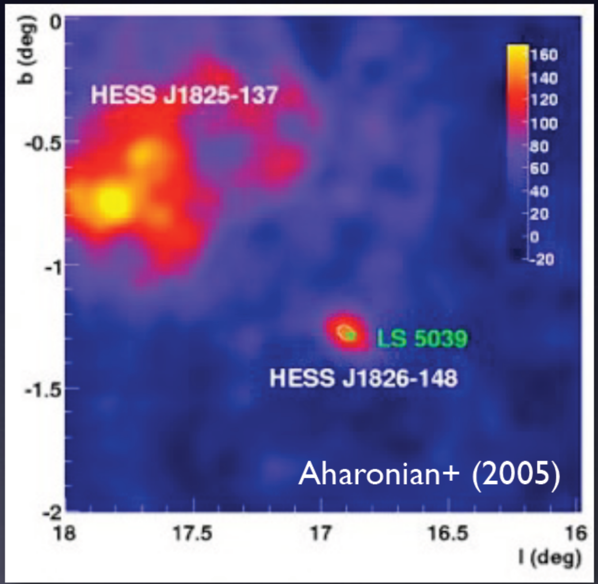

O star + ?
H.E.S.S. detected
Periodicity (3.9 days)

LS I +61° 303

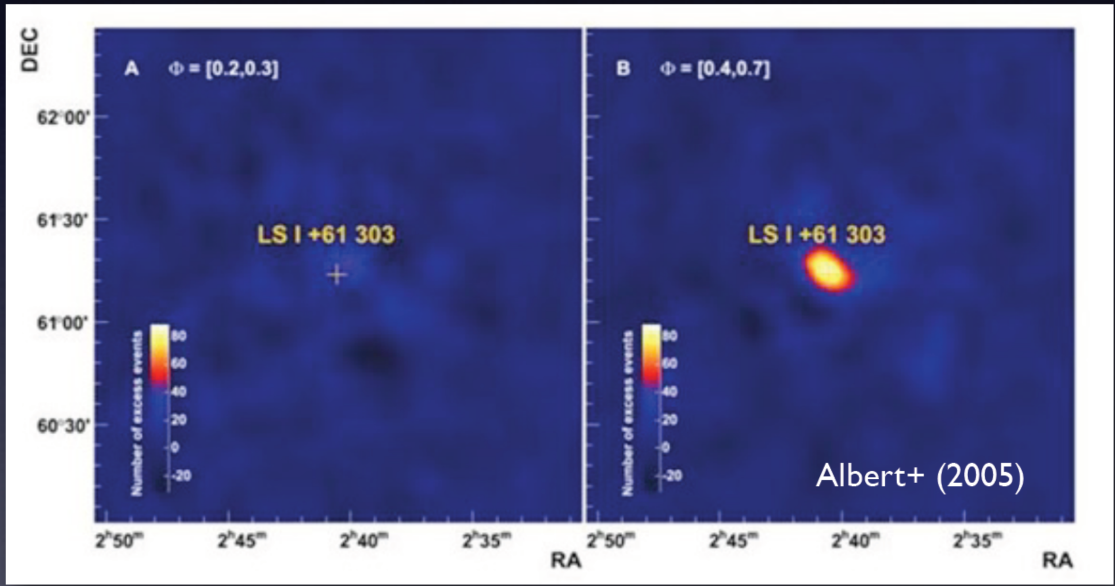

Be star + ?
MAGIC & VERITAS detected
Periodicity (26.5 days)

Emission Mechanism?

Mirabel (2006)

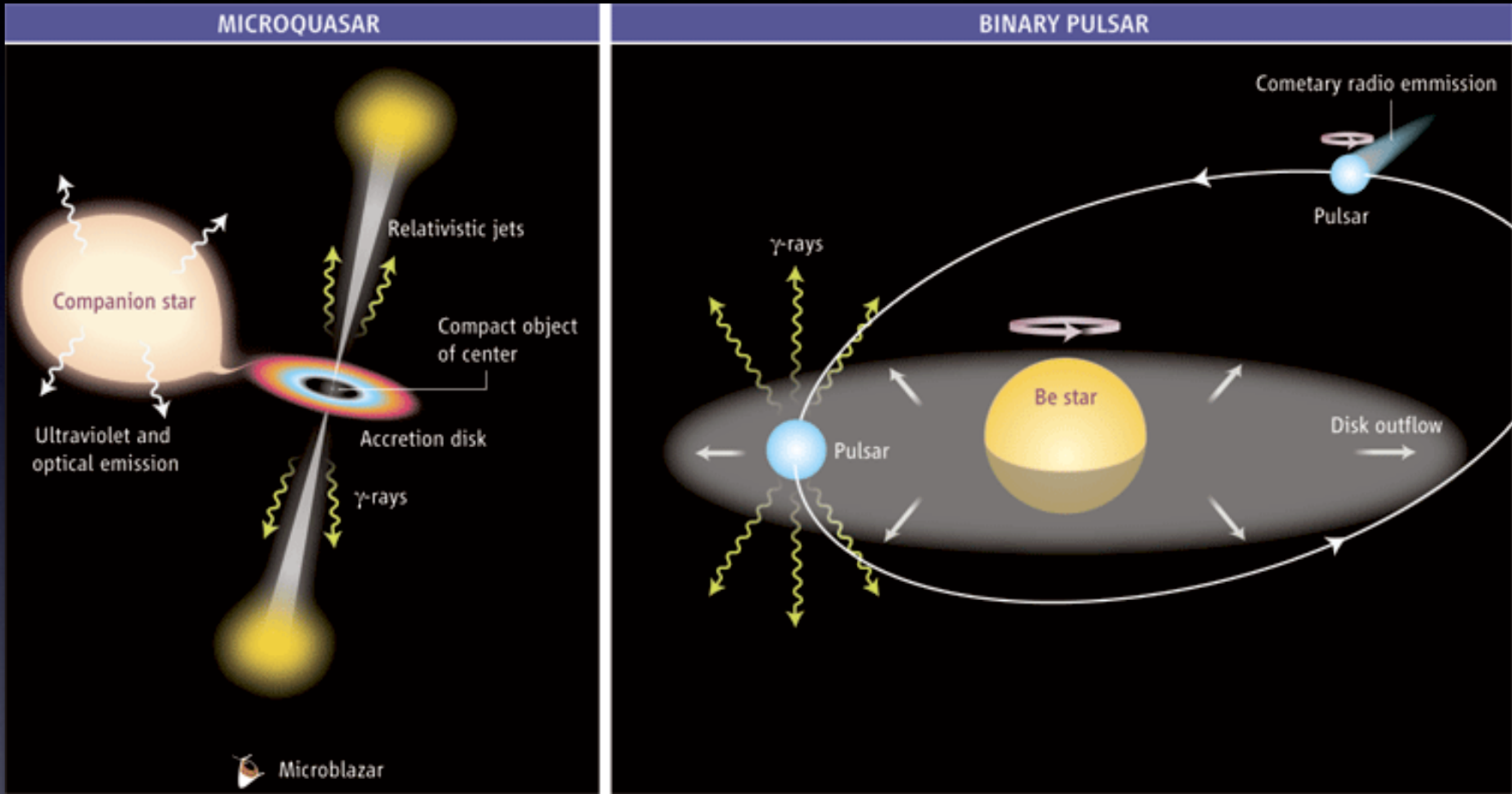

Tanaka et al 2012

Possible Scenarios

Particles accelerated at a jet from the compact object

or

at a shock generated by interaction between stellar wind and pulsar wind

LS 5039 by Fermi LAT

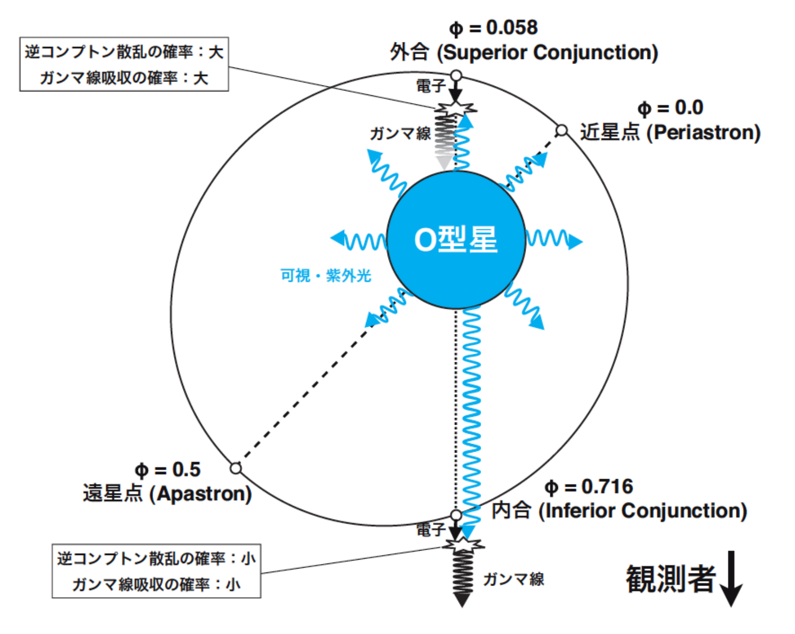

Tanaka et al 2012

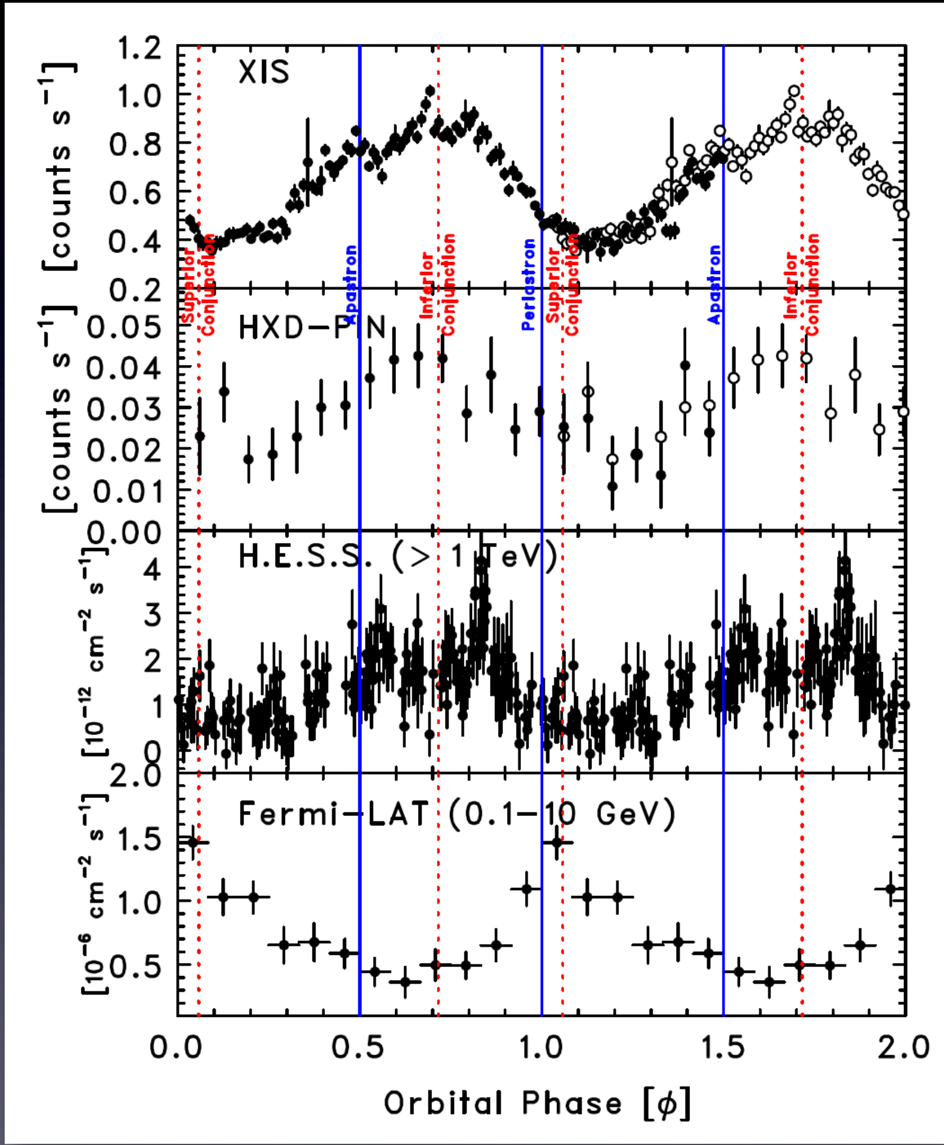

Anti-correlation between GeV and TeV flux as predicted Abdo+ (2007)

LS 5039 Gamma-ray Spectrum

Hadasch+ (2012)

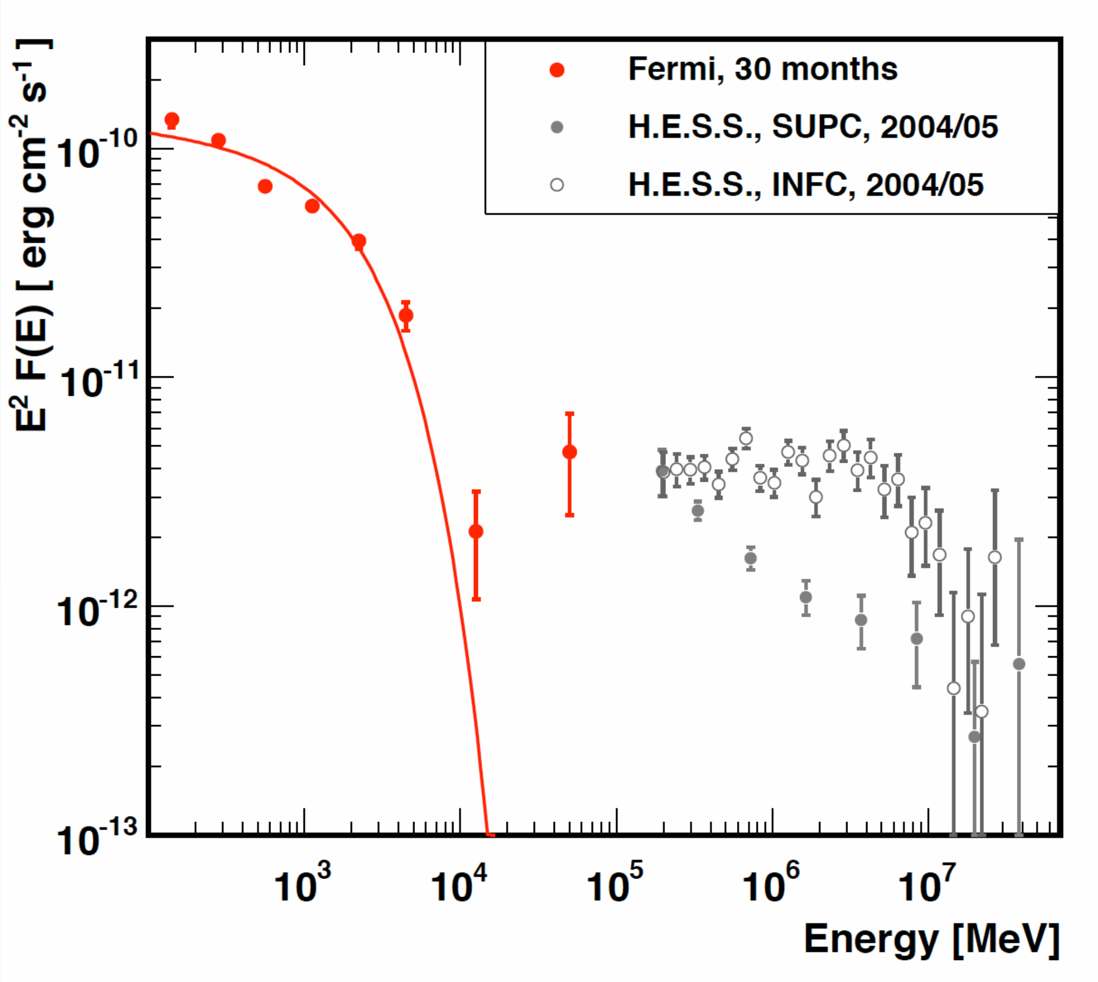

Tanaka et al 2012

Cutoff energy of 2.2 GeV is too low compared to that expected from γγ absorption (> 30 GeV)

Galactic globular clusters

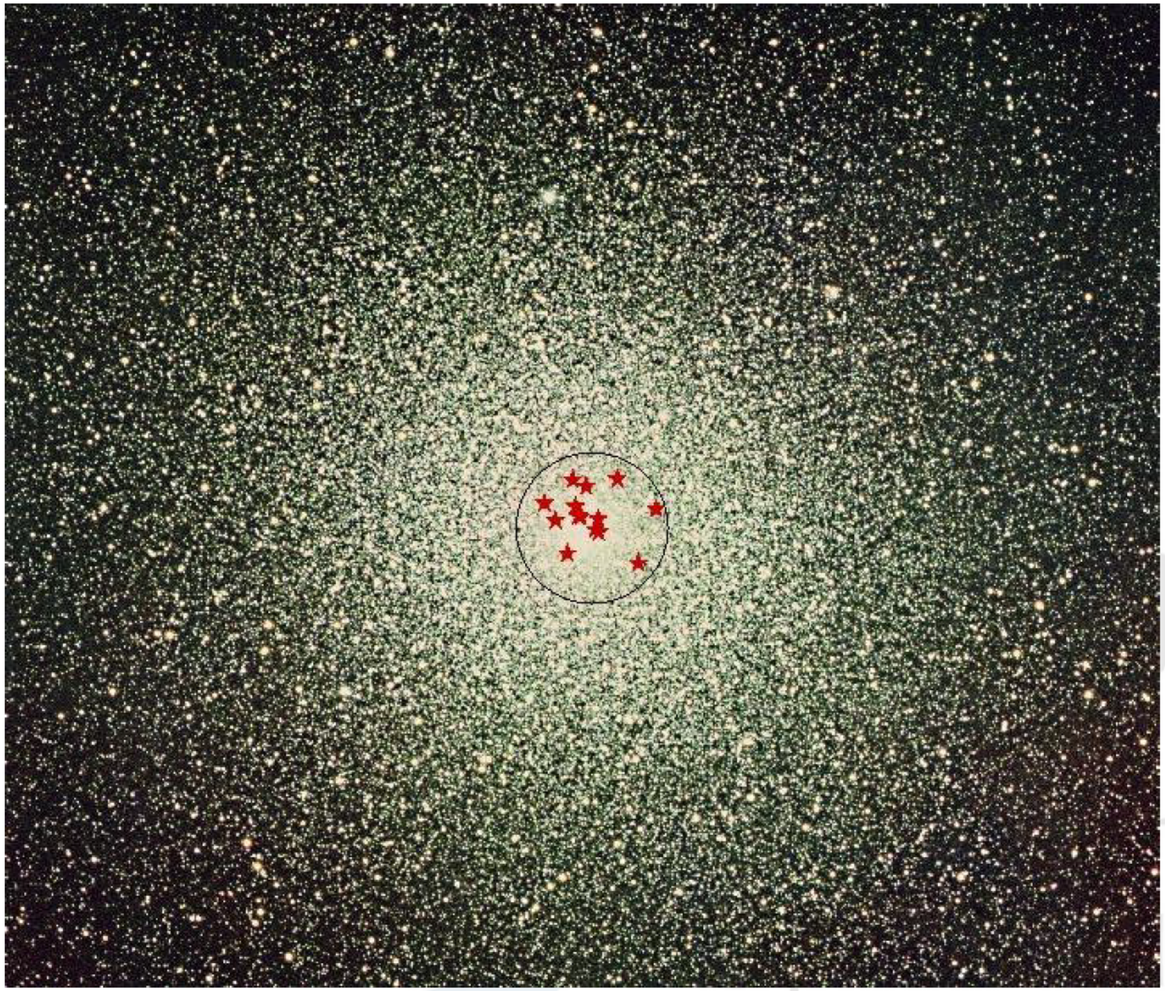

47 Tuc, Anglo-Australian Observatory
Red stars = radio MSPs

- Dense groups of old stars (10^{5-6} stars)
- Stable on dynamical timescales ($\sim 10^6$ yr)
- Unstable on thermal timescales ($\sim 10^9$ yr)

Webb 2010

Globular cluster energy sources

Compact binaries:

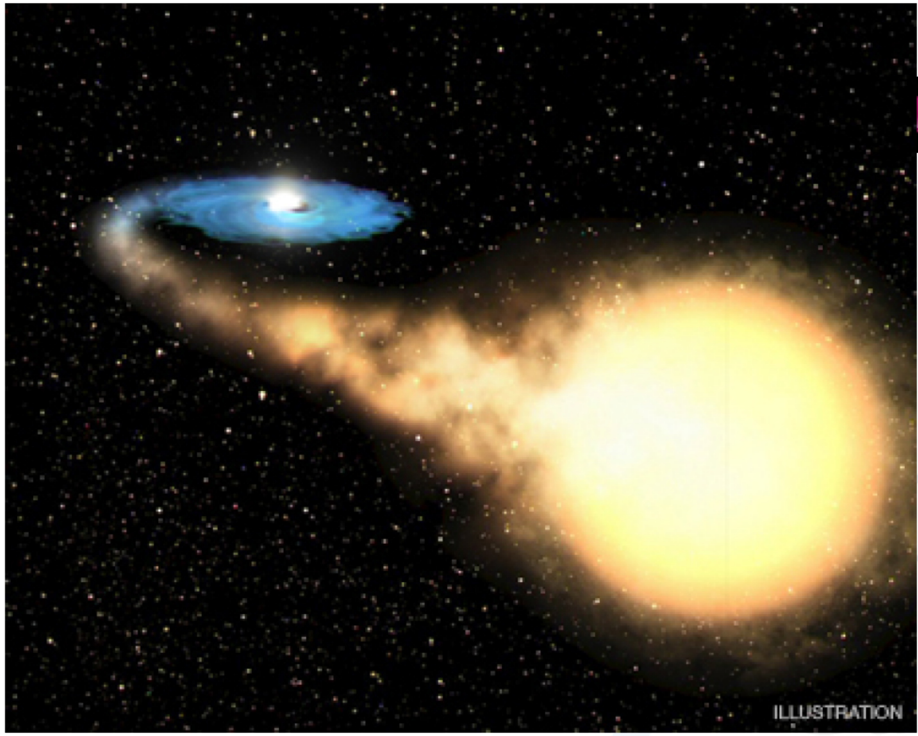

Artist's impression of an X-ray binary (Credits: ESA, NASA and Felix Mirabel)

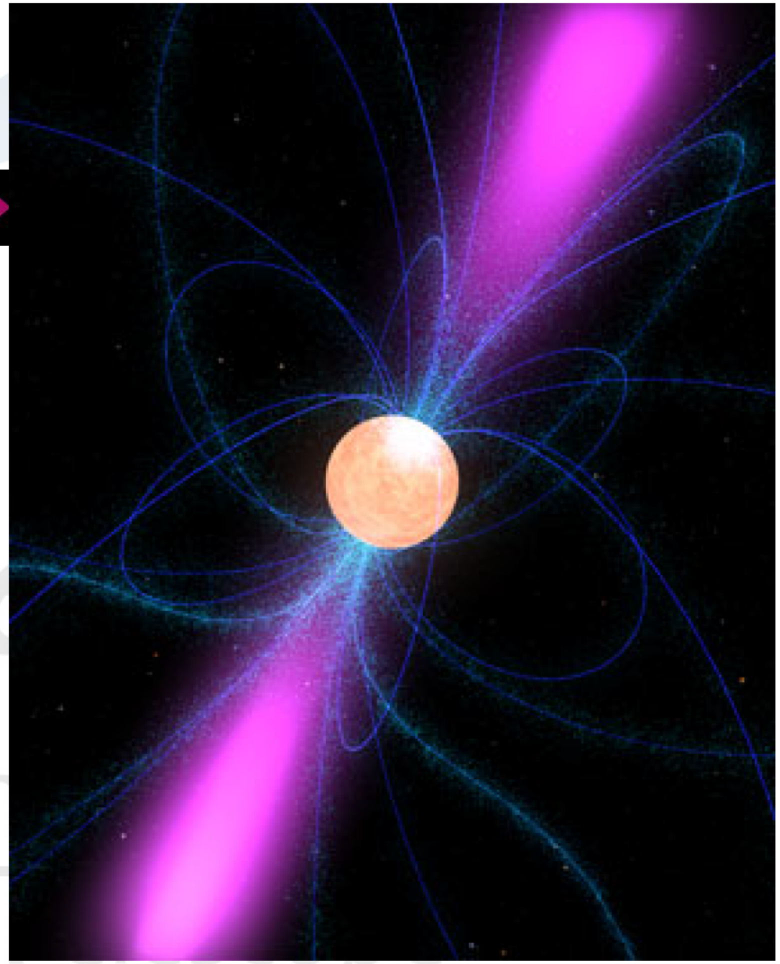

Artist's impression of a pulsar (Credit: NASA)

Webb 2010

High energy emission from pulsars

Webb 2010

- **Three models:**
  - **polar cap**
  - **outer gap**
  - **slot gap**

- **Inverse Compton scattering/ curvature radiation $\rightarrow \gamma$-rays**

- **Discovery of γ-ray emission from MSPs (Abdo et al. 2009a,b)**

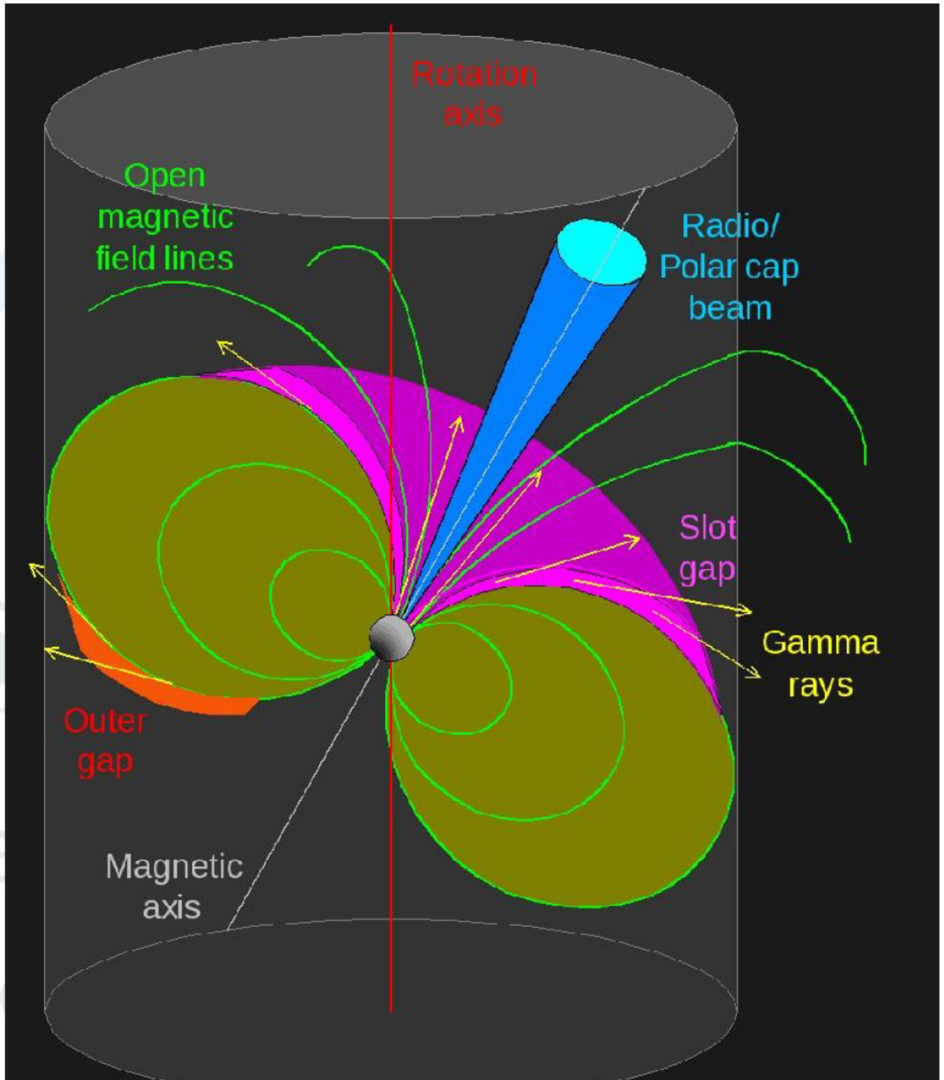

$M \sim 1.4\ M_{\odot}$, $R \sim 10$ km, $B \sim 10^{7-9}$ G

47 Tucanae

Webb 2010

- 23 millisecond pulsars known (radio detection, Freire[a])
- γ-ray emission detected with the Fermi LAT (17 σ)
- $L_{(200MeV-10GeV)} =$ $(4.8\pm1.2) \times 10^{34}$ erg s^{-1} (distance $= 4.0 \pm 0.4$ kpc)

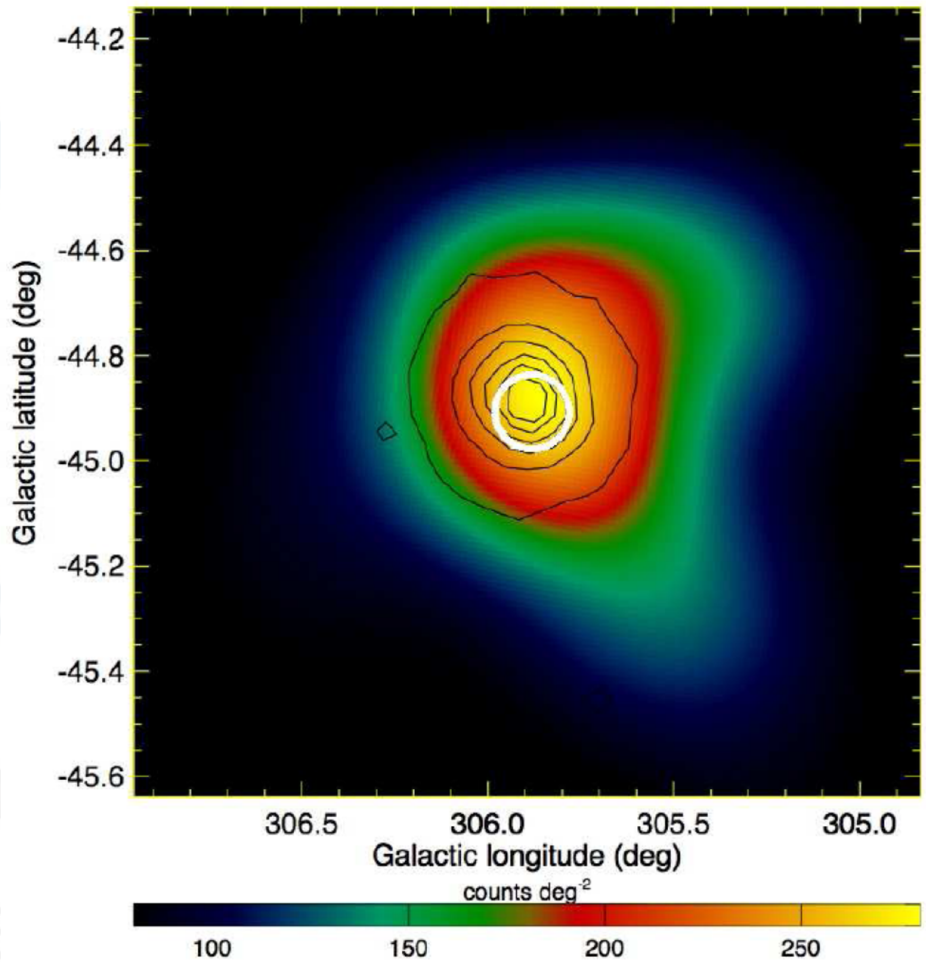

Circle: 95% confidence region for the location of the gamma-ray source.

[a] http://www.naic.edu/ pfreire/GCpsr.html

Gamma-ray spectrum of 47 Tuc

Webb 2010

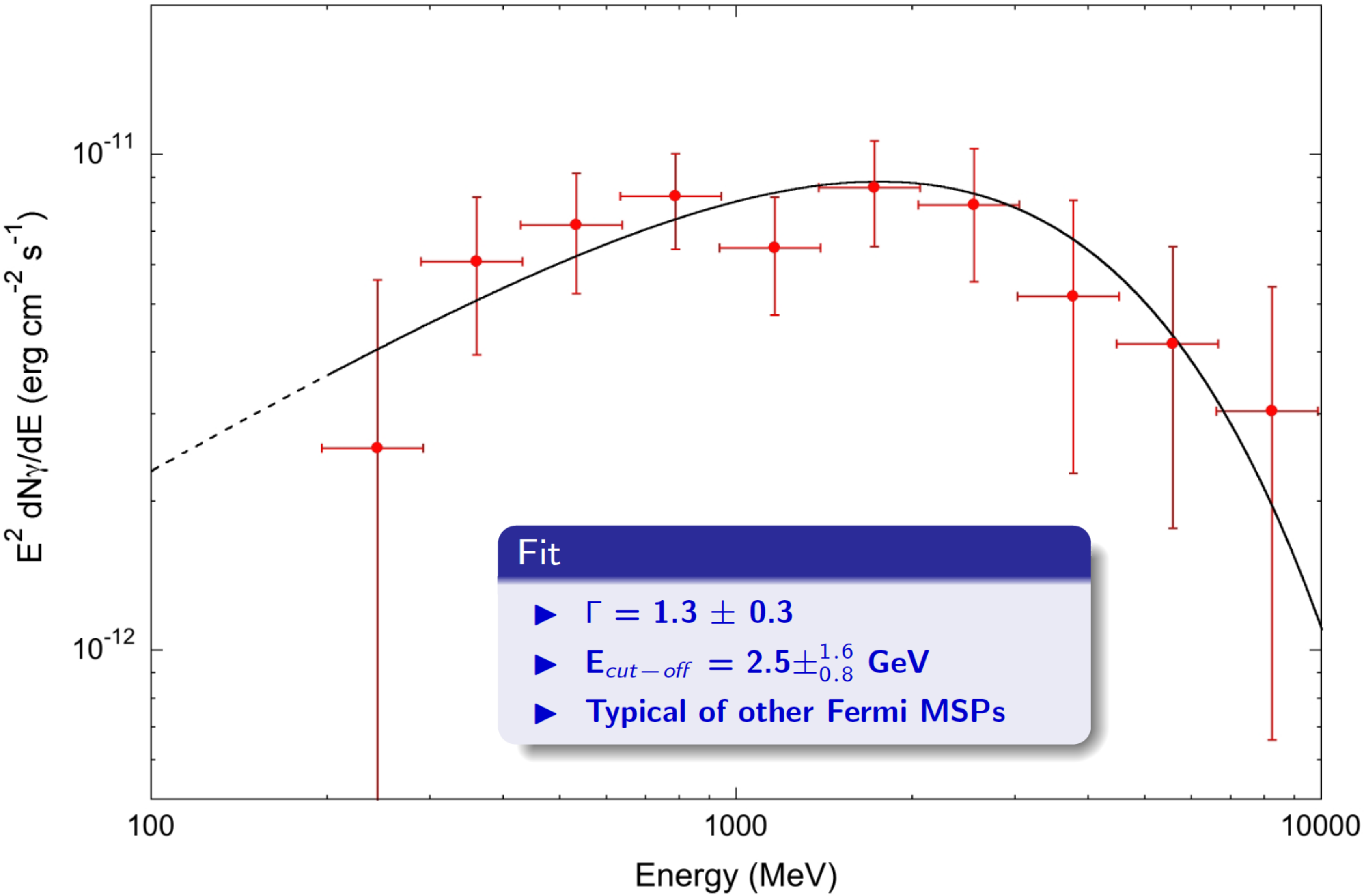

Fit

- $\Gamma = 1.3 \pm 0.3$
- $E_{cut-off} = 2.5\pm^{1.6}_{0.8}$ GeV
- Typical of other Fermi MSPs

...and what about other Galactic globular clusters?

Webb 2010

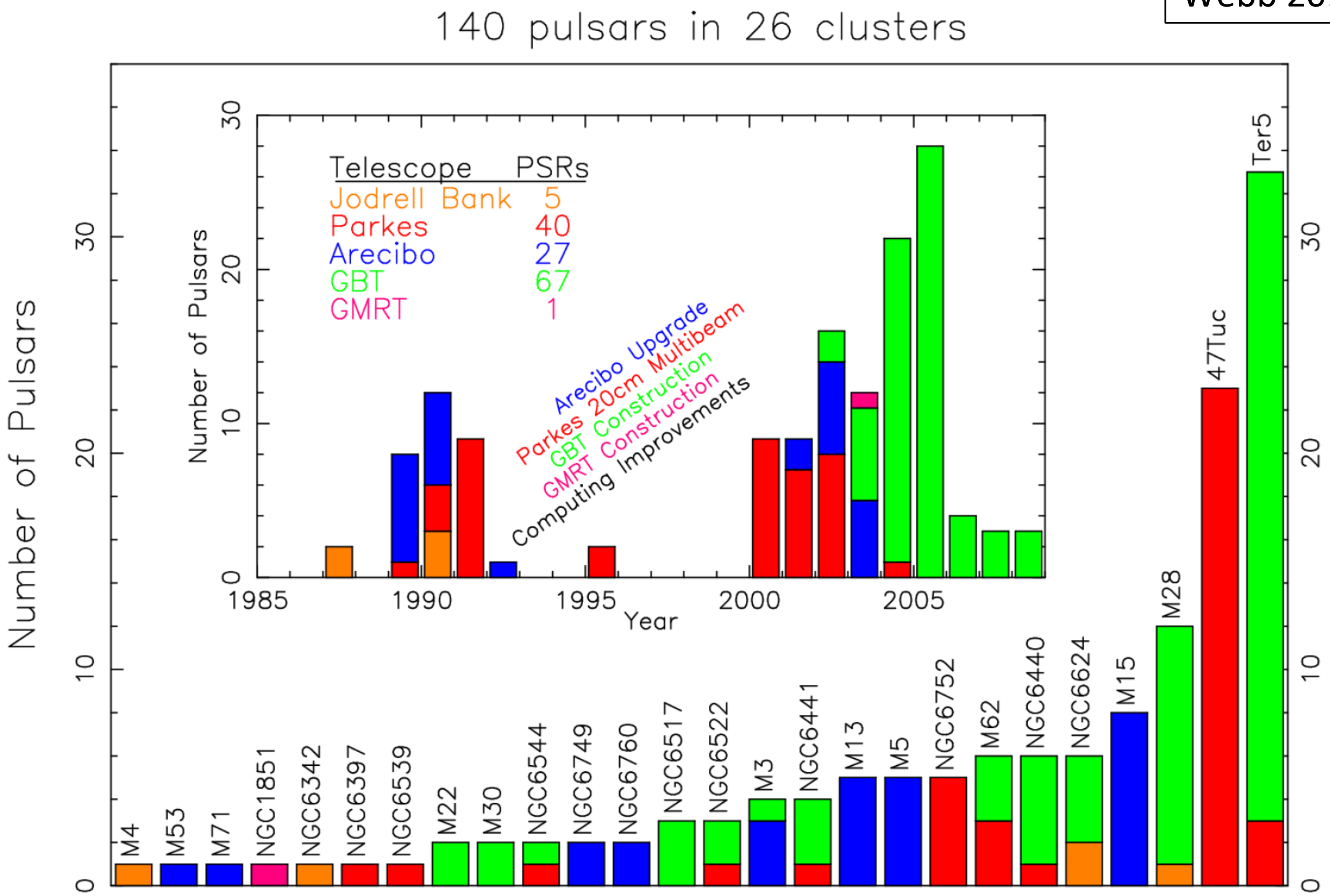

The Gamma-ray Flares of Cyg X-3

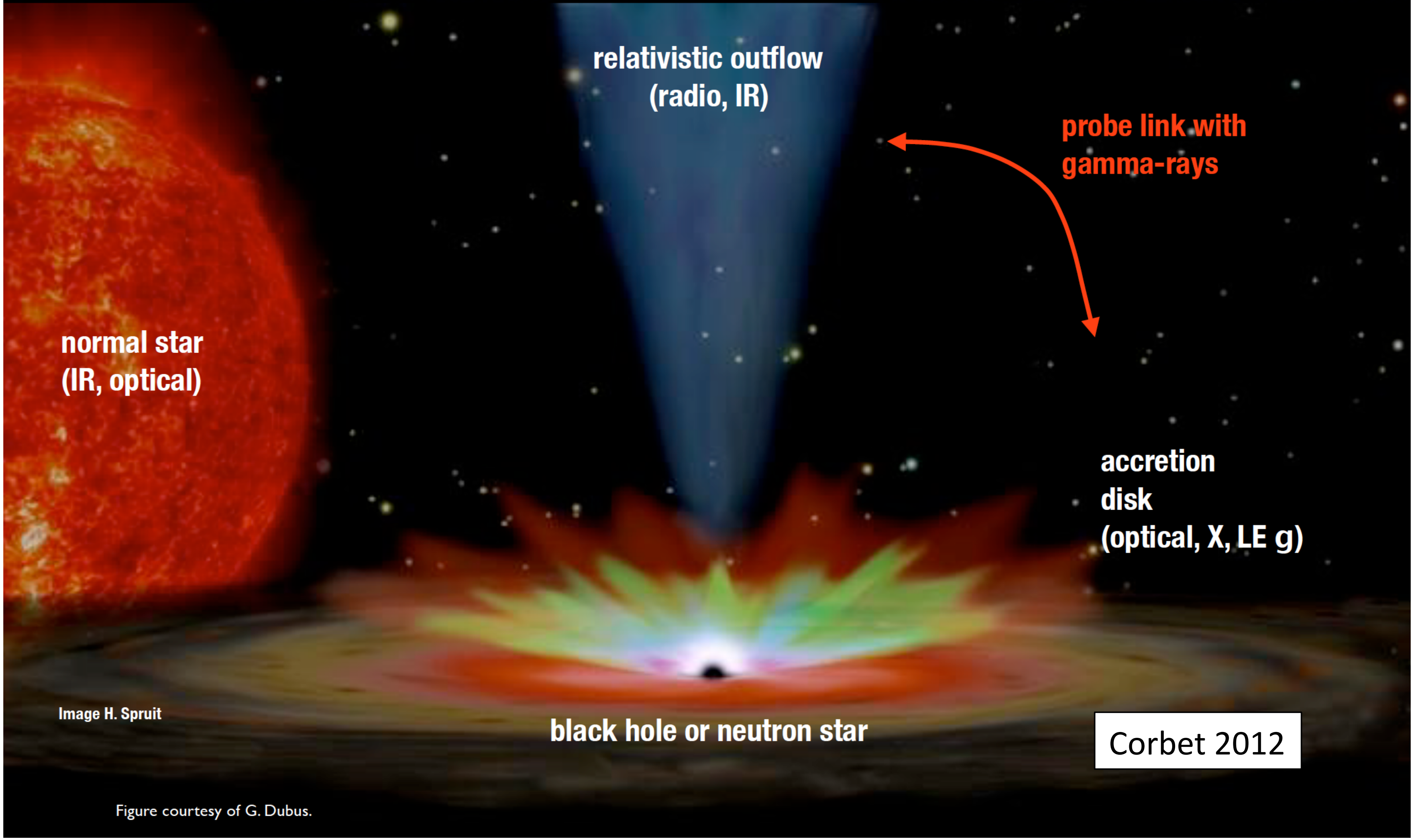

Cyg X-3: a microquasar in γ-rays

AGILE & Fermi/LAT detections

Tavani+ 2009, Abdo+ 2009, Williams+ 2011, Bulgarelli+ 2011, Corbel+ 2012

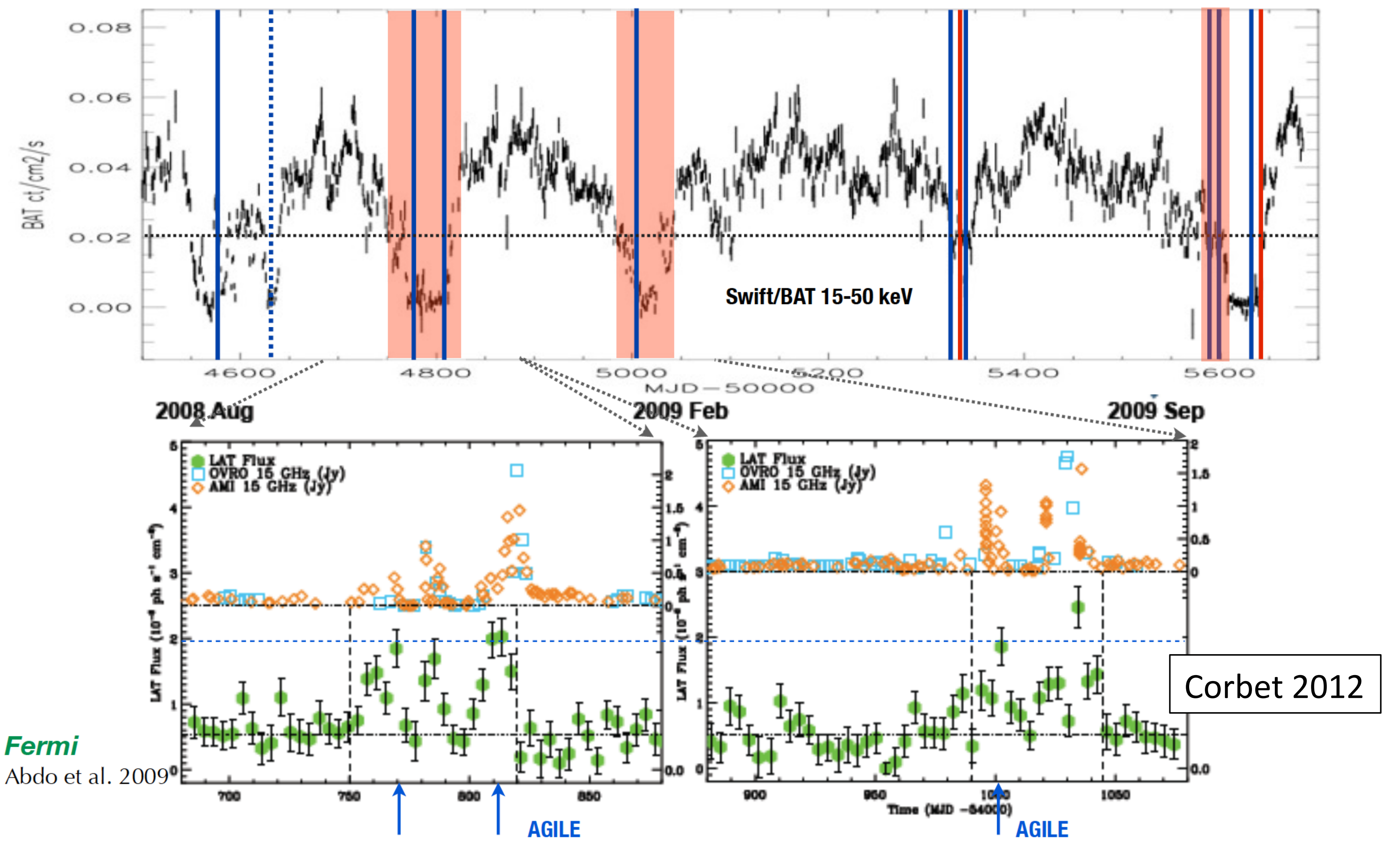

Orbital Modulation in Cyg X-3

- During the first two outbursts from Cyg X-3 (2008, 2009) modulation of LAT flux on the orbital period was clearly detected.
- Modulation also detected in 2011 outburst. But investigation hampered by short duration.
- Analysis being undertaken using Pass 7 with improved soft response...

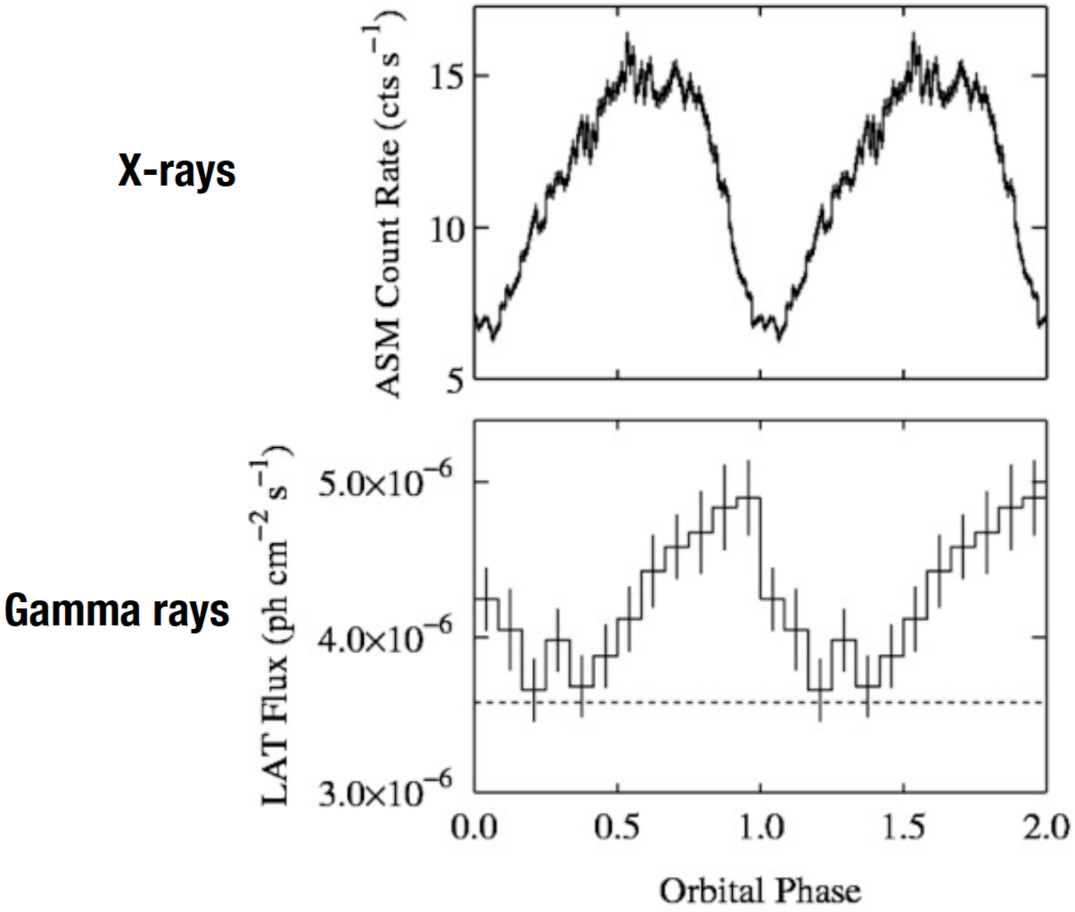

Corbet 2012

Possible scenario

(7-12 Jan 2012, 219th AAS, Texas, Anna Szostek et al.)

- Shock forms at various distances along the jet (Lindfors et al. 2007; Miller-Jones et al. 2009)

- Transition **IN**/**OUT** of the ultrasoft X-ray state signal a **decrease**/**increase** in jet efficiency with non-thermal region moving **CLOSER**/ **FURTHER** from the compact object

- Gamma-ray emission is most efficient at "sweet-spot" bounded by strong pair production on thermal X-rays and declining seed photon density for inverse Compton scattering (Cerutti et al. 2011; Sitarek & Bednarek 2011)

- Detections prior to and after the quenched state when shock moves through this region

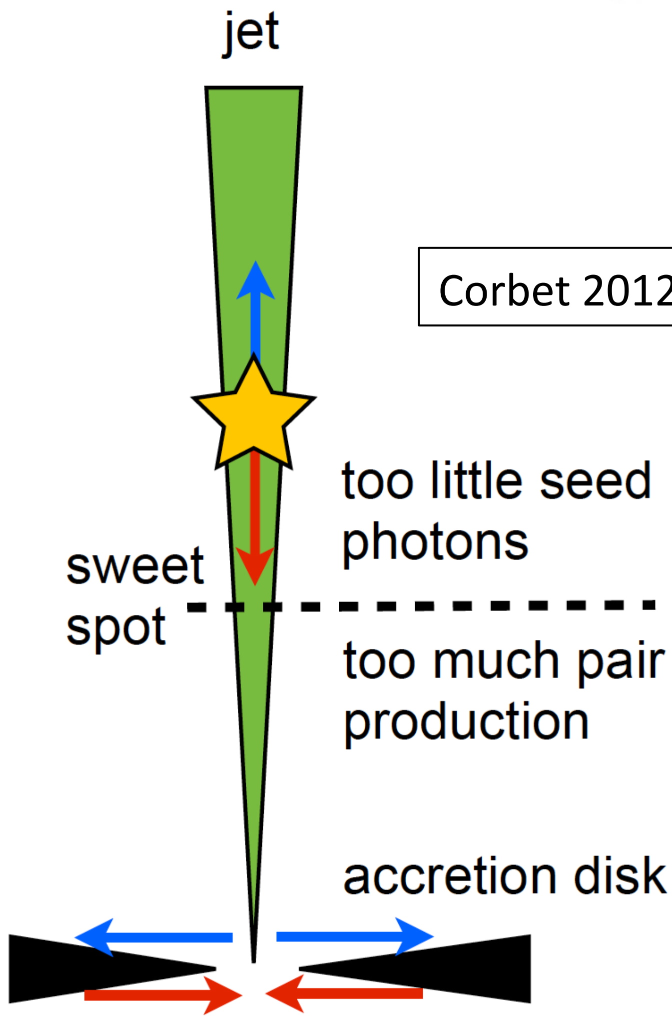

Corbet 2012

Fermi Discovery of a Nova – the First

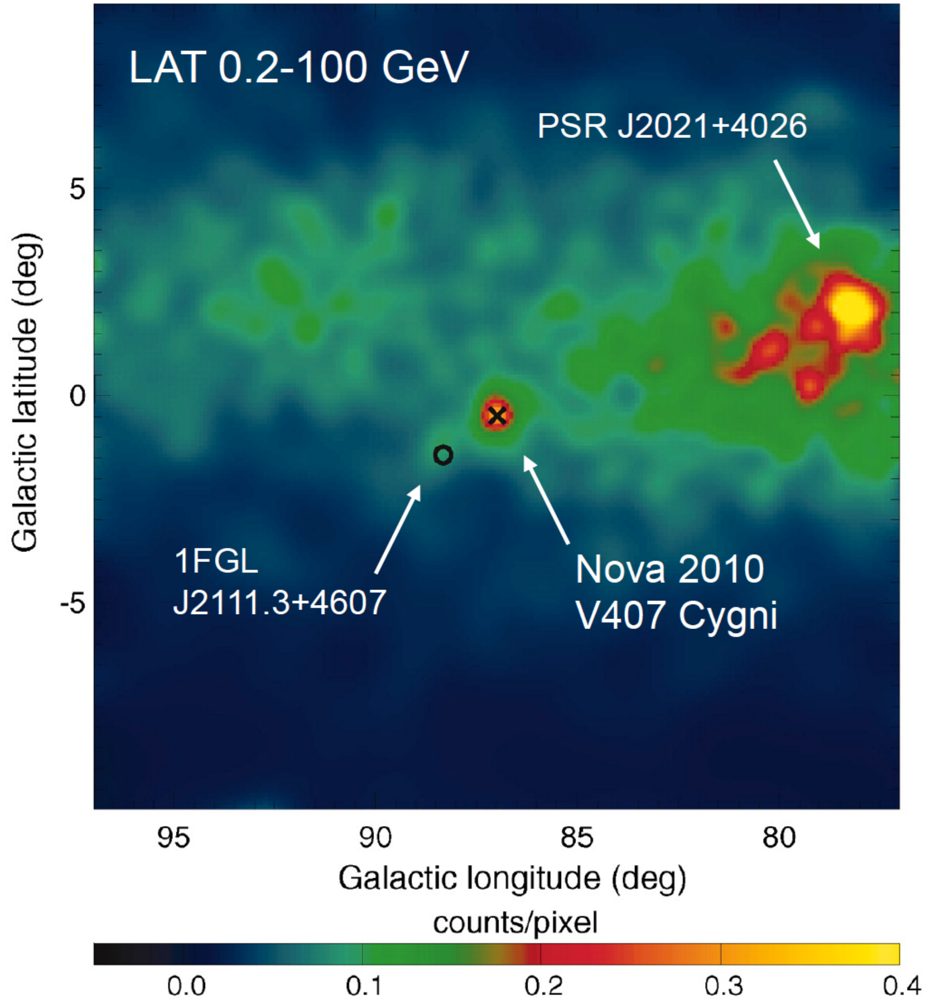

- γ-ray ID via spatial ($r_{95\%}$=3.7') + temporal coincidence with a *symbiotic recurrent nova*
- LAT detections March 13-14 by "Flare Advocates" (Cheung, Donato, et al. ATel #2487)
- Subsequently found initial LAT detection March 10, same day as nova V407 Cyg optical discovery
  - *White dwarf in binary system*

Abdo et al. 2010 Science, 329, 817

Cheung 2012

Fermi Discovery of a Nova – the First

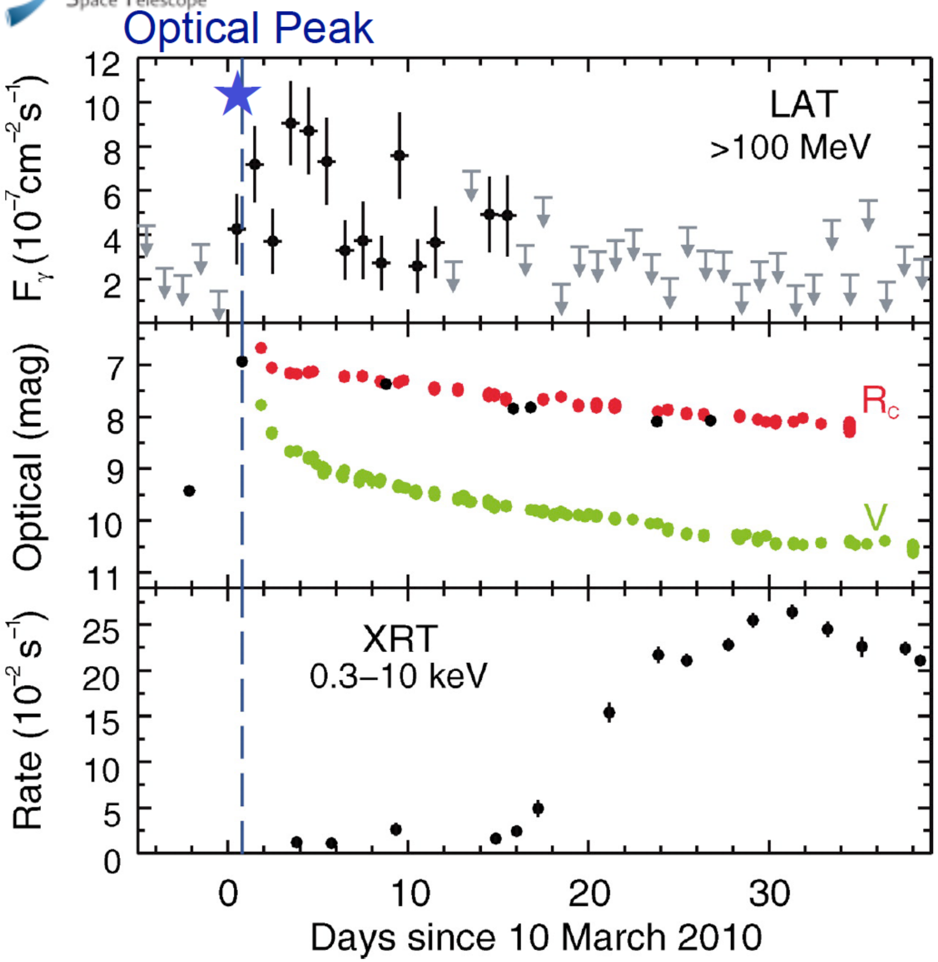

- γ-ray ID via spatial ($r_{95\%}$=3.7') + temporal coincidence with a *symbiotic recurrent nova*
- LAT detections March 13-14 by "Flare Advocates" (Cheung, Donato, et al. ATel #2487)
- Subsequently found initial LAT detection March 10, same day as nova V407 Cyg optical discovery
  - *White dwarf in binary system*

Abdo et al. 2010 Science, 329, 817

Cheung 2012

Our Understanding of γ-ray Novae (ca. ~2010)

Compact cataclysmic variable:

WD + Main Sequence

↓

Roche lobe overflow

γ-ray sources e.g., V407 Cyg

Symbiotic system:

Massive WD + Red Giant

↓

accretion from a red giant wind

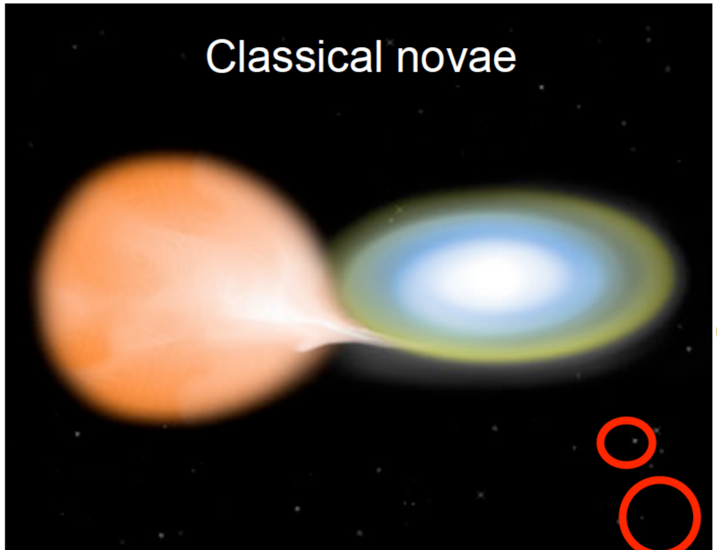

Hydrogen burning in degenerate conditions on top of the white dwarf

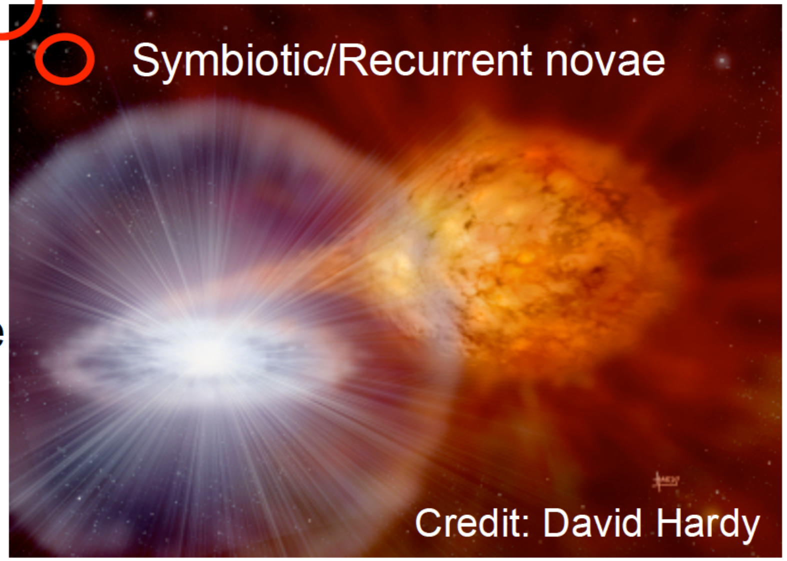

- a ~ 10^{11}cm ~ $R_\odot$
- P_{rec} >~10^4 yr; P_{orb}~hr-day
- rate ~35/yr in Galaxy

Not γ-ray sources

- a ~ 100's $R_\odot$
- P_{rec} <100 yrs; P_{orb}~years
- ~10 known

Adapted from M. Hernanz X-ray Universe 2011 talk

Cheung 2012

LAT Non-Detections

KT Eri 2009 Classical Nova
(white dwarf + Main sequence star)

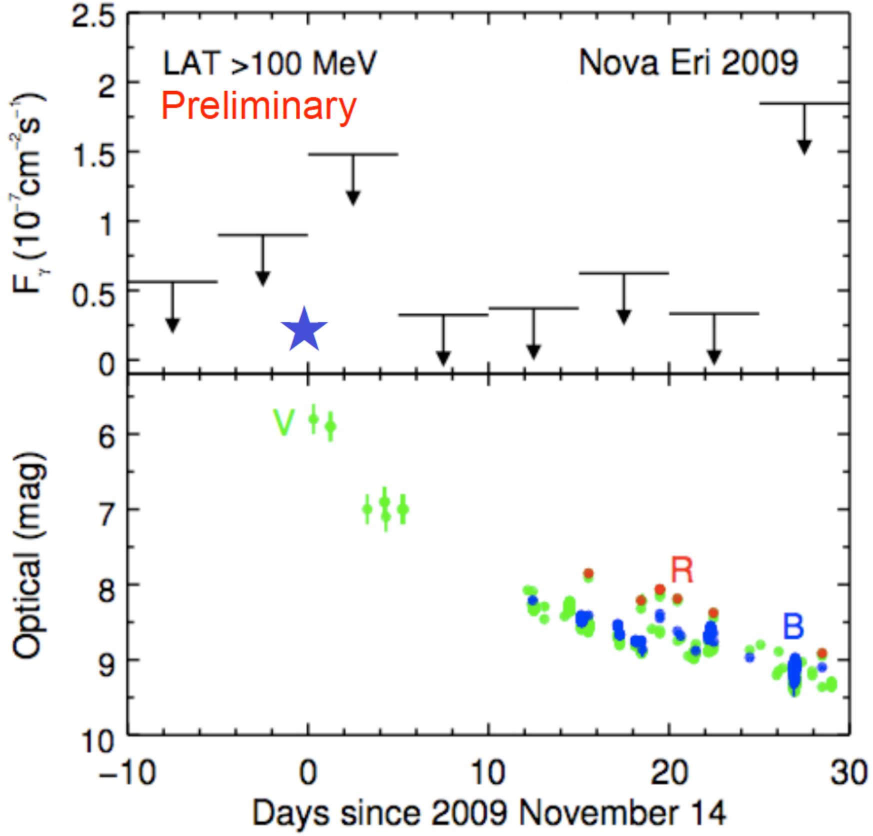

V407 Cyg Symbiotic Recurrent Nova
(white dwarf + Red Giant)

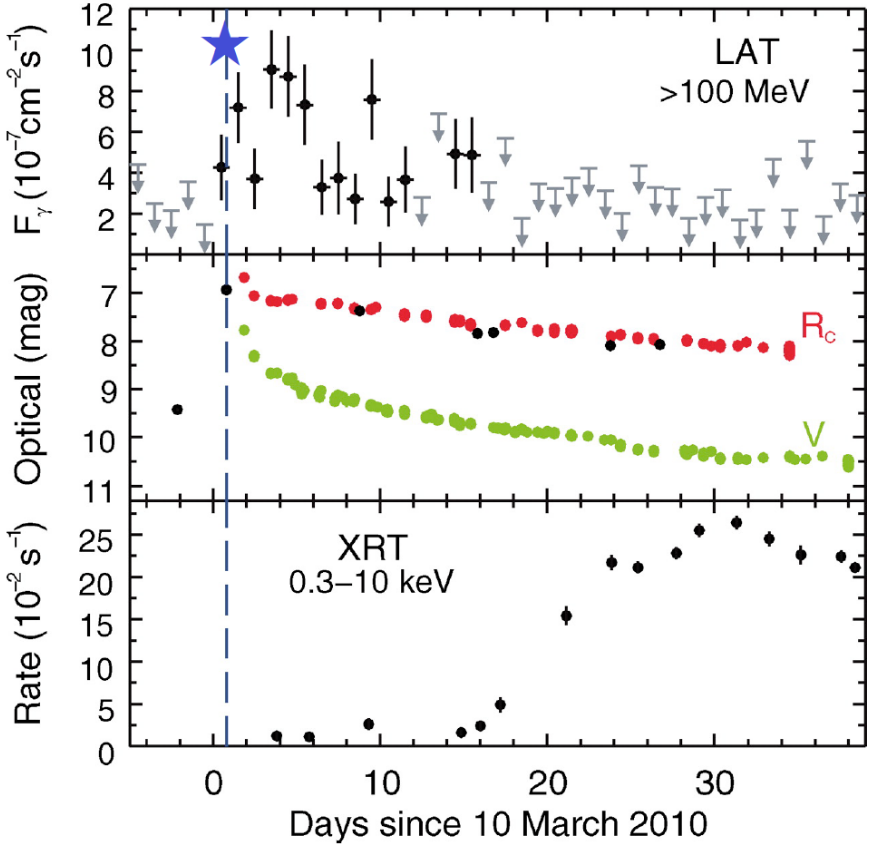

Other novae typically <~10x fainter than V407 Cyg γ-ray peak – why?

Cheung 2012

Fermi Detection of Nova Sco 2012

Nova Sco 2012 Classical Nova (?)
(white dwarf + Main sequence star)

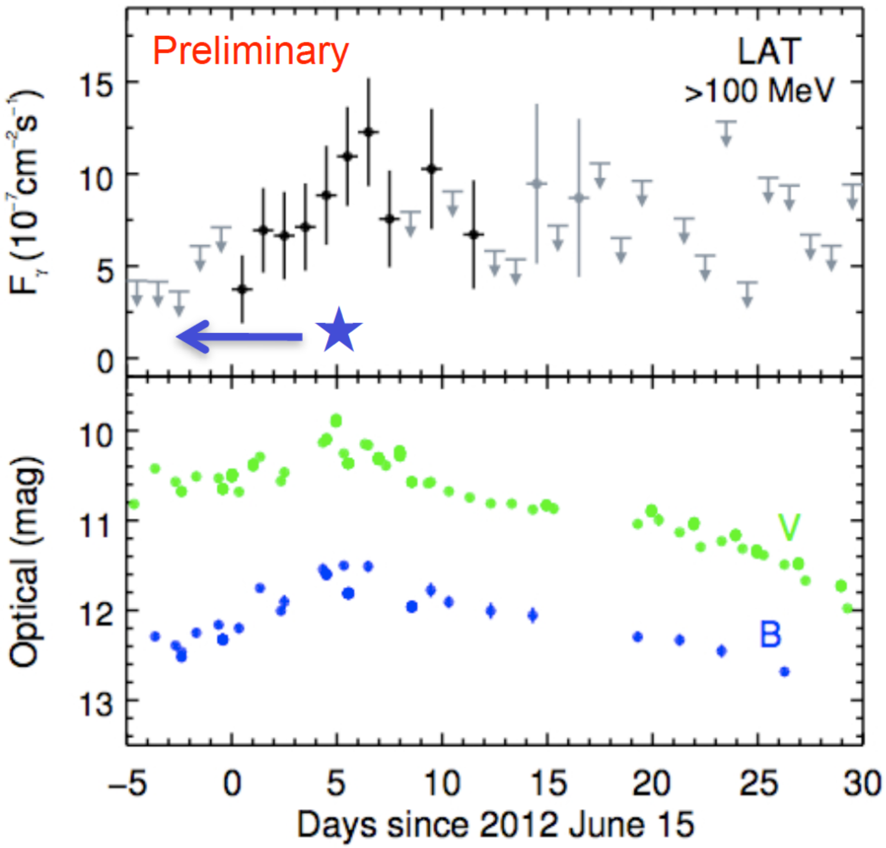

Nova Sco 2012

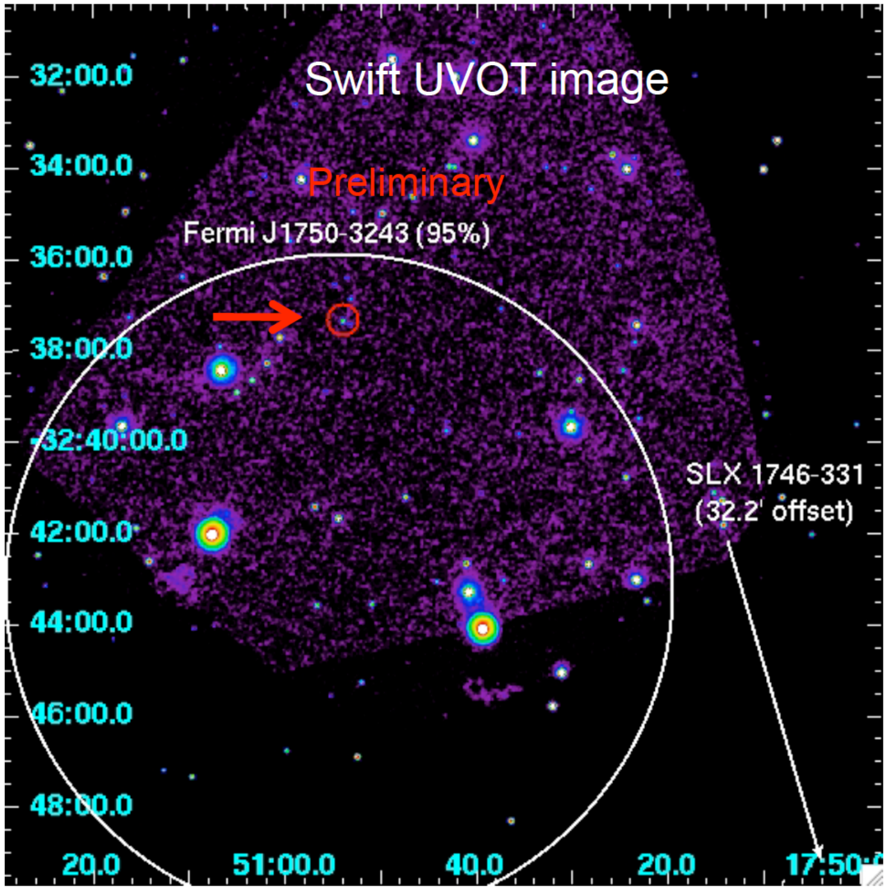

See Adam Hill et al. poster for details

Cheung 2012

Fermi *Discovery* of Nova Mon 2012

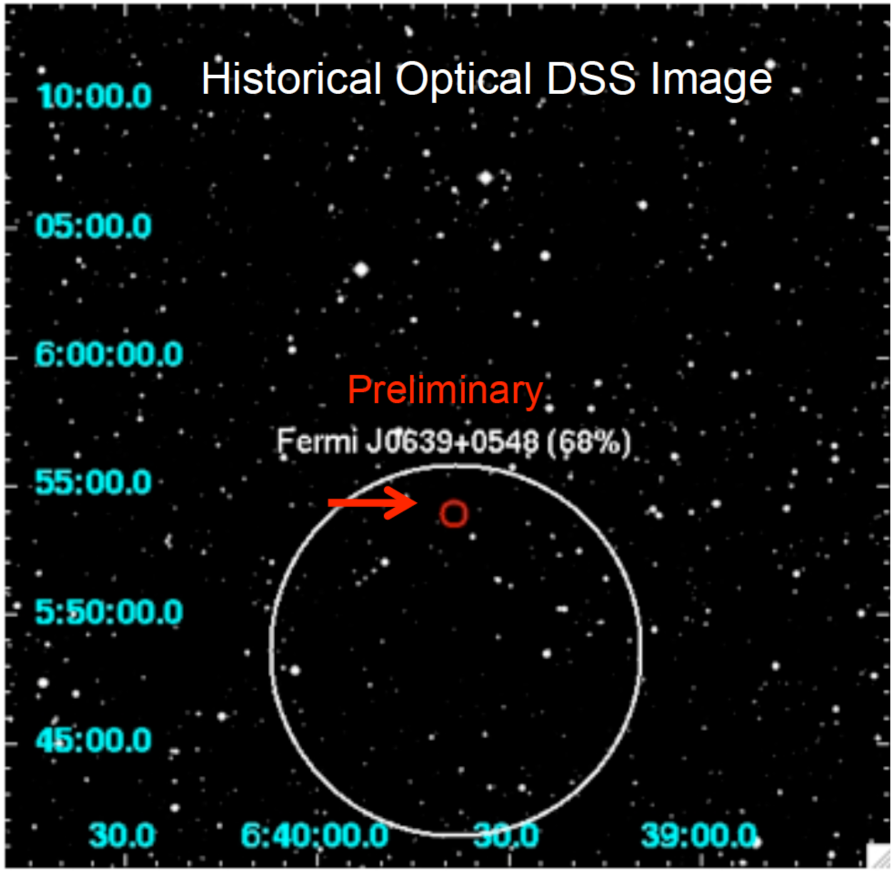

- Initial LAT discovery of Fermi J0639+0548, ~20º from Sun in late-June (Cheung et al. ATel #4224)
- Optical discovery of possible nova August 9 (S. Fujikawa, CBET#3202)
- Amateur and Nordic Optical Tel spectroscopic confirmation Aug 14-16 as ONe type classical nova ~50 days after outburst, 3-4 kpc away, and LAT association with Nova Mon 2012 (Cheung, Shore et al. ATel #4310)

Cheung et al 2012

Fermi *Discovery* of Nova Mon 2012

Before

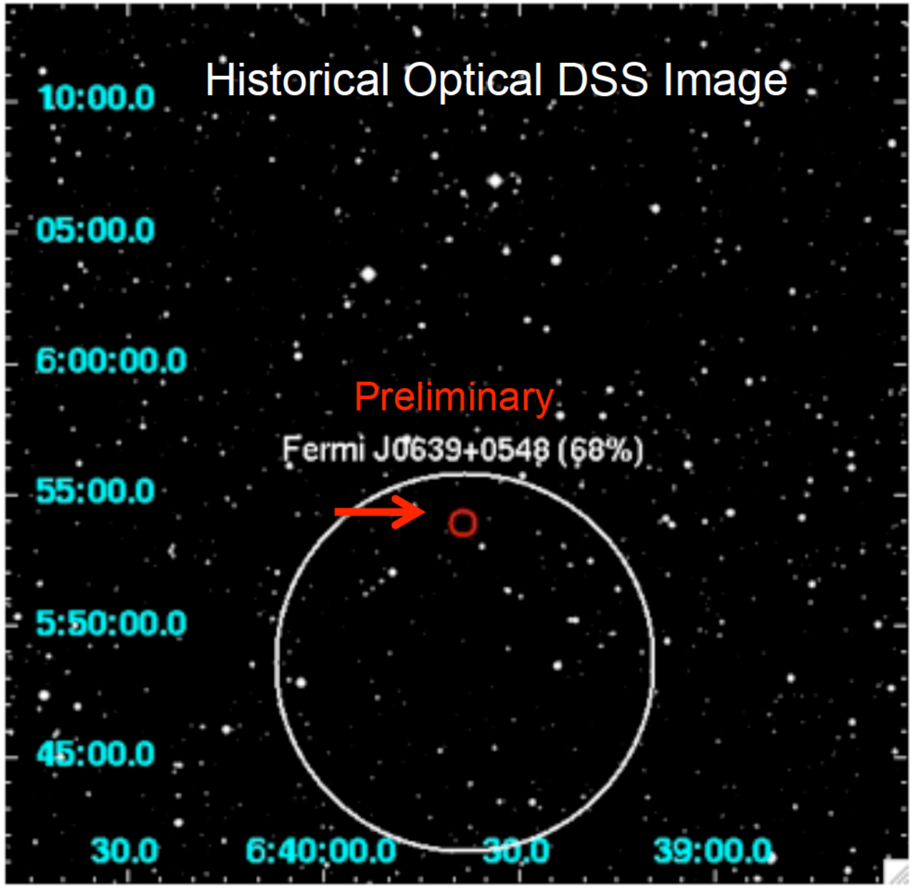

Nova

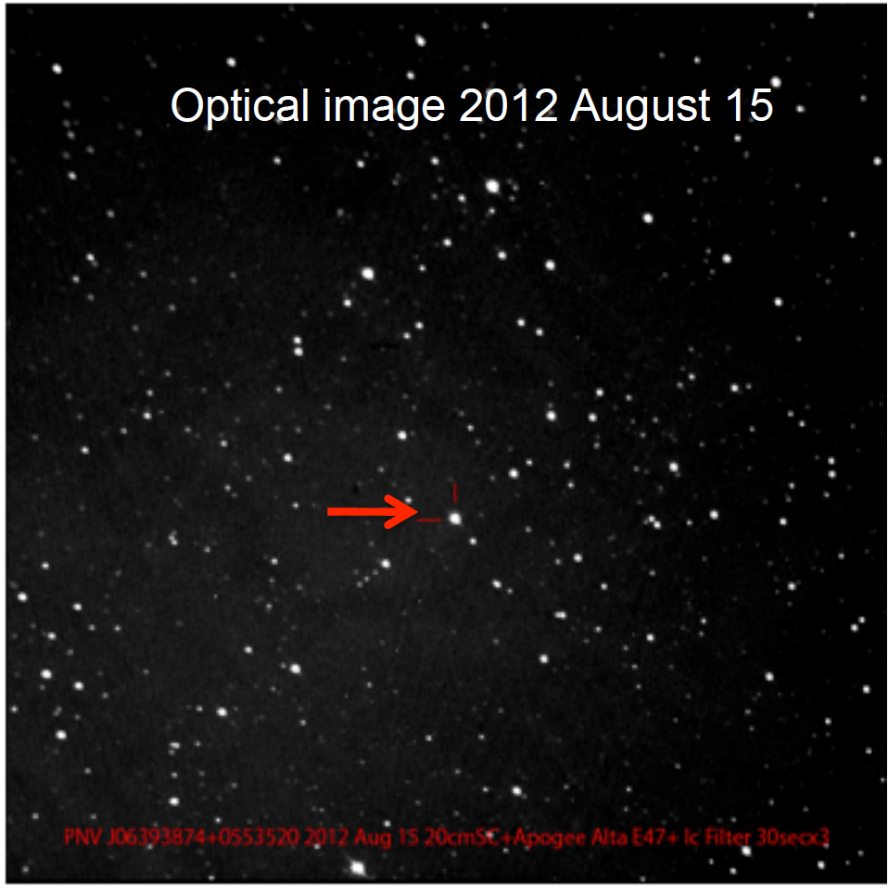

Image: Seiichiro Kiyota (Tsukuba, Japan)

Cheung 2012

Similarity of LAT γ-ray Spectra

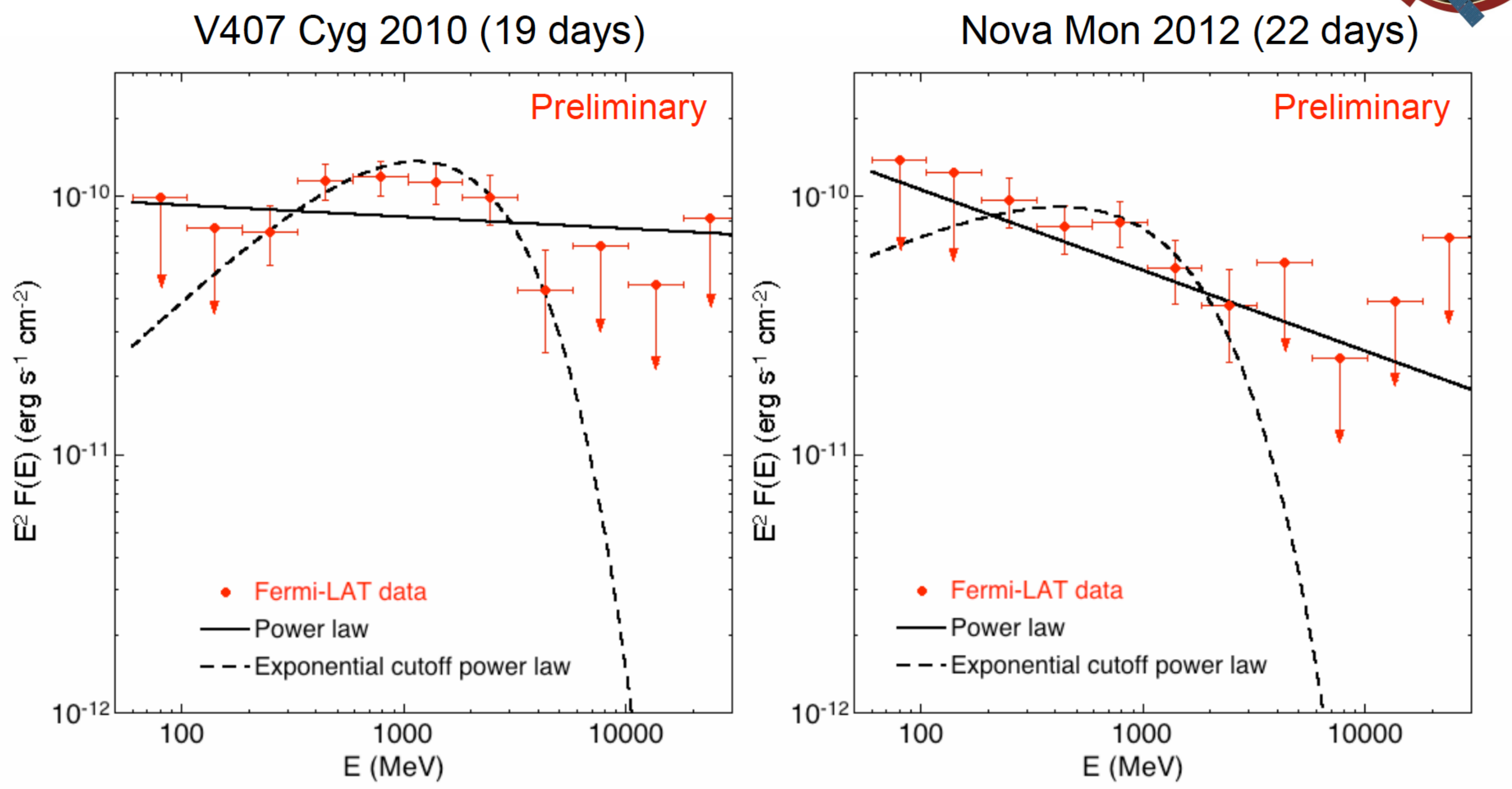

LAT spectra with P7V6 selection; Courtesy Pierre Jean

Cheung 2012